ABSTRACT

Title of Dissertation: FUNCTIONAL FOODS THAT MANIPULATE THE GUT MICROBIOTA COMPOSITION AND REGULATE THE INTESTINAL IMMUNE SYSTEM-*Urtica dioica* a CASE STUDY

Si Fan, Doctor of Philosophy, 2024

Dissertation directed by: Assistant Professor, Diana Obanda, Department of Nutrition and Food Science

The prevalence of obesity and its comorbidities, such as insulin resistance and type 2 diabetes are major concerns. Diet-induced obesity and insulin resistance are associated with gut microbiota dysbiosis, specifically, a reduction in diversity and an increase in bacteria taxa linked with host tissue inflammation and extra energy harvest. Prevention strategies focusing on modification of diet and physical activity levels are beneficial, effective, and cost-efficient but difficult to maintain in the long term.

Urtica dioica is widely used as a food in several cultures and its extract has been widely studied for intervention against several diseases, but the molecular mechanisms involved are unclear. In addition, most studies have focused on the extract but not the plant as a whole food. Because *U. dioica* exerts pleiotropic effects in several tissues, we hypothesized that its

phytochemicals get into the systemic circulation to reach target tissues, such as abdominal adipose tissue and skeletal muscle but also impact obesity and insulin resistance through pathways involving the gut microbiota and ultimately the gut immune system.

The data presented herein was acquired in a mouse model of obesity and insulin resistance. Supplementing the food with whole *U. dioica* vegetable, attenuated high fat (HF) diet-induced weight gain, fat accumulation, insulin resistance and changed the gut microbiota composition, by increasing diversity and promoting the proliferation of species from the genus *Clostridium*. This taxon has associated with lower body weight and activation of regulatory T cells (Tregs) in the intestinal immune system. In a second study, we confirmed that *U. dioica* induced T cells antigenic stimulation, promoted the activation of Tregs and overall protected against HF diet inflammation. Furthermore, besides attenuating HF diet induced fat accumulation, *U. dioica* promoted the browning or beiging of adipose tissue as evidenced by enhanced gene expression of key markers of this process. Brown or beige adipose tissue displays enhanced fat oxidation. Finally using enteroids derived from small intestinal tissue, we show that in presence of excess nutrients, supplementation with *U. dioica* reduces the amount fatty acids and glucose absorbed. In conclusion, supplementing a HF diet with *U. dioica* attenuates fat accumulation and insulin resistance via mechanisms involving the gut microbiota composition and function, the gut immune system and associated inflammation and moderation of amounts of macronutrients absorbed.

FUNCTIONAL FOODS THAT MANIPULATE THE GUT MICROBIOTA COMPOSITION AND REGULATE THE INTESTINAL IMMUNE SYSTEM-*Urtica dioica* a CASE STUDY

by

Si Fan

Dissertation submitted to the Faculty of the Graduate School of the
University of Maryland, College Park, in partial fulfillment
of the requirements for the degree of
Doctor of Philosophy
2024

Advisory Committee:
Assistant Professor Diana Obanda, Chair
Professor Liangli Yu
Associate Professor Seong-Ho Lee
Professor Zhengguo Xiao
Associate Professor Rohan V. Tikekar

Dedication

To

My Parents

Zhongxiao Fan and Yan Luo

And my fiancé

Hao Dong

Thank you for your unconditional love and support

Acknowledgments

I am grateful to acknowledge all the people who supported me through the process of my Ph.D. studies and my dissertation over the past five years.

I would like to thank my principal advisor, Dr. Diana N. Obanda, who provided me with a precious opportunity to become a Ph.D. student, her endless patience, support and mentorship throughout my entire Ph.D. career. Without her advice, I would not have finished my dissertation successfully.

I would also like to thank all my committee members for supporting my dissertation work and contributing valuable inputs: Dr. Liangli Yu, Dr. Seong-Ho Lee, Dr. Zhengguo Xiao and Dr. Rohan Tikekar. I appreciate their precious time and valuable suggestions.

Furthermore, I also want to express my special thanks to Dr. Md Shahinozzaman, a postdoctoral fellow who worked with us, and my lovely lab mates, Samnhita Raychaudhuri, Ujjwol Subedi, Opeyemi Osahonruwen Ogedengbe and Victor Moronge Mochama, who worked with me to complete some of the studies, deliberate and troubleshoot issues together. I am grateful to have all of them and have the opportunity to work with them.

Finally, I will express my deepest gratitude to my parents, Yan Luo and Zhongxiao Fan. Without their sincere support and encouragement, I would not have completed my Ph.D. degree. Also, I would like to give special thanks to my beloved, Hao Dong, who showed up in my life and loved me so much. They all keep me going forever.

Table of Contents

List of Tables

List of Figures

List of Abbreviations

T2DM	Type 2 Diabetes Mellitus
DIO	Diet-Induced Obesity
HOMA-IR	Homeostatic Model Assessment of Insulin Resistance
U. diocia or UT	*Urtica dioica*
Low Fat	LF
High Fat	HF
LFUT	LF supplemented with 1.6% of *U. dioica*
HFUT2	HF supplemented with 2% of *U. dioica*
HFUT4	HF supplemented with 4% of *U. dioica*
HFUT/HFUT9	HF supplemented with 9% of *U. dioica*
WHO	World Health Organization
CDC	Centers for Disease Control and Prevention
AOAC	Association of Analytical Chemists
IACUC	Institutional Animal Care and Use Committee
RT	Room Temperature
GF	Germ-Free
FMT	Fecal Microbial Transplant
ROS	Reactive Oxygen Species
FFAs	Free Fatty Acids
SCFA	Short-Chain Fatty Acids
BCAAs	Branched-Chain Amino Acids

GABA	Gamma-Aminobutyric Acid
BA	Bile Acid
FFAR	Free Fatty Acid Receptor
FIAF/ANGPTL4	Fasting Induced Adipocyte Factor
AMPK	AMP-Activated Protein Kinase
TLR4	Toll-Like Receptor 4
LPL	Lipoprotein Lipase
FXR	Farnesoid X Receptor
PYY	Peptide YY
GLP-1	Glucagon-Like Peptide-1
GLP-2	Glucagon-Like Peptide-2
CCK	Cholecystokinin
5-HT	Neurotransmitter
AKT	Protein Kinase B
VAT	Visceral Adipose Tissue
WAT	White Adipose Tissue
iBAT	Interscapular Brown Adipose Tissue
ORO	Oil Red O
LDL	Low-Density Lipoprotein
HDL	High-Density Lipoprotein
ELISA	Enzyme-Linked Immunosorbent Assay
RNA	Ribonucleic Acid
DNA	Deoxyribonucleic Acid

RT-PCR	Real Time Reverse Transcription Polymerase Chain Reaction
qPCR	Quantitative PCR
NTC	Non-Template Controls
NGS	Next Generation Sequencing
ISPs	Ion Sphere Particles
OTUs	Operational Taxonomic Units
PCA	Principal Component Analysis
LEfSe	Linear Discriminant Analysis Effect size
PICRUSt2	Phylogenetic Investigation of Communities by Reconstruction of Unobserved States
KEGG	Kyoto Encyclopedia of Genes and Genomes
KO	KEGG Ortholog
PERMANOVA	Permutational Multivariate Analysis of Variance
GI	Gastrointestinal
SI	Small Intestine
LP	Lamina Propria
PP	Peyer's Patches
ILCs	Innate Lymphoid cells
Tregs	Regulatory T cells
Tfh	T follicular helper cells
Th17	T-helper type 17 cells
IgA	Immunoglobulin A
sIgA	secretory Immunoglobulin A

RORγt^{+}	Retinoids Orphan Receptor gamma t
MyD88	Myeloid Differentiation primary response 88
ICOS	Inducible T-cell co-stimulator
RBP	Plasma Retinol Binding Protein
GPR	G-Protein coupled Receptor
LPS	Lipopolysaccharide
FBS	Fetal Bovine Serum
DPBS	Dulbecco's Phosphate-Buffered Saline
RPMI	Roswell Park Memorial Institute
EDTA	Ethylenediaminetetraacetic Acid
DTT	Dithiothreitol
7AAD	7-Aminoactinomycin D
APC	Allophycocyanin
FITC	Fluorescein Isothiocyanate
PE	Phycoerythrin
PMA	Phorbol 12-Myristate 13-Acetate
GCDR	Gentle Cell Dissociation Reagent
BSA	Bovine Serum Albumin
DMEM	Dulbecco's Modified Eagle Medium
DMEM/F-12	Dulbecco's Modified Eagle Medium/Nutrient Mixture F-12
ROCK	Rho-associated, coiled-coil containing protein kinase
TEER	Transepithelial Electrical Resistance
HEPES	(2-hydroxyethyl)-1-piperazine ethanesulfonic acid

NaCl	Sodium Chloride
KCl	Potassium Chloride
$MgSO_4$	Magnesium Sulfate
$CaCl_2$	Calcium Chloride
IL-1	Interleukin 1
IL-1β	Interleukin 1 beta
IL-6	Interleukin 6
IL-10	Interleukin 10
IL-17A	Interleukin 17A
IL-21	Interleukin 21
IL-22	Interleukin 22
IFNγ	Interferon-γ
TNFα	Tumor necrosis factor-α
NFκB	Nuclear Factor kaapa-light-chain-enhancer of activated B cells
iNOS	Inducible Nitric Oxide Synthase
FOXO	Forehead Box O
CD36	Cluster of Differentiation 36 (Platelet glycoprotein 4)
Mogat1	Monoacylglycerol O-acyltransferase 1
MTTP	Microsomal Triglyceride Transfer Protein
NPC1L1	Niemann-Pickk C1-Like 1
LIPE	Lipase E
DGAT1	Diacylglycerol O-acyltransferase 1
DGAT2	Diacylglycerol O-acyltransferase 2

FABP1	Fatty-Acid-Binding Protein 1
FABP4	Fatty-Acid-Binding Protein 4
UCP1	Uncoupling Protein 1
CIDEA	Cell-death Inducing DFFA like Effector A
PRDM16	PR domain containing 16
PPARα	Peroxisome Proliferator-Activated Receptor alpha
PPARγ	Peroxisome Proliferator-Activated Receptor gamma
PGC-1	Peroxisome proliferator-activated receptor gamma coactivator 1
Dio2	Iodothyronine deiodinase 2
EBF2	EBF transcription factor 2
FGF21	Fibroblast Growth Factor 21
BMP7	Bone Morphogenetic Protein 7
LXR	Liver X Receptors
SIRT1	Sirtuin 1
COX8b	Cytochrome c oxidase subunit 8b
ASK1	Apoptosis Signal-regulating Kinase 1
SENP2	SUMO specific peptidase 2
TGF-β	Transforming Growth Factor beta
HMGS	Mitochondrial Hydroxymethylglutaryl-CoA Synthase
CPT	Carnitine Palmitoyl Transferas

Chapter 1: Introduction

1.1. Obesity

According to the World Health Organization (WHO), by 2016, more than 1.9 billion adults aged 18 years and older were designated as being overweight. Among these, over 650 million were classified as overly obese (Winer et al., 2016). In the United States, obesity prevalence is even higher. According to the Centers for Disease Control and Prevention (CDC), 41.9% of the population in the United States was identified as obese between 2017 and 2020 (Patel et al., 2013). Being obese predisposes one to different non-communicable diseases, including insulin resistance and type 2 diabetes mellitus. The worldwide surge in the prevalence of obesity and its corresponding increase in associated comorbidities is a crucial cause of concern. Prevention strategies focusing on modification of diet to modulate energy intake and increasing levels of physical activities are beneficial, cost-effective, and safe. However, changes in lifestyle to modify dietary intake and activity level are difficult to sustain in the long term (Mokdad et al., 2003; Portero McLellan et al., 2014). Although the etiology of obesity or fat accumulation is linked to a long-term energy imbalance between energy intake and expenditure, the molecular mechanisms involved are sophisticated and involve several tissues, organs, and the gut microbiota and its metabolites (Gérard, 2016).

1.2. Gut Microbiota

Trillions of microbes, including bacteria, viruses, fungi, and protozoa, inhabit the human gastrointestinal (GI) tract (García-Montero et al., 2021; Greer et al., 2016). The bacteria from over 800 species are mostly non-pathogenic and contribute to the host metabolism and health (Carding et al., 2015). The intestinal microbiota composition varies highly amongst individuals

based on genetic differences and environmental factors, such as dietary behaviors and social environment (Turnbaugh et al., 2008). Diet-induced obesity has been linked to alternations in gut microbiota composition and diversity, which in turn, leads to perturbations in the metabolic activities of the microbes in the GI tract (David et al., 2014; Turnbaugh et al., 2008). Consequently, while the host influences the composition of the intestinal microbiota, the gut microbiota influences the obesity phenotype as well. Research with rodent models of obesity and diabetes has consistently shown that gut bacteria communicate with the host either through direct contact with the intestinal cells or indirectly via its bacterial metabolites, impacting the host cellular homeostasis, inflammatory mechanisms, and subsequently the obesity phenotype (Carding et al., 2015).

1.3. Dysbiosis and its Links to Obesity

Several mechanisms related to energy metabolism and gut microbiota have been proposed. A large volume of data associated with the composition and functional potential of the gut microbiota showed that the microbiota of healthy individuals confers health benefits relating to pathogen protection, nutrition, host metabolism, and immune modulation. In addition, the data showed that the number of diseases that have been linked with alternations in the gut microbial community (dysbiosis) has expanded. Gut bacteria impact digestion, metabolizing phytochemical components of food into forms that are absorbed and ultimately impact other tissues.

Although several studies have identified particular bacterial species associated with healthy gut microbiota in both human and rodent models, there is no clear definition of what constitutes a ‘healthy’ microbiota. Dysbiosis or microbial imbalance is the perturbation in the gut

microbiota that is associated with the development of diseases, including obesity (Carding et al., 2015). Dysbiosis can occur due to poor diet, toxins, drugs, e.g. antibiotics, or invasion of pathogens, thus contributing to chronic conditions (Carding et al., 2015). Differences in the gut microbiota composition between individuals may impact energy balance: intake vs expenditure. Individuals predisposed to obesity may harbor a dysbiotic gut containing bacterial species that more efficiently extract energy and thus promote energy storage from a given diet, compared with the bacterial species in leaner individuals (Ley et al., 2005). Bacteria that enhance extra calorie harvest from host indigestible complex carbohydrates produce excessive short-chain fatty acids (SCFA) that are eventually stored as fat. Dysbiosis is associated with increased gut permeability, inflammation, and insulin resistance. An obesity-associated microbiota produces metabolites that promote the storage of triglycerides in adipocytes by suppressing intestinal and adipose tissue expression of fasting-induced adipocyte factor (FIAF/ANGPTL4) (Mandard et al., 2006). The protein FIAF is a circulating lipoprotein lipase inhibitor and also regulates energy expenditure via modulation of AMP-activated protein kinase (AMPK) activity which ultimately impacts fatty acid oxidation (Mandard et al., 2006).

It has also been shown that dysbiosis arising from diet or disease disrupts the amount and composition of bile acids secreted in the GI tract. Activation of bile acid receptors and overall dysregulation of intestinal bile acid homeostasis may precipitate into gastrointestinal or metabolic disease (Sagar et al., 2015).

Dysbiosis results in an increase in the proportions of bacterial species (gram-negative species) that produce the endotoxin lipopolysaccharide (LPS), which translocated from the lumen into the circulation. Once bound to the receptors toll-like receptor 4 (TLR4), even low-level exposure of the cells to LPS can initiate a well-characterized signaling cascade involving

many pro-inflammatory pathways, leading to chronic disease conditions, including obesity (Boutagy et al., 2016). Further evidence that rodents injected with low levels of bacterial LPS every day for four weeks develop obesity despite consuming a normal diet reinforces the fact that LPS induces fat accumulation (Cani et al., 2007).

1.4. Gut Immune System Links to Obesity

About 70–80% of immune cells are located beneath the mucosal layer and epithelial layer of the small and large intestines (Wiertsema et al., 2021). The microbiota and intestinal immune system are linked by T cells and secretory immunoglobulin (sIgA), produced by B cells in the lamina propria (LP). T cells promote B cell-secreting antibodies, especially regulatory T cells. Changes in the number of IgA-producing cells, sIgA levels, and the phenotype of Tregs are associated with dysregulated immune homeostasis and obesity phenotype (Kubinak et al., 2015; Luck et al., 2019). Obesity-induced reductions in sIgA levels have been shown to worsening insulin sensitivity, reduced gut barrier integrity to enhance microbiota encroachment, and increased inflammation in metabolic tissues (Kim et al., 2016). Foods may act as foreign antigens in the intestines and/or change the gut microbiota composition to produce bacterial antigens, resulting in corresponding immune activities (Kim et al., 2016). Thus, host dietary intake, digested compounds, and bacterial metabolites can modulate the phenotype of intestinal immune cells and, hence cytokines releases.

1.5. Functional Foods in Obesity and Gut Microbiota Health

Since prevention or treatment of obesity based on the modification of dietary intake and physical activity levels is challenging to sustain in the long term, more recent research has targeted the

molecular mechanism involved. The usage of pharmaceuticals in this regard has untoward side effects. Alternatively, the consumption of natural products from plants and/or functional foods harbors beneficial and safer prevention of obesity. Functional foods such as whole fruits and vegetables or fortified supplements can be consumed as part of a regular diet but beyond fundamental nutrition benefits. Additional functions in health promotion or disease prevention are associated with compounds that target particular metabolic molecular pathways.

Diet or obesity-induced gut dysbiosis can be manipulated by specific functional food components or prebiotics which promote the proliferation of beneficial bacteria taxa through direct contact with host cells or indirectly via their metabolites. Specific functional foods or prebiotic vegetables have been shown promotion in gut microbiota health and diversity, including chicory, garlic, Jerusalem artichokes, and stinging nettles (genus *Urtica*).

1.6. Stinging Nettle (*Urtica dioica*)

Nettles grown in Europe, North America, Asia, and North Africa (Devkota et al., 2022), are used as food in several cultures worldwide, and have been widely studied and used as an intervention for several medical conditions for years. Shoots harvested before flowering are used as a spinach alternative (Orčić et al., 2014a; Upton, 2013b). Of the 25 species of plants within the genus *Urtica*, the perennial *Urtica dioica* is the species commonly found in North America. *U. dioica* grows very easily and widely all over North America, and seeds are available from several reputable vendors, e.g., Baker Creek Heirloom Seed Company (Mansfield, MO).

1.6.1. Preliminary Data on Stinging Nettle (*U. dioica*)

The extract of *U. dioica* has been widely studied for decades for intervention against several diseases, but the molecular mechanisms involved are unclear and ill-defined. The extract or whole food exerts pleiotropic effects in several metabolic organs. It has been previously shown that the water/ethanol extract of *U. dioica* prevents high-fat diet-induced insulin resistance and promotes glucose homeostasis (Obanda, et al., 2016a; Obanda, et al., 2016b). Since obesity and insulin resistance are associated with gut microbiota health, composition, and function, we hypothesize that the beneficial effects of *U. dioica* are linked to its impact as a whole vegetable as well through its phytochemical compounds acting on the gut microbiota and immune system.

1.7. Justification and Rationale

Although *U. dioica* grows abundantly all-over North America and dietary supplements are freely available, little is known about the efficacy and mechanistic pathways targeted in the medical conditions for which it is marketed. While the beneficial effects of *U. dioica* have been studied, not much has been done to elucidate mechanisms that cause the positive systemic effects exerted. In the search for anti-obesity agents, the use of functional foods and/or nutraceuticals is a safe, alternative, and achievable strategy. Obesity predisposes one to insulin resistance and the association between obesity and insulin resistance has been established as a cause-and-effect relationship. Almost 40–50% of individuals with insulin resistance, which is the hallmark of pre-diabetes, progress to T2DM over their lifetime. Timely intervention against obesity-associated insulin resistance prevents or delays the onset of overt T2DM. Attenuating or reversing insulin resistance prevents progression to T2DM. Conventional medications for obesity and insulin resistance include the lipase inhibitor Orlistat and thiazolidinediones respectively. While the

former is modest in efficacy and must be used together with a lower-calorie diet, the latter has been largely withdrawn due to its adverse side effects. There remains a critical need to identify therapeutic agents from abundant natural resources that are effective in preventing or attenuating obesity and restoring insulin sensitivity and ultimately maintaining glucose homeostasis. Plant-based foods that address mechanisms involved in the etiology of excessive fat accumulation and insulin resistance serve as an attractive complementary and alternative approach instead of drugs. However, the lack of knowledge on the reliability, safety, and mechanisms of action contributes to skepticism about their efficacy. Diet interventions may dominate over host genetics to influence the incidence and development of metabolic diseases which in part, is due to the modulations of gut microbial communities and metabolism.

Obesity-induced dysbiosis can be attenuated by manipulating the gut microbiota to the targeted proliferation of beneficial bacterial taxa. These taxa directly impact communication with the host intestinal cells or indirectly via bacterial metabolites. The development of therapies that modulate the gut microbiota has critical implications for public health because of the links between the microbiota and metabolic disorders. The role of *U. dioica* on the composition and function of gut microbiota has not yet been studied. It is likely that components of *U. dioica* impact fat accumulation and insulin resistance through impacts on the gut microbiota composition and function and through impacts on the immune responses in the gut.

This research is significant because developing interventions that can maintain the gut microbiota health, attenuate obesity, and preserve insulin sensitivity, despite living in an obesogenic environment has critical implications for public health. It has the potential to limit the cost of treating chronic diseases such as full-blown T2DM and overall improve quality of life in the long term. This work provides justification and significance for clinical efficacy trials

toward the development of safe natural and cost-effective solutions to promote health. It also yields data supporting new functional food approaches, incorporating functional foods into regular diets for optimal health options and disease prevention.

1.7.1. Objective

The overall goal of this study was to elucidate the mechanisms by which the vegetable *U. dioica* attenuates diet-induced fat accumulation and prevents insulin resistance. We hypothesize that phytochemicals from *U. dioica* get into the systemic circulation to reach targeted tissues such as adipose tissue, liver, and skeletal muscle but also impact obesity and insulin resistance through pathways involving the gut microbiota composition and function and ultimately the gut immune system.

Chapter 2: Literature Review

2.1. Obesity

The prevalence of obese and overweight individuals has been substantially increasing worldwide in the last 30 years. Epidemiological studies show that this high incidence of obesity is attributed to several factors which include the type of diet, energy expenditure, early life influences, sleep deprivation, disruption of the hormone system, chronic inflammation, and the gut microbiome (Sun et al., 2018). The concern about health risks associated with rising obesity is universal. Comorbidities of obesity include insulin resistance, type 2 diabetes (T2DM), high blood pressure, cardiovascular disease, atherosclerosis, stroke, non-alcoholic liver disease, arthritis, certain types of cancer, sleep disorders, and some immune-related disorders (Gérard, 2016; Patel et al., 2013; Winer et al., 2016).

2.2. Links between Obesity, Gut Microbiome Composition and Function

While direct causality has not been proven, data from various research groups support the fact that a strong relationship exists between the gut microbiota composition, its metabolic activity (e.g., metabolite production), and host metabolism. Thus, the activity of the gut bacteria may influence health and the risk of developing diseases like obesity. Evidence of a causal role of intestinal microbiota in obesity mostly originates from animal studies. Germ-free (GF) mice are resistant to HF diet-induced obesity despite a higher food intake (Turnbaugh et al., 2008). Furthermore, colonization of GF mice with fecal contents from obese persons (obese microbiota) resulted in a significantly greater increase in total body fat than colonization with fecal contents from lean persons (lean microbiota) (Ridaura et al., 2013). Similarly, reducing the abundance of

intestinal microbes by administering antibiotics partially protects mice against diet-induced obesity and related metabolic disorders (Muccioli et al., 2010)

Although obesity results from long-term energy imbalances between energy intake and expenditure, gut microbiota composition and function have been shown to influence energy balance through several mechanisms. The microbiota impacts the host obesity phenotype through direct contact with the local tissues: intestinal cells. However, via bacterial metabolites, the gut microbiota has indirect effects beyond local tissues, with adipose tissues considered a primary target. Other tissues affected indirectly in host cellular mechanisms include the brain, liver, and skeletal muscle. Besides synthesizing metabolites, the gut microbiota influences the synthesis (in the host tissues) of host hormones, enzymes, cytokines, neurotransmitters, nitric oxide, and hydrogen sulfide. These all impact host physiology and health.

Variation in the bacterial species that comprise the gut microbiota plays an important role in the pathogenesis of obesity. The composition of gut microbiota in obese individuals differs from that in lean individuals, although inconsistent changes have been reported. Persons exhibiting higher adiposity, insulin resistance, and dyslipidemia harbor a microbiota with low bacterial diversity and richness. On the other hand, lean individuals have a microbiota that is richer and more diverse in the bacterial species (Le Chatelier et al., 2013)

The data linking specific taxa of bacteria to the obese or lean phenotypes is inconsistent. However, multiple lines of evidence link dysbiosis to obesity. The gut microbiota impacts local and distant organs and contributes to obesity development and progression through different mechanisms. Several mechanisms have been highlighted and demonstrate that the gut microbiota communicates with host organs through several pathways. Metabolites produced by the degradation of nutrients or host products (e.g., SCFAs, neurotransmitters like serotonin, bile

acids, bioactive lipids) and the production of specific hormones stimulated by the action of such metabolites on key receptors and specific nervous routes have been described.

Two previous studies have shown that the abundance of bacteria from class Clostridia (phylum Firmicutes) and specifically genus *Clostridium* is associated with a lean phenotype. Outbred Sprague-Dawley CD rats that have a higher abundance of *Clostridium* remain lean, while those with a relatively lower abundance of *Clostridium* will rapidly gain weight when placed on a high-fat diet (Obanda et al., 2020 and 2021). Recent literature comparing the gut microbiota of people in western industrialized countries where obesity is rampant and hunter-gatherer groups in which there are no obesity issues have shown that the lower abundance of certain members of phylum Firmicutes in non-western populations may play a role in obesity prevalence (Rampelli et al., 2015). A similar observation has been shown in studies of paleofeces (1000-2000 years old). These feces obtained in caves came from an era when obesity was nonexistent and show the prominence of phylum Firmicutes before obesity became a problem. Over the years, there has been a reduction in Firmicutes and an increase in Bacteroidetes as the major phylum in the gut microbiota of western populations (Wiertsema et al., 2021). However, variations in specific bacterial genera or species rather than phylum-level differences may be more important.

2.2.1. Impacts of Gut Microbiota on Local Tissues

In local tissues, the obesity-associated gut microbiota has an increased capacity to harvest energy from the diet. Undigested carbohydrates and dietary fibers are substrates of the gut microbes and the fermentation products; short-chain fatty acids (SCFAs) provide an extra 10% of the daily energy (Lee et al., 2020). However, excessive fermentation by some species can produce

excessive SCFAs, which may increase energy harvest, reverse positive metabolic effects, and result in increased gut permeability and inflammatory activities. Besides SCFAs, gut bacteria or their metabolites stimulate gene reprogramming in the colon, change polypeptide hormones and other bioactive molecules released by intestinal enteroendocrine cells, decrease the intestinal barrier, and change immune homeostasis. By impacting the secretion of bioactive molecules released by intestinal host cells, the microbiota impacts the uptake of fatty acids by enterocytes and the transport of fatty acids and monoglycerides to intracellular sites for triacylglycerol biosynthesis.

Knowledge of the role of specific bacterial species in the causation of the obese phenotype or resistance to becoming obese is minimal. However, it has been shown that some genera among Firmicutes, particularly *Clostridium* impact host obesity phenotype by increasing IgA secretion by immune cells (B cells) in the intestine and reducing host lipid absorption through modulation of the protein involved in the transport and absorption of fat in the small intestines e.g. of the expression of CD36 (Petersen et al., 2019). The gut microbiota also has direct effects beyond the gastrointestinal tract, notably on organs that are interdependent on the levels of glycemia including the brain, liver, adipose tissue, and skeletal muscle (Gizard et al., 2020).

2.2.2. Impacts of Gut Microbiota on Adipose Tissues

The gut microbes communicate with host adipose tissue through metabolites. Fasting-induced adiposity factor (FIAF; also known as angiopoietin-like protein 4), is a circulating lipoprotein lipase inhibitor whose expression is normally suppressed in the gut epithelium by the microbiota (Bäckhed et al., 2007). FIAF plays a central role in triglyceride metabolism by inhibiting

lipoprotein lipase (LPL) production in adipose tissue and modulating fatty acid oxidation in skeletal muscle. Some specific bacterial species may suppress FIAF in the intestinal epithelia and potentially stimulate host weight gain by impairing triglyceride metabolism and promoting fat storage.

Under obese conditions, circulating levels of fatty acids increase and activate TLR4 signaling in adipocytes and macrophages (Lee et al., 2003). TLR4 is the receptor for LPS, the metabolite produced by gram-negative bacteria. Increased circulating LPS (endotoxemia) initiates a well-characterized signaling cascade that elicits many pro-and anti-inflammatory pathways when bound to TLR4. Furthermore, infusion of LPS in mice induces fat accumulation (Cani et al., 2007). Thus, the abundance of LPS-producing bacteria from phylum Bacteroidetes and Proteobacteria as is the case in western populations as a result of diet may precipitate in obesity through increased endotoxemia. A HF diet and dysbiosis that cause increased LPS levels compromise the gut-intestinal barrier. LPS increases tight junction permeability by increasing TLR4 expression. A healthy microbiota is ensured by a diverse microbiome with activities contributing to immune and metabolic homeostasis, notably through reinforcing the intestinal barrier to attenuate fat accumulation and inflammation (Rastelli et al., 2019).

2.2.3. Impacts of Gut Microbiota on Skeletal Muscle

Skeletal muscle responds and changes quickly in response to environmental factors such as exercise and nutrition. Being the major site of insulin-stimulated glucose uptake and fatty acid oxidation, skeletal muscle plays a key role in metabolism and is one of the dominant metabolic organs in the body (Kelley et al., 1999; Lahiri et al., 2019). A reduction in skeletal muscle mass and function results in metabolic disorders and sarcopenia, underscoring the role of skeletal

muscle in the maintenance of health. Compared to mice that have a gut microbiota, germ-free mice lacking a gut microbiota display reduced skeletal muscle weight, and atrophy and have decreased expression of insulin-like growth factor 1, and transcription genes involved in skeletal muscle growth and mitochondrial function and key metabolites. Transplanting germ-free mice with the gut microbiota of conventional mice restores muscle mass and function; restoring key metabolites like amino acids glycine and alanine improves the oxidative metabolic capacity of the muscle and elevates the expression of neuromuscular junction assembly genes.

Interactions between the host and its gut microbiota are mediated by diverse metabolites including SCFAs generated from the bacterial fermentation of soluble dietary polysaccharides. The diverse biosynthetic activity of the gut microbiota beyond SCFAs ensures its impacts on multiple host converging pathways to regulate host muscle function. Some other gut microbiota byproducts, such as phenolic products, secondary bile acids, and conjugated linoleic acid, can impact skeletal muscle glucose homeostasis, energy expenditure, protein synthesis, and physical performance (Gizard et al., 2020).

Because skeletal muscle cells express the LPS receptor TLR4, elevations in plasma LPS concentrations found in obese and T2DM subjects could play a role in the pathogenesis of insulin resistance. Antagonists of TLR4 or TLR4 deficiency may improve insulin action in these individuals (Cani et al., 2007; Lee et al., 2003). Other specific bacterially produced metabolites that influence skeletal muscle growth and function are not yet elucidated. Skeletal muscle expresses receptors for inflammatory cytokines that are released by the adipose tissues, such as TNF-α and IL-6. Similar to adipose tissue, skeletal muscle also produces low-grade inflammatory cytokines that can dampen insulin sensitivity (Bleau et al., 2015).

2.2.4. Impacts of Gut Microbiota on Liver

The intestinal microbiota and bacterial products can, directly and indirectly, affect the liver through various mechanisms. The liver and gut microbiome closely interact because the liver receives 75% of its blood supply from the intestines via the portal vein and the liver releases bile acids into the intestines (Tripathi et al., 2018). As a result, the gut microbiota may contribute to liver function or liver diseases through several mechanisms that can be influenced by bacterial composition, bacterial metabolism of bile acids, dietary components, and bacterial metabolites of dietary components such as SCFAs and choline. The gut microbiota influences the size and composition of the bile acid pool through the conversion of primary bile acids to secondary bile acids (BAs). Bile acids are directly associated with intestinal mucosal integrity and the synthesis of antibacterial peptides by epithelial cells. When BAs bind to the farnesoid X receptor (FXR), it stimulates the production of antimicrobial peptides, such as angiogenin 1. These peptides prevent the encroachment of bacteria through the mucus and epithelial layer and thus improve gut-barrier function (Parséus et al., 2017). In addition, bile acids also function as signaling molecules to influence physiological processes which include the regulation of glucose and lipids metabolism through FXR activation and binding of G-protein-coupled bile acid receptor 1.

Increased LPS levels compromise gut barrier integrity. Through the portal vein, LPS gets to the liver where it induces hepatic inflammation and hepatic injury. Other bacterial products and metabolites translocate through the intestinal barrier into the portal system, and then the liver. Translocation of LPS increases TLR4 expression, which activates the pro-inflammatory cytokines (TNF-α and IL-6), thus trigger systemic inflammation. Inflammasomes, which are proteins made up of leucine-rich repeat-containing units and nucleotide-binding domains, govern the cleavage of pro-inflammatory cytokines.

Bacterial fragments and products can also recruit and activate hepatic immune cells, further contributing to liver disease progression (Arrese et al., 2016). Kupffer cells of the liver, are critical components of the innate immune system in the liver. Kupffer cells can be activated by various endogenous and exogenous stimuli, including LPS. Activation of Kupffer cells triggers the production of inflammatory cytokines (TNF-α and IL-6) and reactive oxygen species (ROS), which can produce tissue damage in the liver (Baffy, 2009). Microbiota-derived antigens also influence the composition and activation of hepatic natural killer cells, impacting hepatic function (Baffy, 2009), ultimately impacting glucose metabolism and fat accumulation in the liver and pathogenesis of liver diseases.

2.2.5. Impacts of Gut Microbiota on Brain and Appetite

Abnormal regulation of appetite can cause eating disorders and obesity. The gut microbiota and appetite system are highly associated. Recent research exploring the gut-microbiota-brain axis suggests that the gut microbiota can act as an effective regulator of host body weight. The gut microbiota and its metabolites and components impact appetite regulation via modulating hormone secretion, neural signals, and immune system function (Han et al., 2021). Gut microbial metabolites stimulate enteroendocrine cells to release the appetite-related/anorexigenic hormones (PYY, GLP-1, and CCK) and neurotransmitter (5-HT) and promote the secretion of peripheral hormones (leptin, ghrelin, and insulin). All these have an impact on feelings of satiety during food intake and, thus amounts of food ingested and appetite (Han et al., 2021; Noble et al., 2018). Bacterial metabolites include SCFAs, amino acids, branched-chain amino acids (BCAAs), organic acids, fatty acids, succinate, and bacterial proteins.

SCFAs can activate ghrelin-related signaling and inhibit insulin secretion by activating free fatty acid receptor 3 (FFAR3, GPR41) in islets. They can inhibit appetite by binding to the free fatty acid receptor 2 (FFAR2, GPR43), which further activates the release of GLP-1, PYY, insulin, and leptin to signal to the appetite system (Li et al., 2018). Microbial metabolites derived from amino acids e.g., tryptamine from tryptophan, affect the production and secretion of 5-HT, which is a neurotransmitter that conveys signals from the gut to the brain and mediates appetite control. Glutamine can be metabolized by gut microbiota to produce Gamma-aminobutyric acid (GABA), a neurotransmitter that regulates the secretion of appetite-related hormones and intestinal motility. Gut microbiota is involved in the biosynthesis and transport of BCAAs. An imbalance in amounts of BCAAs can influence the 5-HT production in the hypothalamus. Modulating gut microbial composition using dietary interventions, probiotics, prebiotics, can specifically and precisely change the microbial metabolites and thus appetite and satiety and hence obesity mechanisms.

2.3. Obesity Links to Insulin Resistance

Obesity is the most important identified factor contributing to insulin resistance. Systemic insulin resistance measured as decreased glucose disposal rate in response to a specific level of insulin results from impaired insulin action in metabolically active organs and tissue, including skeletal muscle, liver, and adipose tissue (Hardy et al., 2012).

Visceral fat accumulation results in insulin resistance because visceral fat itself is inherently diabetogenic; it secretes adipokines that impair insulin sensitivity in the liver and muscle. The adipokines thus increase upon expansion of fat depot. Secondly, excess lipid accumulation causes the accumulation of macrophages and other immune cells that release

inflammatory cytokines (TNF-α and IL-6) and chemokines, which can impair insulin sensitivity. Thirdly, adipose tissue lipolysis results in lipotoxicity (from excess circulating FFAs) all contributing to systemic insulin resistance (Hardy et al., 2012). Lipotoxicity products include ceramides and by-products of incomplete fatty acid oxidation, which induce insulin resistance. Despite being highly evolved to sequester or store fat, the storage capacity of single adipocytes is finite. After a HF diet, enlarged adipocytes due to excessive fat accumulation display insulin resistance without much immune cell infiltration into adipose tissue (Lee et al., 2011).

2.4. Obesity Links to Gut Immune System

The intestinal immune system is an important contributor to obesity and obesity-related insulin resistance. Similar to other metabolic organs, like visceral adipose tissue (VAT) and the liver, altered immune homeostasis has also been observed in the small and large intestines during obesity.

During diet-induced obesity, many subsets of adaptive immune cells within the gut adopt a pro-inflammatory phenotype. This is demonstrated by T cells producing pro-inflammatory cytokines, such as IFN-γ. This shift is accompanied by a reduction in proportions of regulatory T cells (Tregs) and innate lymphoid cells (ILCs) and T-helper type 17 (Th17) T cells, which produce IL-22 that helps maintain intestinal homeostasis (Luck et al., 2015). During high fat diet feeding and obesity, a significant shift occurs in the microbial populations and ultimately the intestinal immune system. This shift reduces the proportions and numbers of retinoid orphan receptor gamma t, (RORγt^{+}) Th17 and Treg and increases IFN-γ-producing Th1 cells. Consistently, Tregs are decreased in the small intestine and colon of obese patients compared with lean control human subjects (Luck et al., 2015). Immune cells express receptors for gut

bacterial metabolites such as SCFAs. Signals from SCFAs, stimulate G-protein receptor (GPR), which is generally expressed in gut immune cells. Among them, GPR43 on Treg cells and GPR109 on dendritic cells are important for gut homeostasis.

Another link between the gut microbiota and the intestinal immune system is the immune-derived molecule immunoglobulin A (IgA), a B-cell antibody primarily produced by plasma cells in the gut lamina propria. Production of IgA is influenced by dendritic cells and pathogen-sensing pathways, such as toll-like receptor 2. Together with antimicrobial peptides, mucus, and host defense molecules, IgA is essential for maintaining gut homeostasis through the protection of the mucosal surface from pathogens while tolerating commensal bacteria (Gutzeit et al., 2014). IgA regulates metabolic disease. IgA levels are reduced during obesity and the loss of IgA worsens insulin resistance and increases intestinal permeability, microbiota encroachment, and downstream inflammation in metabolic tissues. The number of IgA-producing cells is reduced within the intestinal immune system of high-fat diet-fed mice. Commonly used therapies for diabetes such as metformin and bariatric surgery can alter cellular and stool IgA levels (Luck et al., 2019).

Young T-*Myd88*$^{-/-}$ mice (the T cells have disabled Myd88 signaling) exhibit reduced follicular cell responses and defective IgA targeting of their gut bacteria, thus altering the composition of the microbiota. Despite eating a normal mouse diet, these mice show hallmarks of metabolic syndrome with age; they gain more weight, accumulate more fat, and show greater insulin resistance compared with control wild type mice. Petersen et al. (2019) showed that the composition of the microbiota in these mice was driven by defective T follicular helper cell (Tfh cells) responses and that IgA in these mice inappropriately targets bacteria from class Clostridia but allows for the expansion of *Desulfovibrio*. Clostridia suppress host lipid absorption by

modulating CD36 expression while *Desulfovibrio* enhances it, thus contributing to increased energy harvest and fat accumulation. T-*Myd88*$^{-/-}$ mice absorbed more long-chain fatty acids, suggesting that the microbiota regulates lipid absorption. Clostridia-colonized germ-free animals have down-regulated CD36, a receptor that mediates the binding to and uptake of fatty acids down-regulated, whereas the addition of *Desulfovibrio* up-regulated the expression of this receptor and thus enhanced fat absorption. In summary, immune control of the microbiota can maintain beneficial microbial populations that impact lipid metabolism, thus preventing obesity and insulin resistance.

2.5. Obesity Links to Browning of White Adipose Tissues

Adipose tissue is considered an endocrine organ. It secretes either adipokines or regulating cytokines, which play vital roles in health and maintaining host homeostasis. White adipose tissue and brown adipose tissues are two distant types of adipose tissues with functional and morphological differences. These two types of adipose tissue can interchange through white adipose tissue browning, the process of non-shivering thermogenesis. The process involves in upregulation UCP1 gene expression, which uncouples respiratory chain to produce heat out of the host. During browning process, thermogenic genes upregulated included PPARα, PPARγ, PRDM16, PGC-1α, CIDEA, DIO2 and UCP1 (Machado et al., 2022).

2.6. Functional Foods in Modulation of Obesity, Gut Microbiota Health and Immune Function

Modulation of the gut microbiome through dietary intervention is a potential intervention for obesity. Although an individual's microbiome composition is partially established early in life, it

is susceptible to change. Dietary factors are a key determinant of host-microbiome diversity and structure. Data suggests that up to 57–60% of the gut microbial composition is explained by diet alone, while genetic variation accounts for only 12% (Zhang et al., 2010). In addition, the effects of the dietary intervention are rapid and dramatic and restructure the gut microbiota within as little as 24 hours (David et al., 2014). Thus, using dietary interventions to improve the integrity of the gut microbiome and potentially reverse dysbiosis states associated with pathological metabolic states offers an effective and minimally invasive means of combatting obesity and its associated comorbidities. Diet-induced dysbiosis can be prevented or attenuated by manipulation of the microbiota to target the optimum growth of bacterial species that through direct contact with host cells or indirectly via bacterial metabolites influence metabolic functions.

A high-fat, obesogenic western diet significantly reduces bacterial diversity and richness in the GI tract of mice. This effect is readily reversible upon reverting back to a normal chow diet. However, the deleterious effect of western diets or an HF diet in rodents has been demonstrated to be compounding in nature. Persistent microbial signatures during repeated cycles of HF diet lead to enhanced metabolic derangements and accelerated weight gain (David et al., 2014; Sonnenburg et al., 2016). Such sustained diet-driven changes in the microbiota may span further than an individual's lifetime and induce the extinction of some commensal bacterial strains across generations. Restoration of diversity and reemergence of specific lost microbes in this context cannot be achieved by diet switching but can be attained by fecal microbial transplant (FMT) (Sonnenburg et al., 2016).

Prebiotic fibers serve as metabolic substrates for intestinal bacteria which convert them via fermentation into SCFAs and other metabolites. Prebiotic vegetables which promote microbiota health and diversity include asparagus, garlic, leeks, onions, bananas, Jerusalem

artichoke, chicory, wheat bran, barley (Florowska et al., 2016) and nettles (genus *Urtica*). Numerous experimental studies have demonstrated the benefits of prebiotics in combatting obesity and metabolic abnormalities through various mechanisms of action. Specifically, the prebiotic-induced proliferation of beneficial commensal microbial strains positively alters the structure of the gut mucosa, leading to decreased translocation of bacterial endotoxin (LPS) and attenuating activation of TLRs at the luminal surface (Langlands et al., 2004). This prebiotic effect may be further enhanced by increasing the production of intestinal hormones such as glucagon-like peptide 2 (GLP2), which is known to reinforce gut barrier function through the upregulation of critical tight junction proteins in the epithelium (Langlands et al., 2004). Besides altering the expression of metabolic genes that regulate lipid homeostasis, prebiotic fermentation and bacterial metabolism products promote enteroendocrine L-cell differentiation and increase both luminal and plasma levels of intestinal hormones PYY and GLP1, which increases satiety and hence reduces energy intake. Metabolic genes that are altered include those involved in adipocyte differentiation, energy expenditure, and lipogenesis.

Changes to the gut microbiota ultimately also impact the gut immune system. Foods and components of foods act as antigens in the intestines and/or change gut microbiota composition to produce bacterial antigens that impact immune cells (Kim et al., 2016). Gut bacteria also metabolize phytochemical components of food into forms that are absorbed and ultimately impact immune cells and other tissues (Kim et al., 2016). Both microbial and dietary antigens are essential for the normal development of the mucosal immune system. Intestinal Treg cells and B cells are controlled by specific signals from the local environment which is comprised of dietary ingredients and bacterial metabolites. Dietary or prebiotic changes in IgA-producing cells, sIgA levels, and T cells will impact immune homeostasis and diet-induced obesity, insulin resistance,

intestinal permeability, microbiota encroachment, and inflammation in metabolic tissues (Luck et al., 2019).

Being a polygenic disease, the etiology of obesity is multi-factorial and very complex. However, recent research strongly implicates gut dysbiosis as a key contributor to its development and associated metabolic abnormalities. Therefore, modulation of the gut microbiome to restore balance is an area of research with great interest. Even though there is no precisely defined mechanism of action, current research clearly supports the efficacy of prebiotic foods or functional foods in alleviating obesity-associated and microbiome linked perturbations to glucose metabolism and lipid metabolism, and homeostasis.

2.7. Stinging Nettle (*Urtica dioica*)

Though they are considered weeds and are rarely a cultivated crop, nettle (genus *Urtica*) grows easily and is widespread throughout Europe, North America, Africa, and parts of Asia. Nettles are used as food and as traditional medicine in several international cultures over many years and have been widely studied as an intervention for several medical conditions. Of the 25 species within the genus, *Urtica dioica* (*U. dioica*), or stinging nettle is the species commonly found in North America. The shoots are harvested before flowering for use as a vegetable (spinach alternative) (Orčić et al., 2014; Upton, 2013).

The benefits of *U. dioica* are attributed to the rich phytochemical component (polyphenols), high protein content, a high percentage of linoleic and linolenic acids in the lipid fraction, and high soluble and insoluble fiber. The soluble and insoluble fiber may contribute to beneficial effects through the action of the gut microbiota. The shoot also contains several phytochemicals and micronutrients which include carotenoids, lutein, fatty acids, essential amino

acids, vitamins, polysaccharides, and polyphenols: phenolic acids; p-hydroxybenzoic acid, gentisic acid, protocatechuic acid, vanillic acid, quinic acid, ferulic acid, p-coumaric acid, caffeic acid and, 5-Ocaffeolylquinic acid (Kregiel et al., 2018). The second large group of compounds are flavanols which include kaempferol, kaempferol 3-O-glucoside, quercitrin, quercetin 3-O-glucoside, quercetin 3-O-rutinoside (rutin), and isorhamnetin. Others are the bioflavonoids amentoflavone and the catechin a flavan-3-ol. *U. dioica* is richer in polyphenols than cranberry juice, dandelion, and most other vegetable (Orčić et al., 2014; Upton, 2013). Nettles possess antimicrobial compounds, such as miconazole nitrate, amoxicillin-clavulanic acid, ofloxacin, and netilmicin.

Nettles have been used as medicinal plants for many diseases or medical conditions. These include bladder disorders to reduce blood in the urine (Kregiel et al., 2018), autoimmune diseases, such as rheumatoid arthritis, through their anti-inflammatory activities (Upton, 2013), and joint pain because of osteoarthritis. More recently, nettles have been shown to possess anti-diabetic properties, and the safety of aqueous extracts was studied *in vitro* and *in vivo* models (Kregiel et al., 2018).

In this study, we investigate the impact of *U. dioica* on the gut microbiota composition and function, its role in intestinal immune cells and function, and how these may ultimately impact obesity and insulin resistance.

2.7.1. Preliminary Data on Stinging Nettle (*U. dioica*)

The extract of *U. dioica* has been widely studied for decades for intervention against several diseases, but the molecular mechanisms involved are unclear and ill-defined. The extract or whole food exerts pleiotropic effects in several metabolic organs, thus suggesting that a common

cellular or molecular metabolism may exist. The water/ethanol extract of *U. dioica* prevents high-fat diet-induced insulin resistance and promotes glucose homeostasis (Obanda, et al., 2016a; Obanda, et al., 2016b). Since obesity and insulin resistance are associated with gut microbiota health, composition, and function, we hypothesize that the beneficial effects of *U. dioica* may be linked to its impact on the microbiome. Furthermore, we hypothesize that the whole vegetable as well the phytochemical compounds may exert benefits through impacting the gut microbiota and immune system.

Chapter 3: *Urtica dioica* Whole Vegetable as a Functional Food Targeting Fat Accumulation and Insulin Resistance-A Preliminary Study in a Mouse Pre-Diabetic Model*

Abstract

The shoot of *Urtica dioica* is used in several cultures as a vegetable or herb. However, not much has been studied about the potential of this plant when consumed as a whole food/vegetable rather than an extract for dietary supplements. In a 12-week dietary intervention study, we tested the effect of *U. dioica* vegetable on high fat diet induced obesity and insulin resistance in C57BL/6J mice. Mice were fed ad libitum with isocaloric diets containing 10% fat or 45% fat with or without *U. dioica*. The diet supplemented with *U. dioica* attenuated high fat diet induced weight gain ($p < 0.005$; $n = 9$), fat accumulation in adipose tissue ($p < 0.005$; $n = 9$), and whole-body insulin resistance (HOMA-IR index) ($p < 0.001$; $n = 9$). Analysis of gene expression in skeletal muscle showed no effect on the constituents of the insulin signaling pathway (AKT, IRS proteins, PI3K, GLUT4, and insulin receptor). Notable genes that impact lipid or glucose metabolism and whose expression was changed by *U. dioica* include fasting induced adipocyte factor (FIAF) in adipose and skeletal muscle, peroxisome proliferator-activated receptor-α (Ppar-α) and forkhead box protein (FOXO1) in muscle and liver, and Carnitine palmitoyltransferase I (Cpt1) in liver ($p < 0.01$). We concluded that *U. dioica* vegetable protected against diet induced obesity through mechanisms involving lipid accumulation and glucose metabolism in skeletal muscle, liver, and adipose tissue.

*The article was published in the journal of *Nutrients*: Fan S, Raychaudhuri S, Kraus O, Shahinozzaman M, Lofti L, Obanda D.N. Urtica dioica Whole Vegetable as a Functional Food Targeting Fat Accumulation and Insulin Resistance-a Preliminary Study in a Mouse Pre-Diabetic Model. *Nutrients*. 2020; 12(4):1059.

3.1. Introduction

Though they are considered weeds and are rarely a cultivated crop, nettles grow in a broad range of climate conditions and are widespread throughout Europe and North America, North Africa, and in parts of Asia. Nettles (genus *Urtica*) have been used for centuries in traditional medicine in several cultures and have been widely studied as intervention for several medical conditions. Dietary supplements based on *Urtica* supplement extracts are widely available. About 25 different species exist within genus *Urtica*. *U. dioica* is the species commonly found in North America, New Zealand, Turkey, and Europe (Kregiel et al., 2018). Actively growing *U. dioica* shoots are harvested before flowering for consumption as an herb or spinach alternative (Rutto et al., 2013 and Adhikari et al., 2016).

Most studies on *U. dioica* have been performed using its ethanolic or water extract particularly the extract of the leaves and stem which is rich in polyphenols. This extract has been shown to be richer in individual polyphenols than other plants such as dandelion and cranberry juice (Kregiel et al., 2018 and Adhikari et al., 2016).

U. dioica extract has been studied for several different disease conditions including autoimmune diseases, such as rheumatoid arthritis, allergy, eczema, atherosclerosis, cancer, as well as age-related degenerative brain disorders. It has also been studied for alleviating bladder disorders, hemorrhaging and inflammation (Klingelhoefer et al., 1999; Mukundi et al., 2017 and Sharafetdinov et al., 2017). More recent studies show that *U. dioica* extract possess anti-diabetic properties (Mukundi et al., 2017 and Sharafetdinov et al., 2017). A comprehensive review on studies using the extract as intervention for diabetes shows that over 21 studies (Sharafetdinov et al., 2017). Obesity induced insulin resistance caused by accumulation of certain lipid metabolites is a key pathophysiologic feature of T2DM (Obanda, et al., 2016a; Obanda, et al., 2016b).

Progression of insulin resistance into overt T2DM can be prevented or delayed by timely intervention. Treatment of insulin resistance is directed at increasing insulin sensitivity in peripheral tissues such as skeletal muscle and adipose tissue. Because of the high societal and economic cost of treating diabetes, timely intervention for insulin resistance has important medical, economic, social, and human implications. Therefore, conventional medications that address insulin resistance are a major focus for drug development (Portero McLellan et al., 2014).

Our previous studies using cell culture models showed that *U. dioica* extract activates the proteins AKT1 and AKT2 which are components of the insulin signaling pathway by enhancing their phosphorylation in presence of excess fat metabolites (Obanda, et al., 2016a; Obanda, et al., 2016b). Rather than use the extract, in this study we incorporated whole *U. dioica* vegetable in the diet. Our laboratory focus was on whole foods or class of foods that promote health rather than purified supplements. We thus designed a diet to focus on whole-vegetable effects and formulated the control diets to be isocaloric to the diet containing the vegetable. Furthermore, we tested the efficacy of the vegetable in preventing fat accumulation and insulin resistance when used from the beginning of the study. We report on effects of the vegetable on a HF diet induced fat accumulation, insulin resistance, inflammation, endotoxemia and the expression of genes encoding proteins that are involved or impact the insulin signaling pathway in the skeletal muscle of C57BL/6J mice.

3.2. Materials and Methods

3.2.1. Acquisition of Plant Sample

Urtica dioica L. from spring growth was harvested as the total herb above the root mass as the total herb from the Green Farmacy Garden, a medicinal garden located in Fulton, Maryland. The exact latitude is 39.1454180, and the longitude is -76.9213600. A voucher sample was conserved in the herbarium of the University of Maryland. The stems and leaves were rinsed, chopped into small pieces, oven-dried for 6 hours at 50°C, and powdered using a coffee grinder. The powder sample subjected to nutritional analysis before formulating into study diets.

3.2.2. Nutritional Analysis of *Urtica dioica*

The powder sample was analyzed by Medallion Labs (Minneapolis, MN) using the Association of Analytical Chemists (AOAC) methods. Calorific value and proximate analysis methods used shown in Table 1, including moisture, carbohydrate, total lipid, fatty acid profile, protein, ash, soluble fiber, and insoluble fiber.

Table 1. Nutrient Analysis of Leaves and Stems of *Urtica dioica*

	Amount %	Analytical Method used
Proximate Analysis		
Ash	12.8	AOAC: 923.03
Carbohydrates	64.1	By Calculation
Protein (6.25)	16.1	AACC 46 - 30*; AOAC 992.15
Total Fat	2.2	AOAC: 996.06
Fat		AOAC: 996.06*
Saturated Fat	0.54	
Monounsaturated Fat	0.16	
cis-cis polyunsaturated Fat	1.40	
Trans Fat	0.05	
Moisture	5.0	AOAC: 945.43*, 934.01
Fiber		AOAC: 991.43*
Insoluble Dietary Fiber	48.3	
Soluble Dietary Fiber	4.9	
Total Dietary Fiber	53.3	
Calories per 100 g		By Calculation
Calories	340.26	
Calories, 2020	136.74	
Calories from Fat	20.67	
Calories from Saturated Fat	4.77	
Calories (insoluble fiber subtracted)	14.31	

3.2.3. Formulation of Study Diets

In the preliminary study, three different diets were formulated: the low-fat control diet (LF), the high-fat control diet (HF), and the HF diet containing 9 percent of *U. dioica* (HFUT). The LF contained 10% fat, while the HF and HFUT diets contained 45% fat. The HF and HFUT diets were formulated to be isocaloric (3961 Kcal per Kg), as shown in Table 2. Diets were formulated to contain the same amount of sucrose and protein, considering that the *U. dioica* has about 16% protein content.

Table 2. Diet Formulation

	LF	HF	HFUT
Ingredient (g)			
Corn starch	452.2	72.8	63.94
Maltodextrin 10	75	100	100
Sucrose	172.8	172.8	172.8
Cellulose	50	50	6.34
Soybean oil	25	25	23.16
Lard	20	177.5	177.5
Casein	200	200	185.3
L-Cystein	3	3	3
Mineral Mix	10	10	10
Di calcium phosphate	13	13	13
Calcium carbonate	5.5	5.5	5.5
Potassium citrate	16.5	16.5	16.5
Vitamin mix	10	10	10
Choline Bitartrate	2	2	2
Urtica dioica dried powder	0	0	82
Total weight (g)	1055.05	858.15	870.82
kcal			
Protein	716	716	716
Carbohydrate	2840	1422.4	1422.4
Fat	405	1822.5	1822.5
Total kcal	3961	3960.9	3961

3.2.4. Study Animals

All animal procedures and experiments were performed in accordance with a protocol approved by the Institutional Animal Care and Use Committee (IACUC) of the University of Maryland. Twenty-seven male C57BL/6J mice at the age of 7 weeks were ordered separately from Jackson Laboratories, Inc. (Bar Harbor, Maine, USA). They were all singly housed in shoebox cages with corncob bedding. Mice had access to custom diets and water *ad libitum* in controlled environmental conditions at 22°C with a 12-hour light-dark cycle.

3.2.5. Randomization and Feeding Regime

All mice were fed the LF diet for the first week for baseline adaptation. Body weight, fasting glucose, and fasting insulin were collected after one week of feeding the LF diet. Mice were randomized into groups based on body weight and the homeostatic model assessment of insulin resistance (HOMA-IR).

In the preliminary study, groups 1 and 2 were fed with the LF and HF diets for twelve weeks, respectively. Group 3 was fed the HF diet containing *U. dioica* whole vegetable for 12 weeks. The sample size was n = 9 in each group. Food intake (the difference between weight administered and leftover plus spillage) and body weight were monitored and recorded twice weekly. The sample size of n=9-10 for each treatment group was based on a power analysis of insulin resistance results, which showed that 8 is sufficient to generate statistically significant results. To attain a statistical power of 0.90, 8 samples are needed for a one-tailed test and 10 for a two-tailed test.

3.2.6. Determination of Insulin Sensitivity

Six hours of fasting plasma glucose and insulin were determined at baseline for randomization and after six weeks and twelve weeks of feeding customed diets, respectively. Blood was collected by the mandibular bleeding and glucose was measured using a portable glucometer (Milpitas, CA, USA). Fasting insulin was determined using a mouse ELISA kit (Crystal Chem, Downer Grove, IL). Insulin resistance (HOMA-IR index) was calculated: HOMA-IR = fasting glucose (mg/dL) × fasting insulin (ng/mL) / 405 (Roza et al., 2016).

3.2.7. Euthanasia and Tissue Collection

In the preliminary study, after 12 weeks (at 20 weeks of age), animals were anesthetized by isoflurane inhalation. Terminal blood was collected by heart puncture, followed by euthanasia by cervical dislocation. Whole blood was clotted, centrifuged to separate serum, and stored at -80°C for later use. The epididymal, perirenal, and retroperitoneal were excised and collected as abdominal fat pads. Their weights were recorded and summed as total abdominal fat. All tissues were collected snap frozen in liquid nitrogen followed by storing at -80°C for later analysis. Other tissues collected included the liver, skeletal muscle tissues, the small intestine, the content in the small intestine, cecum, cecal contents, colon, colon contents, urine, and feces.

3.2.8. Histology

Tissue samples were collected and fixed in 10% buffered formalin or snap-frozen in liquid nitrogen. The samples fixed in formalin were dehydrated in alcohol and embedded in paraffin before sectioning at a thickness of 2–3 μm. Sections were stained with Oil red O (ORO). The liver snap-frozen samples were cut directly into 3–4 μm sections and stained with ORO without prior alcohol fixation.

3.2.9. Analysis of Triglycerides in Liver and Colon Contents

About 100mg of colon contents or 150mg of liver were separately homogenized in ND40 reagent containing protease inhibitors and analyzed by a triglyceride kit (Cayman Chemical, Ann Arbor, MI). Briefly, after centrifuging at 4°C, the supernatant was diluted 3-fold and reacted with lipoprotein lipase to release glycerol and fatty acids. The glycerol was then quantified by a colorimetric enzymatic reaction according to the kit manufacturer's instructions.

3.2.10. Serum Analysis

Serum samples were analyzed for total triglycerides using a colorimetric kit (Cayman Chemical, Ann Arbor, MI) according to the manufacturer's specifications. Serum total low-density lipoprotein (LDL) cholesterol and high-density lipoprotein (HDL) cholesterol were quantified using mouse ELISA kits. Endotoxin levels were determined by quantifying serum lipopolysaccharide levels using a mouse ELISA kit. All ELISA kits were from Cusabio (Wuhan, China).

3.2.11. RNA Extraction from Tissue and cDNA Synthesis

RNA from 50mg of gastrocnemius skeletal muscle and liver and 100mg of the epididymal fat pad were separately extracted and purified using the RNAeasy mini kit (Qiagen, German Town, MD, USA) according to the manufacturer's specifications. Prior to extraction, the muscle sample was disrupted in TRIzol with bead beating using the FastPrep®-24 (MP Biomedical, Solon, Ohio). Both RNA quantity and quality were determined using the Qubit 4 fluorometer (ThermoFisher Scientific, Rockville, MD). Only RNA samples with a concentration over 2.3 ng/ul and an RNA integrity number greater than 7.8 were used for cDNA synthesis using the High-Capacity cDNA Reverse Transcription Kit (Qiagen, German Town, MD) with 2000ng as starting RNA per sample.

3.2.12. Analysis of Target Genes in Skeletal Muscle, Adipose Tissue, and Liver by qPCR

Primer sets (IDT Technologies, Coralville, IA) were used to analyze selected genes that have been shown to impact adipogenesis, lipogenesis, fatty acid oxidation, and gluconeogenesis. A list

of primers used is shown in 4. RT-PCR cycling conditions on the CFX 96 (Bio-rad, Hercules CA, USA) were 2 mins at 50°C and 2 mins at 95°C, followed by 40 cycles of two-step PCR denaturation at 95°C for 15secs and annealing extension at 60°C for 1 min. Duplicate assay samples contained 10ng cDNA and 6 umol/L primers in 2× PowerUp™ SYBR™ Green Master Mix (ThermoFisher Scientific, Rockville, MD, USA) in a final volume of 20ul. The relative amount of target mRNA was normalized to β-actin levels as the endogenous control gene. Data were analyzed using the $2^{-\Delta\Delta CT}$ method, and fold difference was calculated between LF, HF, and HFUT groups.

Table 3. Primers Used for qPCR

Genes	Forward Primers	Reverse Primers
β-Actin	5'-GGCACCACACCTTCTACAATG-3'	5'-GGGGTGTTGAAGGTCTCAAAC-3'
FIAF	5'-TTTCCCTGCCCTTCTCTACT-3'	5'-GTACCAAACCACCAGCCA-3'
PPARα	5'-ATGCCAGTACTGCCGTTTTCA-3'	5'-GGGCCACAGAGCACCAATCTGTG-3'
PPARγ	5'-GTGCCAGTTTCGATCCGTAGA-3'	5'-GGGCCACAGAGCACCAATCTGTG-3'
CD36	5'-TGGCCTTACTTGGGATTGG-3'	5'-CCAGTGTATATGTAGGCTCATCCA-3'
FOXO1	5'-ACATTTCGTCCTCGAACCAGCTA-3'	5'-ATTTCAGACAGACTGGGCAGCGTA-3'
DGAT1	5'-TGGCTGCATTTCAGATTGAG-3'	5'-GCTGGGAAGCAGATGATTGT-3'
DGAT2	5'-CTTCCTGGTGCTAGGAGTGGC-3'	5'-GCTGGATGGGAAAGTAGTCTCGG-3'
CD11c	5'-CTGGATAGCCTTTCTTCTGCTG-3'	5'-GCACACTGTGTCCGAACTCA-3'
F4/80	5'-CTTTGGCTATGGGCTTCCAGTCC-3'	5'-GCAAGGAGGACAGAGTTTATCGTG-3'

3.2.13. Statistical Analysis

Data are expressed or graphed as mean ± SEM. Differences between two groups were assessed using the unpaired two tailed student t-test. Data sets with more than two groups were assessed using the MIXED procedure of SAS 9.4 for analysis of variance between treatments. Main effects were considered significant at $p \leq 0.05$. Data was analyzed for outliers using studentized residuals. Significant differences observed were followed up using the Bonferroni test of multiple comparisons.

3.3. Results

3.3.1. Nutritional Analysis of *U. dioica* Dried Powder

The analysis showed that the dried powdered leaves and stems contained 5% moisture, 12.8% ash, 64.1% carbohydrates, 2.2% total fat, and 16.1% proteins. Among the carbohydrates, it contains 48.3% of insoluble fiber and 4.9% of soluble fiber. The subsets of the fatty acids include linoleic, linolenic, and palmitic acid, constituting 41.8%, 23.1%, and 18.1%, respectively. The details are shown in Table 4.

Table 4: Fatty Acid Profile of the Leaves and Stems of *Urtica dioica*

Component Name	Normalized by Weight	% (w/w) as Triglyceride in Product
C-12:0 Lauric	1.52%	0.021
C-16:0 Palmitic	18.0%	0.252
C-16:1 t-Hexadecenoic	1.50%	0.021
C-18:0 Stearic	2.24%	0.031
C-18:1 t-Elaidic	0.75%	0.010
C-18:1 Oleic	7.45%	0.104
C-18:2 Linoleic	41.76%	0.585
C-18:3 Linolenic	23.12%	0.324
C-20:0 Arachidic	0.74%	0.010
C-20:4 Arachidonic	0.74%	0.010
C-22:0 Behenic	0.74%	0.010
C-23:0 Tricosanoic	1.48%	0.021
Totals:	100%	1.4

3.3.2. Food Consumption, Energy Intake and Body Weight

In the preliminary study, weekly food consumption (calorie intake) was not significantly different between the HF and HFUT groups (Figure 1 A & B). After 12 weeks, the HF diet group significantly increased body weight compared to the LF group. The HFUT diet induced a reduction in body weight compared to the HF diet (Figure 1C).

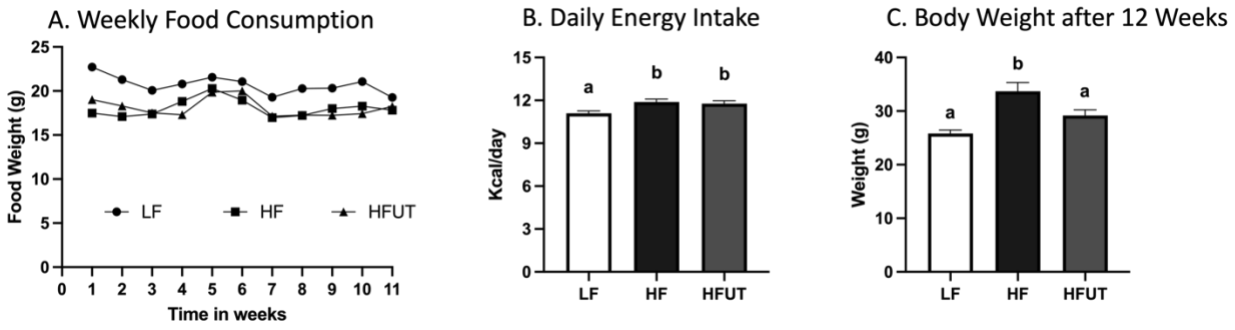

Figure 1. Supplementation with U. dioica vegetable prevented HF diet induced body weight. (A) Weekly food consumption was not different among all groups ($p>0.05$; n=9) (B) The calculated calorie consumption per day was not different among HF groups (n = 9). (C) The HF diet induced greater body weight gain compared to the LF diet. Supplementation of the HF diet with *U. dioica* vegetable lowered body weight compared to the HF diet. [a]Different letters indicate significant differences between the groups ($p<0.05$; n=9).

3.3.3. Fasting Glucose, Fasting Insulin and Insulin Resistance

At the end of the 12 weeks of the preliminary study, the HF diet induced higher fasting glucose, fasting insulin, and the calculated insulin resistance index (HOMA-IR) compared to the LF diet group. Supplementation with *U. dioica* lowered these parameters (Figure 2A, B, & C).

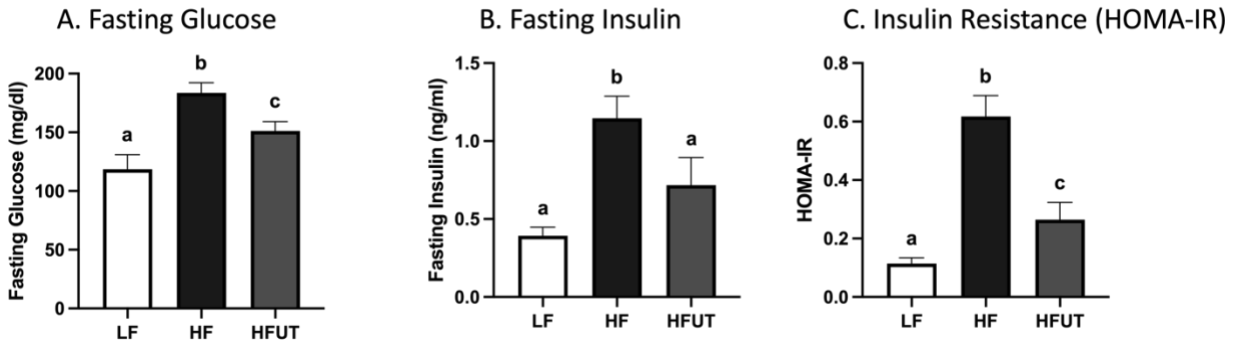

Figure 2. Supplementation with U. dioica reduced fasting glucose, fasting insulin, and enhanced insulin sensitivity.

(A) Fasting glucose after 12 weeks of intervention. The HF diet induced higher fasting glucose compared to the LF diet. HFUT diet group reduced the fasting glucose. (B) Fasting insulin after 12 weeks. The HF diet increased higher fasting insulin compared to the LF diet group, the HFUT diet group reduced the fasting insulin. (C) HOMA-IR after 12 weeks of intervention. The HF diet induced higher HOMA-IR compared to the LF diet group and the HFUT diet group reduced it significantly. [a]Different letters indicate significant differences between the groups ($p<0.05$; $n=9$).

3.3.4. Liver Weight and Triglycerides

In the preliminary study, the weight of the liver was higher in the HF diet group compared to the LF diet group. *U. dioica* supplementation reduced liver weight but not significantly compared to the HFUT group (Figure 3A). *U. dioica* also lowered the liver triglycerides to the level of the LF diet group (Figure 3B). The ORO-stained sections of the liver showed more lipid droplets in liver of HF group compared to LF. Liver from HFUT mice had similar amounts of lipid droplets like those of HF (Figure 3C–F).

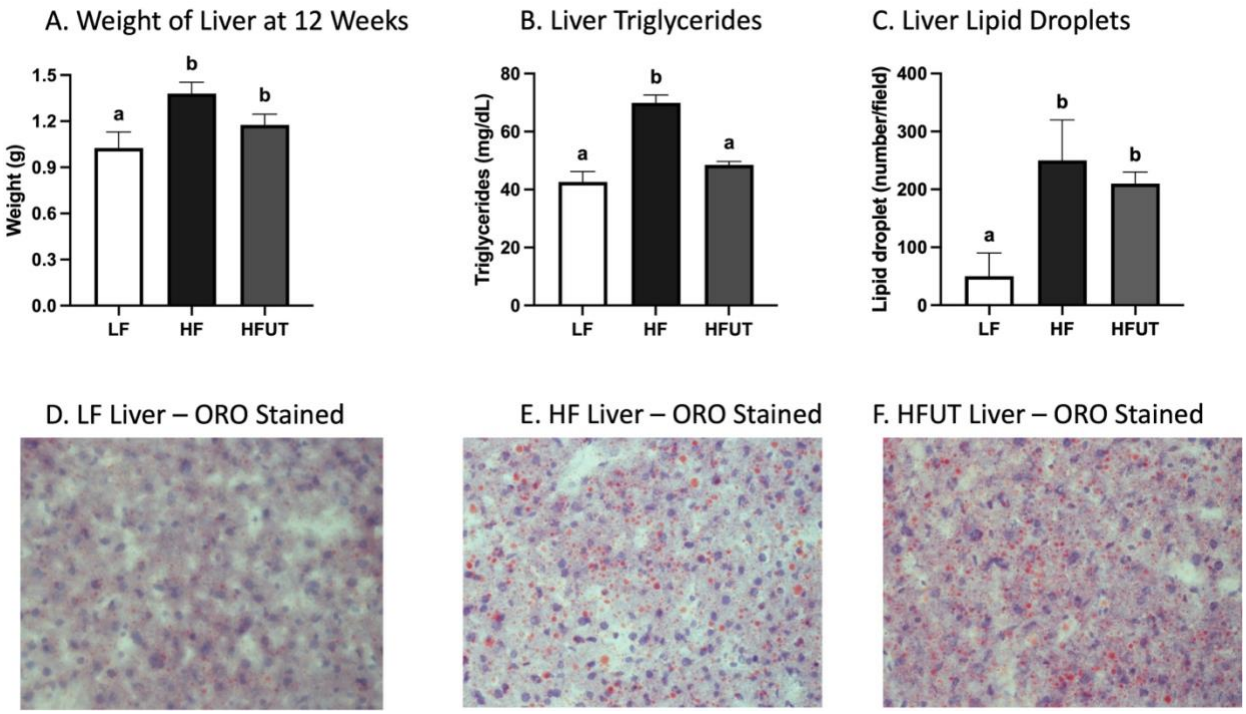

Figure 3. Supplementation with U. dioica attenuated the increase in liver weight and liver triglycerides.

(A) The weight of the liver was higher in HF compared to the LF diet group (n = 9). (B) Liver triglycerides were higher in the HF group compared to the LF diet group (n = 9). Supplementation of the HF diet with *U. dioica* lowered liver triglycerides to levels similar to the LF diet group (n = 9). (C–F) Oil red O (ORO) stained liver slides from HF fed mice showed highly increased lipid droplets compared to the LF group. The lipid droplet number in the HFUT group was not different from that of the HF group. [a]Different letters indicate significant differences between the groups ($p<0.05$; n=9).

3.3.5. Fat Accumulation in Adipose Tissue

In the preliminary study, the sum of the epididymal, retroperitoneal, and perirenal fat pads was higher in the HF diet group compared to the LF diet group. Supplementation with *U. dioica* lowered the weight of fat pads compared to the HF diet group (Figure 4A-C).

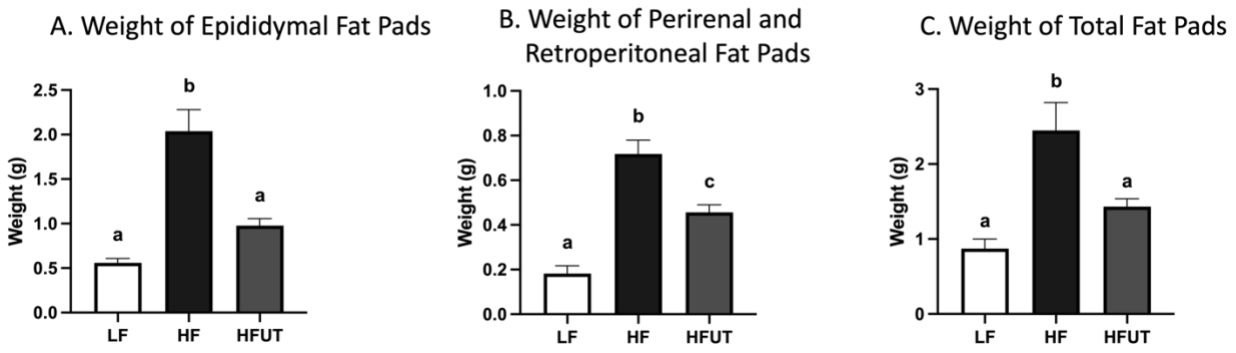

Figure 4. Supplementation with U. dioica attenuated the fat accumulation in the adipose tissues. The different fat depots were dissected and weighed at euthanasia. (A–B) The weight of the epididymal fat pad and the combined weight of perirenal and retroperitoneal fat pads were higher in HF compared to LF fed group ($p < 0.05$; $n = 9$). Supplementation of the HF diet with *U. dioica* lowered overall fat pad weights compared to the HF diet ($p < 0.05$; $n = 9$). (C) The total weight of abdominal fat pads: epididymal, perirenal, and retroperitoneal fat pads was higher in the HF diet compared to the LF diet group. The HFUT diet group lowered overall fat pad weights compared to the HF diet. [a]Different letters indicate significant differences between the groups ($p<0.05$; $n=9$).

3.3.6. Gene Expression in Adipose Tissue

Results from qPCR to determine gene expression were shown in Figure 5. The gene expression of selected genes in the HF and HFUT groups relative to the LF control in the preliminary study. In adipose tissue, the HF diet lowered the expression of genes involved in adipogenesis: peroxisome proliferator-activated receptor gamma (PPARγ), CCAAT/enhancer binding protein alpha (C/EBPα), C/EBPβ, peroxisome proliferator-activated receptor gamma coactivator 1-alpha (PGC1α) ($p<0.05$; $n=3$). The HFUT diet reversed this reduction and enhanced the expression of CD36.

For markers of lipogenesis and triglyceride synthesis, compared to the HF diet, HFUT lowered the expression of fatty acid synthase, (Fasn), diacylglycerol O-acyltransferase 1 (DGAT1), DGAT2, Acetyl-CoA carboxylase (ACC1), and fatty acid binding protein 4 (FABP4) all markers of lipogenesis and triglyceride ($p<0.05$; $n=3$) (Figure 5C). For markers of

inflammation, the HF diet increased the expression of CD11c by over 2-fold but had no effect on F4/80 and the HFUT lowered these two genes to levels below those of the LF diet ($p<0.05$; n=3).

For markers of fatty acid oxidation, The HFUT diet caused a 6-fold increase in fasting induced adipocyte factor (FIAF) ($p<0.001$; n=3) and attenuated the HF diet-induced reduction in the gene expression of PPARα ($p<0.05$; n=3) (Figure 5B). HFUT diet lowered expression of Peroxisomal acyl-coenzyme A oxidase 1 (Acox1), carnitine acyltransferase I (Cpt-1α), and Forkhead box protein O1 (FOXO1) ($p<0.05$).

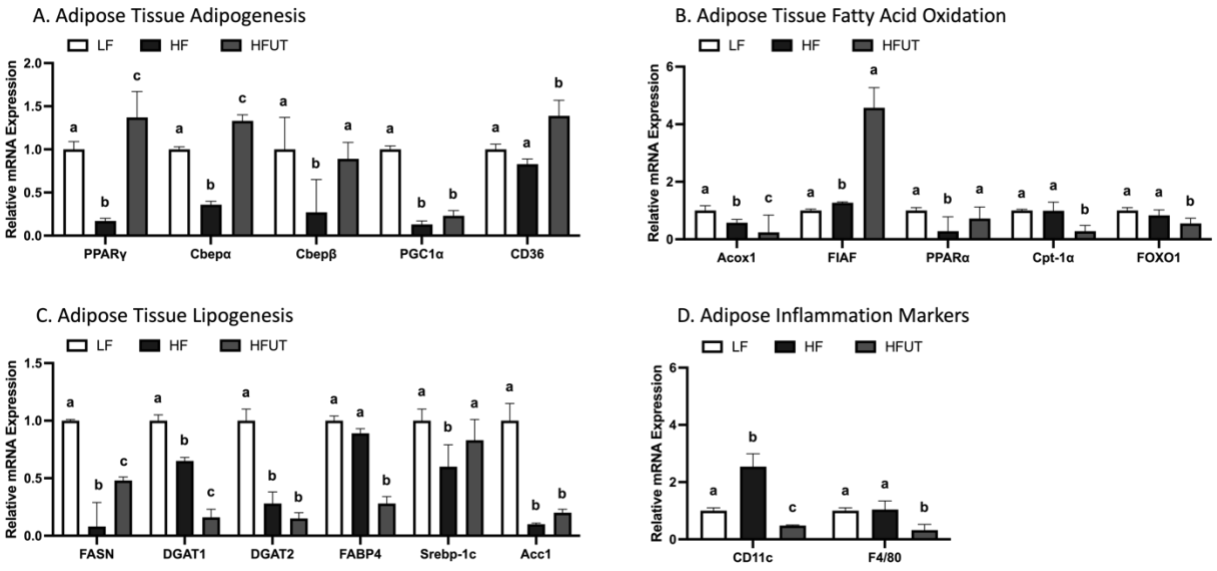

Figure 5. Changes in mRNA expression of genes involved or impact insulin signaling in adipose tissue.

RNA was extracted, cDNA synthesized, and gene expression was determined by qPCR. The threshold cycle (Cq) values for each gene and that of β-actin as a reference gene were used to calculate gene expression by calculating the $2^{-\Delta\Delta CT}$ method. (A) Genes involved in adipose tissue adipogenesis. (B) Genes involved in fatty acid oxidation in adipose tissue. (C) Genes involved in adipose tissue lipogenesis. (D) Markers of inflammation in adipose tissue. [a]Different letters indicate significant differences between the groups ($p<0.05$; n=3).

3.3.7. Gene Expression in Liver and Skeletal Muscle

In the liver, the HFUT diet increased the expression of the fatty acid oxidation markers PPARα, FOXO1, Cpt-1α and increased the expression of CD36 ($p < 0.05$). HFUT had no effect on FIAF, Glucose-6-phosphatase, catalytic subunit (G6PC), and Sterol regulatory element-binding transcription factor 1c (Srebpc-1c) in the liver.

In skeletal muscle, HFUT had no effect on PGC1α and Srebpc-1c but increased FOXO1, CD36, Cpt-1α, FIAF, and PPARα. FIAF was increased by 13-fold while PPARα was increased by 7-fold ($p<0.001$; $n=3$).

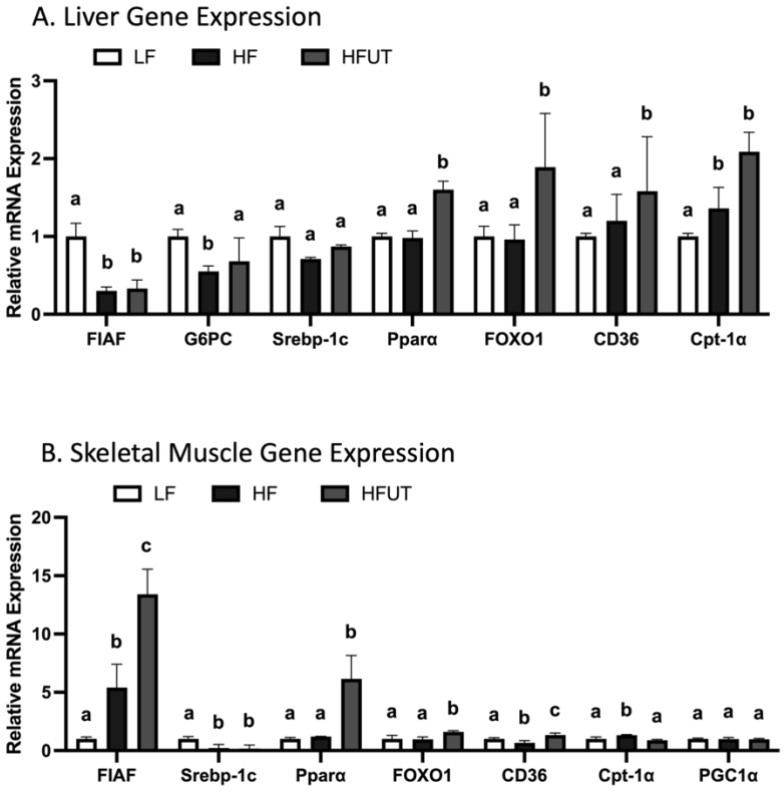

Figure 6. Changes in mRNA expression of genes that involved or impact insulin signaling in the liver and skeletal muscle.

RNA was extracted, cDNA synthesized, and gene expression was determined by qPCR. The threshold cycle (Cq) values for each gene and that of β-actin as a reference gene were used to calculate gene expression by calculating the $2^{-\Delta\Delta CT}$ method. (A) Gene expression in the Liver. (B) Gene expression in skeletal muscle. [a]Different letters indicate significant differences between the groups ($p<0.05$; n=3).

3.4. Discussion

Although diet supplements based on *Urtica dioica* extracts are widely available in the United States, not much is known about the benefits of this plant when consumed as a whole vegetable. In many international cultures *U. dioica* shoots are harvested before flowering for use as an herb or spinach alternative. Some recipes incorporate *U. dioica* leaf flour in bread, pasta, and noodle dough. Besides being high in polyphenols, on a dry weight basis, *U. dioica* leaf is comparable to

common bean (*Phaseolus vulgaris*) and chicken as a source of essential amino acids (Kregiel et al., 2018; Rutto et al., 2013 and Adhikari et al., 2016). In the current study, we show that including the vegetable in a HF diet, attenuates fat accumulation in adipose tissue and whole-body insulin resistance. In our previous study (Obanda et al., 2016) in which we incorporated 0.5% *U. dioica* ethanolic extract into the HF diet, we did not observe a reduction in body weight or body composition; the extract improved insulin signaling despite not having an effect on fat accumulation. Our current findings on reduction of body weight and fat accumulation when the whole vegetable is used instead of the extract, are thus novel and raise new questions on mechanisms involved. It also suggests that other components of the vegetable besides the phytochemicals in the ethanol extract may impact positive effects on body weight.

The HF diet induced a more than 2-fold increase in CD11c compared to the LF diet group. Supplementing the HF diet with *U. dioica* reversed this and downregulated CD11c to levels below those of the LF diet group and also reduced expression of F4/80 another marker of inflammation in adipose (Figure 5D). A specific subset of macrophages that express CD11c and produce high levels of pro-inflammatory cytokines is recruited to obese adipose and muscle tissue. These macrophages are linked to the development of obesity-associated insulin resistance. Using a conditional cell ablation system to deplete $CD11c^+$ cells in obese mouse models, Patsouris et al. (2008) showed that depleting $CD11c^+$ cells result in rapid normalization of insulin sensitivity and leads to a marked decrease in gene expression and protein levels of inflammatory markers. CD11c plays an important role in T-cell accumulation and activation in adipose tissue and contributes to insulin resistance associated with obesity. CD11c messenger RNA positively correlates with MCP-1 in visceral adipose of obese humans with metabolic

syndrome compared with lean humans (Wu et al., 2010). Thus, $CD11c^+$ cells are a potential therapeutic target for the treatment of obesity-related insulin resistance and type II diabetes.

Compared with the HF diet only, supplementing the HF diet with *U. dioica* increased the expression of genes that are involved in fatty acid transport and oxidation in both adipose tissue and skeletal muscle. Specifically, the expression of Angiopoietin-like protein or fasting induced adipocyte factor increased more than 4 fold in adipose and by 13 fold in muscle. FIAF is a circulating inhibitor of lipoprotein lipase and restrains its ability to import and store fatty acids in peripheral tissues. Furthermore, FIAF expression regulates energy expenditure via modulation of AMP-activated protein kinase (AMPK) activity in muscle and adipose. Elevated FIAF levels have been shown to protect against diet-induced obesity (Yoshida et al., 2002). This may be a contributing factor in the lower fat accumulation observed *U. dioica* increased the expression of PPARα in skeletal muscle by more than 6-fold and increased it by 1.6 fold in the liver. In adipose tissue, it prevented the HF induced reduction in expression of PPARα and increased PPARγ expression by 1.4 fold (Figure 5A & B). Activators of both PPARα and PPARγ have been shown to improve insulin sensitivity and normalize impaired glucose tolerance in both humans and rodents. In the liver, PPARα regulates genes involved in lipid and lipoprotein metabolism. When activated, it promotes fatty acid oxidation by inducing expression of mitochondrial acyl-CoA dehydrogenases, acetyl-CoA production, promotes glucose sparing and ketone body synthesis by upregulating mitochondrial hydroxymethylglutaryl-CoA synthase (HMGS), a rate-limiting ketogenesis enzyme (Guerre-Millo et al., 2000 & Goto TLee et al., 2011). It also reduces pyruvate kinase, induces PDK4 expression and reduces weight gain in rodents (Guerre-Millo et al., 2000 & Goto TLee et al., 2011). PPARα activation further reduces plasma triglyceride-rich lipoproteins by increasing the activity of LPL, which hydrolyzes

lipoprotein triglycerides. Thus, through enhanced fatty acid oxidation, *U. dioica* vegetable may impact fat accumulation mechanisms and result in the leaner phenotype. The HF diet lowered PPARγ expression and the *U. dioica* prevented this and enhanced the expression to levels higher than those of the LF group. PPARγ is highly expressed in adipose tissue where its activation alters fat topography, adipose phenotype and upregulates genes involved in fatty acid metabolism and triglyceride storage.

In the liver and muscle, *U. dioica* diet increased the FOXO1 gene by almost 2-fold (Figure 6A and B). FOXO proteins are important in metabolism and energy homeostasis. FOXO1 particularly inhibits hepatic gluconeogenesis. Insulin inhibits FOXO1 activity through the PI3K/AKT signaling pathway, resulting in an inhibition of gluconeogenesis by suppressing the expression of glucose-6-phosphatase and Pck1 (Wondisford et al., 2014). FOXO1 stimulates fatty acid uptake and oxidation in muscle cells. Other genes involved in fatty acid oxidation and energy expenditure and impacted by *U. dioica* were fatty acid translocase (FAT/CD36), carnitine palmitoyl transferase (CPT-1a) (by more than 2-fold in the liver), FABP and Acc2. Overexpression of Cpt1 in skeletal muscle has been shown to enhance fatty acid oxidation and improve high-fat diet-induced insulin resistance (Bruce et al., 2009). The expression of CD36 was enhanced by *U. dioica* in all three tissues. CD 36 promotes adipocyte differentiation and adipogenesis.

Overall, the HFUT diet increased the expression of genes involved in adipogenesis (Pparγ, CEBPα, SREBF1c, FABP4, FASN, and CD36), lowered genes involved in lipogenesis (Acc1, Dgat1, Dgat2, FABP) and increased genes involved in fatty acid oxidation (FIAF, Pparα, Cpt-1). Thus the combination of reduction in lipogenesis genes and increase in and fatty acid oxidation genes contributed to the leaner frame in HFUT fed mice.

Our data clearly showed a relationship between the effects of *U. dioica* vegetable and favorable metabolic parameters but raises several unanswered questions. The limitation of our study is that we assess mRNA changes (transcript abundance) as a proxy for protein levels but have not yet quantified changes in the proteins encoded by these genes. Protein expression levels are highly regulated and protein levels are more conserved than the mRNA levels. In addition to changes in mRNA expression, differences in the translational efficiency of the mRNAs are important. In further studies we shall evaluate protein expression levels, identify the active plant components responsible for the positive effects and metabolites produced in tissues to gain a better understanding of the potential of *U. dioica* as a metabolically favorable functional whole food for obesity and insulin resistance.

Chapter 4: Metagenomic Insights into the Effects of *Urtica dioica* Vegetable on the Gut Microbiota of C57BL/6J Obese Mice, particularly the Composition of Clostridia[*]

Abstract

Urtica dioica vegetable attenuates diet induced weight gain and insulin resistance. We hypothesized that *U. dioica* imparts metabolic health by impacting the gut microbiota composition. We examined effects of *U. dioica* on the cecal bacterial taxonomic signature of C57BL/6J mice fed isocaloric diets: a low-fat diet (LF) with 10% fat, a high fat diet (HF) with 45% fat or the HF diet supplemented with 9% *U. dioica* (HFUT). Among Clostridia, HFUT increased genus *Clostridium* by over 2-fold, particularly the species *C. vincentii* and *C. disporicum* and increased genus *Turicibacter* by three-fold ($p < 0.05$; $n = 9$). Abundance of *Clostridium* and *Turicibacter* negatively correlated with body weight ($p < 0.05$; $R^2 = 0.42$) and HOMA-IR ($p < 0.05$; $R^2 = 0.45$). *Turicibacter* and *Clostridium* have been shown to be more abundant in lean phenotypes compared to obese. *Clostridium* impacts host phenotype by inducing intestinal T cell responses. We conclude that increasing the proliferation of *Clostridium* and *Turicibacter* may be contributing to mechanism(s) by which *Urtica dioica* impacts metabolic health.

[*]The article was published in the *Journal of Nutritional Biochemistry*: Fan S, Raychaudhuri S, Page R, Shahinozzaman M, Obanda D.N. Metagenomic insights into the effects of Urtica dioica vegetable on the gut microbiota of C57BL/6J obese mice, particularly the composition of Clostridia. *J. Nutri. Biochem.* 2021; 91:108594.

4.1. Introduction

The prevalence of obesity, a major risk factor in the development of noncommunicable diseases such as type 2 diabetes, cardiovascular disease, fatty liver disease has significantly increased within the last 50 years (Matthias, 2019). While disproportionate fat accumulation is attributed to energy imbalance, studies have revealed a link between alteration in gut microbiota composition and pathogenesis of obesity. Microbial colonization of germ-free mice results in weight gain and conventional mice gain more weight compared to germ-free mice despite lower calorie consumption (Bäckhed et al., 2004 and Bäckhed et al.,2007). Obesity is associated with an altered gut microbiota composition and diversity. The gut microbiota influences host obesity phenotype through direct contact with intestinal cells or indirectly via bacterial metabolites which act on different host cellular mechanisms.

Diet plays an important role in alteration of gut microbiota population and diversity. Diet or obesity induced dysbiosis can be attenuated by manipulating the microbiota to the target proliferation of bacterial taxa that through direct contact with host cells or indirectly via bacterial metabolites. Prebiotic foods induce the proliferation of beneficial bacteria. The gut bacteria may metabolize the prebiotic food components to produce metabolites that impact host mechanism. Prebiotic vegetables which promote microbiota health and diversity include chicory which has a high content of inulin-type fructan and oligofructose (Liu et al., 2012), Jerusalem artichokes and garlic which also have high amounts of inulin (Ramnani et al., 2010). Nettles (genus *Urtica*) are used as food and have been widely studied as intervention for several medical conditions. Shoots are used as a spinach alternative (Orčić et al., 2014; Upton, 2013). Of the 25 species within the genus, *U. dioica* is the species commonly found in North America. Benefits are attributed to the rich phytochemical component which has been well characterized by several researchers, high

protein content, high percentage of linoleic and linolenic acids and high soluble and insoluble fiber (Orčić et al., 2014; Upton, 2013 and Otles et al., 2012). The vegetable improves several medical conditions through mechanisms that are not clearly elucidated. We have previously shown that the water/ethanol extract of *U. dioica* prevents high fat diet induced insulin resistance (Obanda, et al., 2016a; Obanda, et al., 2016b), while the whole vegetable attenuates fat accumulation and prevents insulin resistance (Fan et al., 2020). The prebiotic properties of *U. dioica* vegetable have not been studied and information on how *U. dioica* alters the microbiota is not available.

We hypothesized that *U. dioica* impacts host obesity phenotype through its effects on gut microbiota composition and diversity. The high proportion of soluble and insoluble fiber and phytochemicals in *U. dioica* may serve as substrates for gut bacteria and result in the proliferation of beneficial bacterial taxa or metabolites that influence host cellular mechanisms. Herein we induce obesity and dysbiosis in C57BL/6J mice using a HF diet and investigate how *U. dioica* prevents or attenuates the dysbiosis, particularly how it impacts bacterial composition. We systematically analyzed changes within each phylum. We reported that supplementing the HF diet with 9% (about 0.23 g) of *U. dioica* vegetable per day, impacted the community structure of the microbiota with the greatest changes attributed to relative abundances of genera and species within phylum Firmicutes specifically genus *Clostridium* and genus *Turicibacter*.

4.2. Materials and Methods

4.2.1. DNA Extraction from Cecal Contents

100 mg of cecal contents from each sample were placed into 2 mL screw-cap tubes filled with beads and disrupted with lysis buffer used FastPrep-24 homogenizer (MP Biomedical, Solon,

Ohio, USA). DNA was extracted individually using the PowerFecal Pro DNA Kit (Qiagen, Germantown, MD, USA) according to the manufacturer's instructions. DNA concentrations were determined by the Qubit 4.0 Fluorometer (ThermoFisher Scientific, Rockville, MD, USA). All extracted DNA was stored at -80°C for further sequencing.

4.2.2. Amplifying the 16s Hypervariable Regions

2 μL of the extracted DNA was input to amplify the 16S hypervariable regions, which are v2-4-8 and V3-6,7-9 using the Ion 16S Metagenomics Kit (ThermoFisher Scientific, Rockville, MD, USA). The thermal cycler conditions were an initial denaturation for 10 min at 95°C, 25 cycles of denaturation at 95°C for 30 s, annealing at 58°C for 30 s, and extension at 72°C for 20 s, and final extension at 72°C for 10 min, and hold at 4°C until taken out. The thermal cycle was done on a CFX Connect Real-Time PCR system (BIO-RAD, Hercules, CA, USA).

4.2.3. Library Preparation, Template Preparation Enrichment, and Sequencing

Purified amplicons were pooled together according to the sample number and added end repair buffer and enzymes to ligate and nick-repair with Ion Xpress Barcode Adapters 1 – 16 kit and 17 – 32 kits separately (ThermoFisher Scientific, Rockville, MD, USA). DNA libraries were prepared using Ion Plus Fragment Library kit (ThermoFisher Scientific, Rockville, MD, USA) and purified in the tubes using Agencourt AMPure XP beads (Beckman Coulter, Nyon, Switzerland) on a DynaMag-2 magnetic rack to remove small mispriming products and primer dimers, followed by washing with fresh 70% ethanol twice on the same magnetic rack, finally eluted into 20 μL Low TE buffer. DNA library quantities were determined using the Qubit dsDNA HS Assay kit (ThermoFisher Scientific, Rockville, MD, USA)

DNA libraries were diluted to a yield of 10 pM input for template preparation performed on an Ion OneTouch 2 System and template-positive Ion Sphere Particles (ISPs) enriched by Ion OneTouch ES. Up to 400 base-pair average inset size libraries were sequenced by loading template positive ISPs into an Ion 530 Chip on Ion GeneStudio S5 System (ThermoFisher Scientific, Grand Island, NY, USA).

4.2.4. Microbial Diversity and Comparative Analysis

Exported sequencing data from 27 samples were analyzed and they were clustered and presented in operational taxonomic units (OTUs) with a 97% similarity threshold referring to the closed-reference OTU picking against the Greengenes v13.5 and MicroSEQ Library v2013.1 database. OTU were presented as counts, percentage of total reads, and percentage of mapped reads.

Alpha and beta diversity were calculated at an even depth of 173,940 sequences per sample. Observed species, Chao 1, Shannon, and Simpson indices were performed for alpha diversity. Alpha rarefaction plots were plotted using the number of sequences against the Shannon index because it takes into account both the richness of the species and the evenness of the species. Principal component analysis (PCA) was calculated and graphed for beta diversity. PCA at the family level was performed by the PLS_Toolbox software using the MATLAB package (Version 9.8) to measure the differences in different treatment groups. Abundance files of all bacteria at all OTU levels as input, linear discriminant analysis scores, and cladograms were gathered as output. Phylogenetic Investigation of Communities by Reconstruction of Unobserved States (PICRUSt2) analysis was performed to predict the metabolic pathways using the Kyoto Encyclopedia of Genes and Genomes (KEGG) Ortholog (KO) database.

4.2.5. Quantifying the Genus *Clostridium* and Genus *Turicibacter* by qPCR

Because sequencing data revealed that the *U. dioica* promotes the representation of *Clostridium* and *Turicibacter* in excrement, we further validate these finds by qPCR. QPCR primers were F: 5' A GCACAAGCAGTGGAGT 3', R: 5' CTTCCTCCG TTTTGTCAA 3' and F: 5' CAGACGGGGACAACGATTGGA 3', R: 5' TACGCATCGTCGCCTTGGTA 3' for *Clostridium* and *Turicibacter* respectively as reported by Kable et al. (2019). Primers were manufactured by Integrated DNA Technologies (Coralville, Iowa).

DNA from all samples were pooled diluted 20 folds and used to generate standard curve by serial 10-fold dilutions. All samples and standards were amplified in targeted regions on the CFX 96 Connect Real-Time PCR system. Conditions used were 50°C for 2 min, 95°C for 2 min, and 40 cycles of 95°C for 15 s and annealing at 60°C for 1 min. Cq values were collected after running and non-template controls (NTC) were used to adjust all values. A standard curve was acquired from amplicon quantities versus cycles-to-threshold. The gene copies per microliter were obtained using the formula by Oldham and Duncan (2012).

$$\frac{[\text{DNA concentration (nanograms per microliter)}] \times [6.02 \times 10^{23}\ \text{(copies per mole)}]}{\left[\text{amplicon length (bp)} \times 6.6 \times 10^{11}\ \frac{\text{ng}}{\text{mol}}\right]}$$ The assumptions were the average molecular mass of the double-stranded DNA base pairs is 6.6×10^{11} ng/mol, and the Avogadro's number of copies per mole is 6.022×102^{3}. The length of the amplicon of *Clostridium* is 141 bp, and of *Turicibacter* is 254 bp.

4.2.6. Statistical Analysis

Data are expressed or graphed as mean ± SEM. Differences between the two groups were assessed using the unpaired two-tailed student T-Test. Data sets with more than two groups were assessed using the MIXED procedure of SAS 9.4 for analysis of variance between treatments.

The main effects were considered significant at $P \leq 0.05$. The linear discriminant analysis effect size (LEfSe) was used to determine the OTUs and clades most likely to explain differences between the 3 treatment groups using standard tests for statistical significance with additional tests for biological consistency and effect relevance as shown by Segata et al. (2011). The LEfSe analysis was done with the abundance information file of all bacteria obtained at all OTU levels. We obtained p-values for the factorial Kruskal-Wallis test among treatment groups and obtained p-values for the pairwise Wilcoxon rankings with an LDA score >3 for any significant taxa between subclasses. Only p-values < 0.05 were significant. Results were analyzed for false discovery rate by Benjamini-Hochberg tests where only p-values < 0.05 and q-values < 0.25 were considered significant for an association between metadata and taxonomy. Relative abundances (%) of bacteria at all taxonomic levels were statistically compared using the MIXED procedure of SAS 9.4 for analysis of variance between treatments with significance set at $p \leq 0.05$. Significant differences were followed up using the Bonferroni test of multiple comparisons. The false discovery rate through Benjamini-Hochberg correction was used as shown above. We performed a correlation of taxa levels that were significantly different against body weight and insulin resistance.

4.3. Results

4.3.1. Alpha Diversity Metrics

The HF diet decreased the alpha diversity compared to the LF diet assessed by Chao1, Observed, and Shannon indices (Figure 7A-C), representing less microbial diversity in the mouse gastrointestinal (GI) tracts. However, the HFUT diet brought the microbial diversity back to the level same as LF diet in the Shannon and Simpson indices, which two indices could demonstrate

not only the richness of species but also the evenness of species. The rarefaction curves reached a similar summit after 30,000 sequences in all different treatment groups, pointing out that the sequencing depth was sufficient to detect all taxa within each sample (Figure 7D).

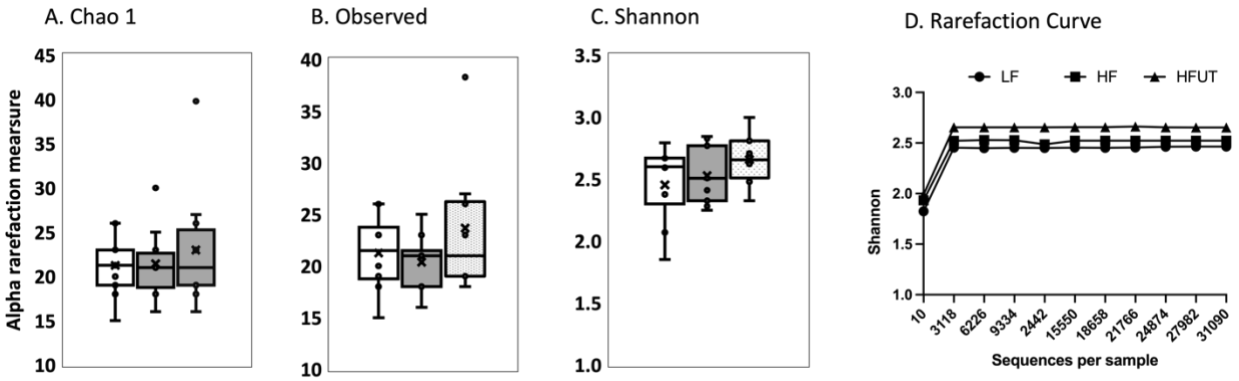

Figure 7. Rarefaction Curve and Alpha Diversity measures.
(A–C) Alpha diversity measures of Chao1, Observed, and Shannon. Shannon index showed differences among groups (n=9). (D) The rarefaction curve reached a summit after 3118 sequences for all treatment groups.

4.3.2. Beta Diversity Analysis

The principal component analysis for beta diversity depicted the first three variations with percentages of 32.34, 23.51, and 18.37, respectively. From PCA diagrams, samples in LF and HF diet groups showed evident different distributions. Whereas the HFUT group showed another direction distinguishing from both LF and HF diet groups. Although the three treatment groups showed some degree of similarity in the gut microbiota composition with overlapping clusters, the HFUT diet presented a different distribution. Permutational multivariate analysis of variance (PERMANOVA) described that the three treatment groups have significant differences (Figure 8, F= 3.11 P=0.001).

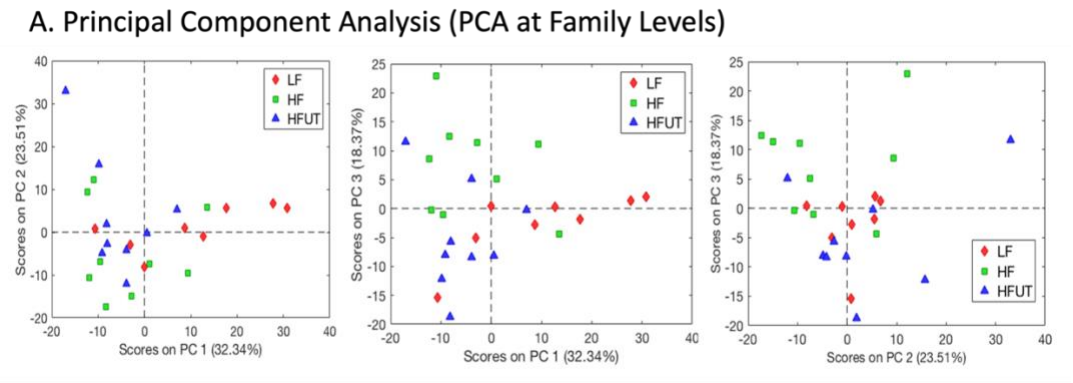

Figure 8. Beta diversity as measured by Principal component analysis (PCA).
The different colors in PCA score plots represent different groups (LF, HF, and HFUT). The closer the sample distance represents the more similar the microbial composition between samples. PERMANOVA showed significant differences (pseudo-F = 3.11, P = 0.001).

4.3.3. Comparative Analysis of the Gut Microbial Composition

At the phylum level, Firmicutes was the most abundant, followed by Bacteroidetes and Actinobacteria (Figure 9A). While the most abundant classes were Actinobacteria, Bacteroides, Bacilli, Clostridia, and Erysipelotrichi (Figure 9B).

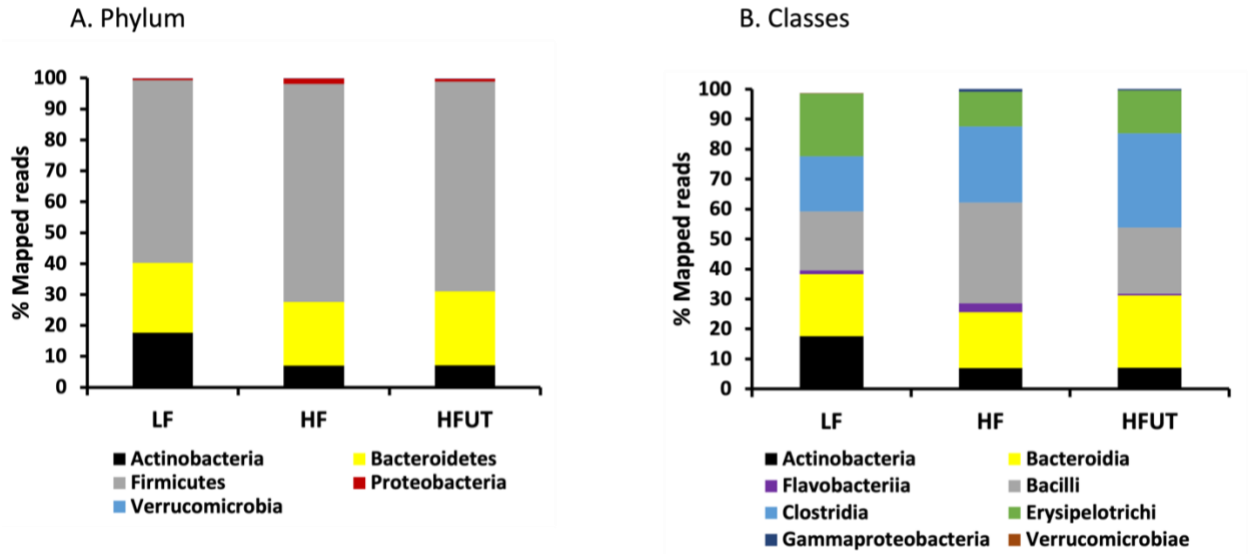

Figure 9. Stacked bars of relative abundance.
The Y-axis represents the relative abundance presented as the percentage. (A) Relative abundance of the top 5 phyla. (B) Relative abundance of the top 8 classes.

4.3.4. Comparative Analysis of the Phylum Firmicutes

The HF diet increased Firmicutes by 19% compared to the LF diet. The HFUT diet lowered the abundance of Firmicutes, but not significantly. Within the phylum Firmicutes, the HFUT diet reduced class Bacilli by 34.3% but further increased the class Clostridia by 24% compared to the HF diet group. Among class Clostridia, the HFUT diet increased genus *Clostridium* compared to both LF and HF diet groups, particularly the species *C. vincentii* and *C.* disporicum (**Error! R eference source not found.**A). Although the HF diet reduced the number of bacteria in class *Erysipelotrichi* and family Erysipelotrichaceae, it increased the genus *Turicibacter* in this class by 3-fold (Figure 10B).

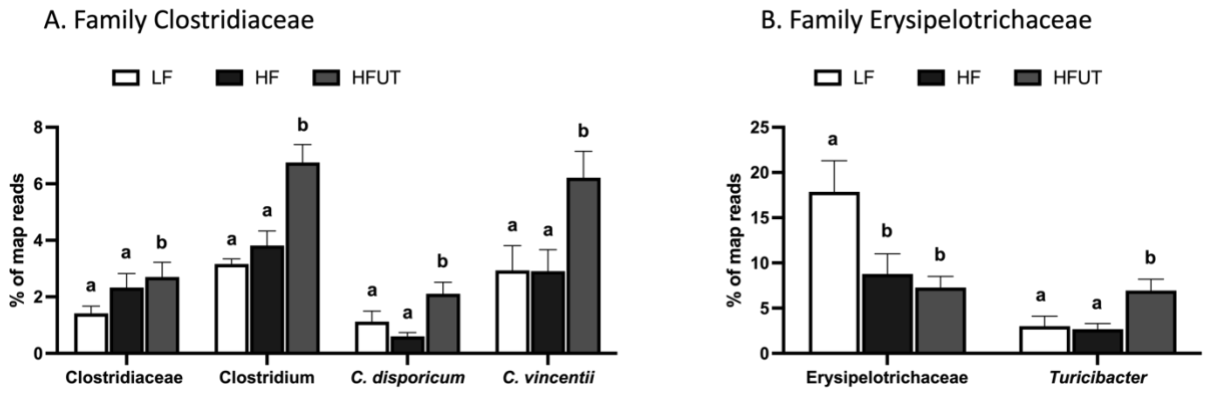

Figure 10. Comparative analysis of phylum Firmicutes.
(A) Among Clostridia, the HF had no effect on Clostridiaceae or *Clostridium*. The HFUT diet increased Clostridiaceae and species among *Clostridium* to levels higher than those of both the HF and LF diets. (B) The HF diet overall lowered Erysipelotrichia/Erysipelotrichaceae compared to the LF diet, while the HFUT had no significant effect. However, HFUT increased the genus *Turicibacter* compared to the LF and HF diets. [a]Different letters indicate significant differences between the groups ($p<0.05$; $n=9$).

4.3.5. Linear Discriminant Analysis Effect Size (LEfSe)

LEfSe was used to identify the taxa accounting for most differences between the diet groups. The effect size was shown by the logarithmic LDA score. At the threshold of 2.0, 25 taxa accounted for differences between the LF and HF diet groups. At the threshold of 4.0. only 12 taxa accounted for discriminative features between them. 28 taxa accounted for differences between the HF diet and HFUT diet groups at the threshold of 2.0, whereas only 10 taxa accounted for discriminative features at the threshold of 4.0 (Figure 11).

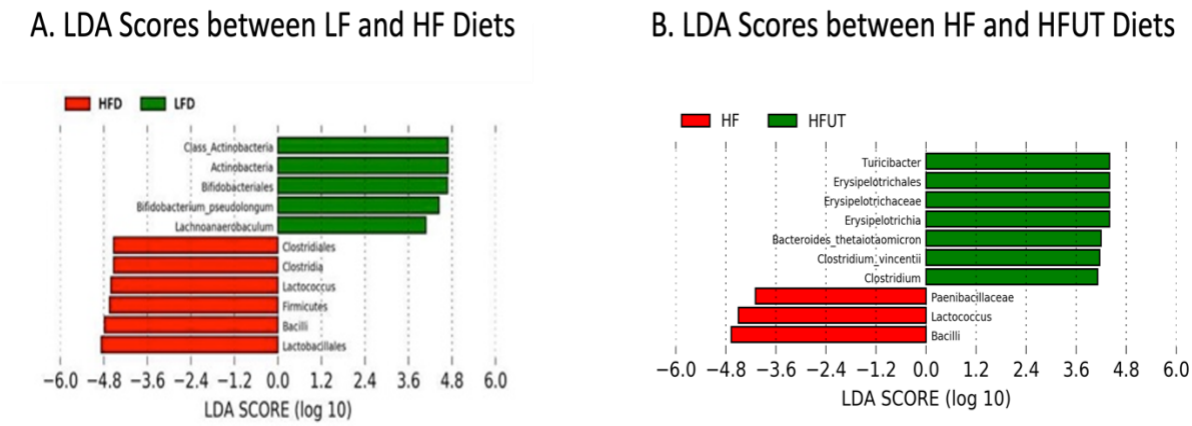

Figure 11. Linear Discriminant Analysis.
Taxonomic differences were detected and ranked according to their effect size between the groups of HF and HFUT diets. A p-value < 0.05 and a score ≥ 4.0 were considered significant.

4.3.6. Quantification of *Clostridium* and *Turicibacter* by qPCR

To validate the results got from 16S sequencing, the real-time qPCR quantification of *Clostridium* and *Turicibacter* genus was performed. The HFUT diet increased both *Clostridium* and *Turicibacter* genus compared to both the LF diet and HF diet groups (Figure 12).

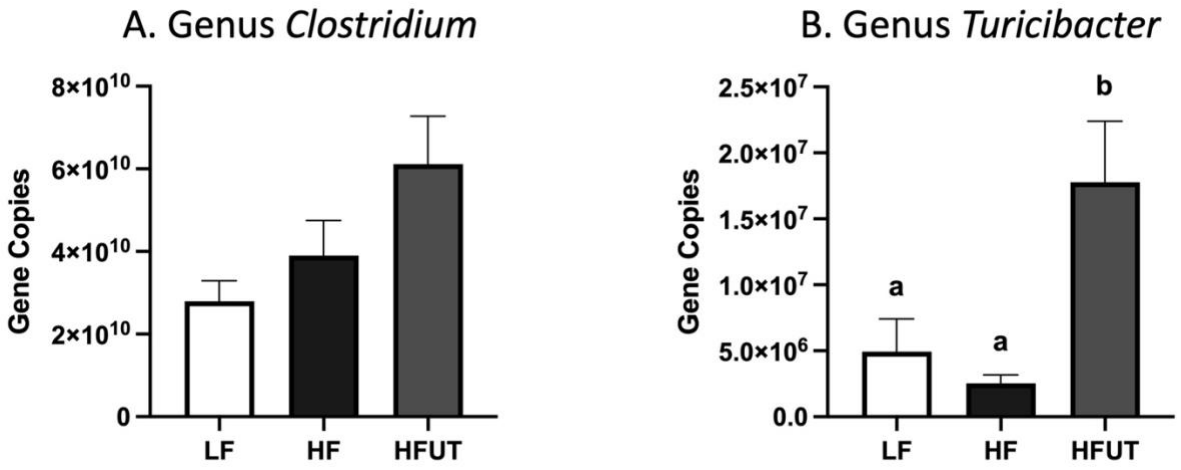

Figure 12. Comparative analysis of genus Clostridium and genus Turicibacter by qPCR. Using specific primers, *Clostridium* and *Turicibacter* were quantified with real-time qPCR, and molar concentrations were converted to gene copies. (A) The HFUT diet increased *Clostridium* (n=9). (B) The HFUT diet increased *Turicibacter* significantly ($p<0.01$, n=9). [a]Different letters indicate significant differences between the groups ($p<0.05$; n=9).

4.3.7. Pearson Correlations

Pearson correlation analyses were performed among mice fed either an HF or HFUT diet. Results demonstrated that the body weight and HOMA-IR were negatively associated with the genus of *Clostridium* and *Turicibacter*, respectively (Figure 13). No correlations were observed among other taxa.

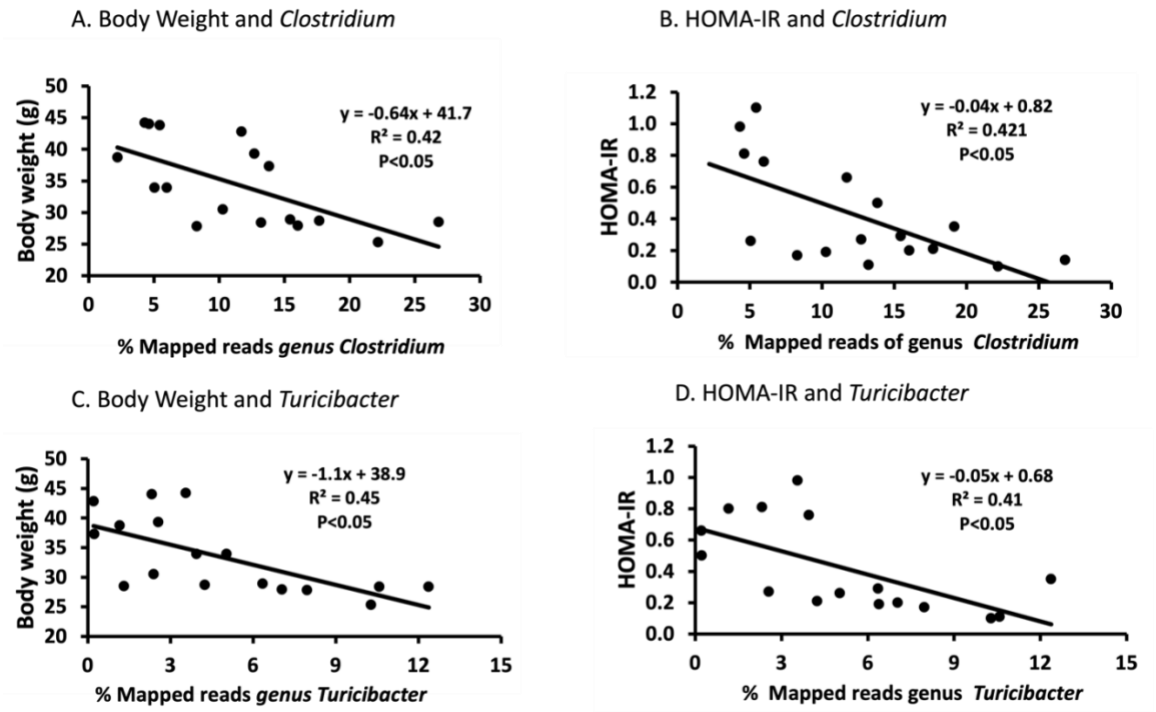

Figure 13. Body weight and insulin resistance negatively correlate with the abundance of the genus Clostridium and the genus Turicibacter.

The correlation analysis included 18 mice fed either HF diet or HFUT. Pearson correlations among body weight, HOMA-IR, and genus *Clostridium* and *Turicibacter* between HF and HFUT diets. (A-B) Correlation of body weight and HOMA-IR with the abundance of the genus *Clostridium* ($p<0.05$, $n=18$). (C-D) Correlation of body weight and HOMA-IR with the abundance of the genus *Turicibacter* ($p<0.05$, $n=18$).

4.4. Discussion

A close relationship between the intestinal microbiota and obesity exists. In agreement with several other studies, we show that diet dominantly shapes gut microbial communities. After LEfSe analysis revealed taxa that account for the differences between the dietary groups, we systematically analyzed the composition of each phylum and class to determine the magnitude by which *U. dioica* vegetable changes specific genera and species and how these correlates with weight gain and insulin resistance. Supplementing the HF diet with *U. dioica* vegetable remodeled the gut microbiota composition with the most impact being among genus and species

within Firmicutes. Specifically, the vegetable prevented HF diet induced increases in members of Bacilli but further increased Clostridia. Among Clostridia the vegetable mainly increased *Clostridium* and *Turicibacter*. In agreement with a number of previous studies we show that the abundance of these two genera negatively correlates with weight gain and insulin sensitivity.

Prebiotic vegetables chicory, Jerusalem artichokes and garlic all promote microbiota health and diversity via gut bacterial fermentation of their inulin-type fructan and oligofructose component (Liu et al., 2012; Ramnani et al., 2010). *U. dioica* did not elicit fermentation by gut bacteria; although the *U. dioica* sample contained 4.9% soluble fiber and 48.3% insoluble fiber (Table 1), there was no increase in weight of the empty and full cecum compared to LF and HF diet groups. We deduced that fermentation of the fiber components is not behind the mechanism by which *U. dioica* benefits the host. The fiber in the vegetable is not fermentable and it is likely that the phytochemicals compounds in *U. dioica* impact the gut bacteria and/or produce metabolic products that are yet to be identified. The wide range of compounds in *U. dioica* elucidated by several researchers include phenolic acids, p-hydroxybenzoic acid, gentisic acid, protocatechuic acid, vanillic acid, quinic acid, ferulic acid, p-coumaric acid, caffeic acid, and 5-O-caffeolylquinic acid. Flavanols include kaempferol, kaempferol 3-O-glucoside, quercitrin, quercetin 3-O-glucoside, quercetin 3-Orutinoside (rutin), and isorhamnetin (Orčić et al., 2014; Upton, 2013 and Otles et al., 2012). All these may individually impact obesity, insulin resistance and microbiota composition in ways that are yet unknown.

Maintenance of the diversity and collective functional capacity of the microbiota is vital for optimal metabolic health throughout life. The microbiota of *U. dioica* fed mice had overall higher alpha diversity than those of the LF or HF diets fed mice (Figure. 7A–C). There was a distinct separation between the microbiota of mice fed *U. dioica* and those fed either LF or HF

(Figure. 8). Persons whose microbiota has low gene richness (low bacterial diversity) are more likely to be obese (Kubinak et al., 2015 and Fadlallah et al., 2018). Higher diversity is associated with better health outcomes.

Supplementing the HF diet with *U. dioica* vegetable remodeled the gut microbiota composition with the most impact being among genus and species within Firmicutes. *U. dioica* did not reverse HF induced increases in Firmicutes, but within Firmicutes, significant changes among Bacilli, Erysipolotrichi, and Clostridia were observed. Specifically, the vegetable prevented HF induced increases in members of Bacilli but further increased Clostridia. Among Clostridia, *U. dioica* increased Clostridiaceae/*Clostridium* (species *C. vincentii* and *C. disporicum*) but had no effect on family Lachnospiraceae which includes Blautia, Ruminococcus, and Roseburia. Our data indicates that *Clostridium* may play an important role in obesity mechanisms and corroborates previous studies that have shown a correlation between the abundance of *Clostridium* and reduced body fat accumulation and enhanced insulin sensitivity (Shang et al., 2016; Obanda et al., 2020; Petersen et al., 2019; Atarashi et al., 2013; Atarashi et al., 2011 and Chiba et al., 2011). *Clostridium* regulates systemic immune responses through the induction of colonic regulatory T cells (Petersen et al., 2019; Atarashi et al., 2013; Atarashi et al., 2011 and Chiba et al., 2011). Petersen et al. (2019) showed that obesity induced by knockout of Myd88 in T cells caused broad reductions in the diversity and abundance of Clostridia, particularly *Clostridium* and Peptostreptococcaceae and led to fat accumulation and inflammation. Atarashi et al. (2013) identified and isolated 17 strains of Clostridia species with a high potency of enhancing intestinal regulatory T cell abundance and inducing anti-inflammatory IL-10 and inducible T-cell co-stimulator (ICOS). When the 17 strains were administered as probiotics to mice, they provided bacterial antigens, stimulated a TGF-β-rich environment,

expanded differentiation of regulatory T cells and attenuated inflammation (Atarashi et al., 2013 and Atarashi et al., 2011). The HF diet lowered class Erysipelotrichi/family Eysipelotrichaceae and *U. dioica* did not affect most taxa in this category except for genus *Turicibacter*, which was increased about 3-fold compared to the LF and HF diets. Our finding raises an important question on whether *Turicibacter* has probiotic properties against microbiota related effects on body weight or fat accumulation. This is supported by the work of other scientists, Liu et al. (2016), Everard et al. (2014), and Guo et al. (2020) have all shown that the abundance of *Turicibacter* is decreased markedly in mice fed HF. Similarly, Chávez-Carbajal (2019) showed that *Turicibacter* was 3-fold more abundant in lean women compared to those with obesity or metabolic syndrome. Linear discriminant analysis of our data to detect biomarkers revealed that among the 12 taxa that account for the differences between the HF and the HFUT diets, genus *Turicibacter* and *Clostridium* (*C. vincentii, C. disporicum*), *B. thetaiotaomicron*, and class Bacilli (Lactococcus and Paenibacillaceae) are key. The data acquired by qPCR corroborated data acquired by sequencing and shows that *U. dioica* vegetable increases the representation of *Clostridium* and *Turicibacter*. In agreement with a number of previous studies, we show that the abundance of these two genera negatively correlates with weight gain and insulin sensitivity.

U. dioica significantly increased phylum Bacteroidetes with the major shift being an increase in genus *Bacteroides*. The changes induced in Bacteroidetes were all among the species *Bacteroides thetaiotaomicron*. The metabolic function of *B. thetaiotaomicron* is to degrade plant polysaccharides. This species produces very high levels of digestive enzymes effective in the breakdown and subsequent digestion of plant polysaccharides (Wexler et al., 2007 and Xu et al., 2003)). Dietary *U. dioica* likely induced its proliferation for the purpose of producing plant polysaccharide digesting enzymes. The HF also lowered Actinobacteria, the bulk of which was

genus Bifidobacterium and *U. dioica* did not change their abundance. Bifidobacterium are saccharolytic and play an important role in carbohydrate fermentation. The lack of *U. dioica* effects on this taxon may be a contributing factor to why fermentation was not observed. The proliferation of phylum Proteobacteria is widely implicated in obesity and other diseases and our data shows that *U. dioica* vegetable prevents the proliferation of classes and families among this phylum.

Metabolic function prediction by PICRUSt2 revealed that *U. dioica* vegetable enhanced metabolism pathways of several amino acids, including beta-alanine, D-arginine, and D-ornithine. It also increased metabolic pathways for xenobiotics and riboflavin (vitamin B2). In diet induced obese rats, dietary arginine supplementation and increased metabolism have been shown to reduce fat gain, serum glucose and triglyceride concentrations, and increase skeletal muscle mass insulin sensitivity (Jobgen et al., 2009). Plasma free amino acid profile is a potential biomarker for the early detection of lifestyle related diseases and metabolic variables (Wiklund et al., 2016). Thus, the impact of *U. dioica* supplementation on amino acid metabolism may be a contributing factor to its impact on body weight and insulin resistance. Because the microbiota recognizes plant polyphenols as xenobiotics, the increased xenobiotic or drug metabolism pathway noted may have a profound role in the metabolism of phytochemicals in *U. dioica* ensuring that the metabolites are available to the host.

Overall, the significance of our finding on the role of *U. dioica* in modulating class Clostridia was further reinforced by the negative correlation observed between body weight/insulin resistance and abundance of *Turicibacter* and *Clostridium* (Figure. 13). We conclude that *U. dioica* vegetable promotes the representation of bacterial taxa associated with a lean phenotype, and enhanced insulin sensitivity. Metabolic function prediction further

demonstrates that *U. dioica* enriches amino acid metabolism pathways that contribute to reducing body weight and increasing insulin resistance. It is likely that yet to be identified bacterial metabolites from *U. dioica* phytochemicals influence bacterial composition and host phenotype. Out study is limited because it does not determine causality but, identification of *U. dioica* as a food that promotes the representation of microbes associated with the lean phenotype provides evidence of a food suitable for obesity prevention. Another limitation is that we did not sequence the diets alone to detect or ascertain dietary introduced DNA. Some HF diets containing casein introduce *Lactococcus* during manufacturing. While the HF and LF diets had equal amounts protein (casein) the diet supplemented with *U. dioica* had less casein because *U. dioica* contains about 16% protein. The HF diet elicited much higher levels of *Lactococcus* in the microbiota and HFUT prevented this. This may have partly caused the reduced amount of *Lactococcus* in the group fed *U. dioica* diet. We will aim at including this aspect in follow-up studies involving *U. dioica* vegetable.

Chapter 5: Impacts of the Vegetable *Urtica dioica* on the Intestinal T and B Cell Phenotype and Macronutrient absorption in C57BL/6J Mice with Diet-Induced Obesity*

Abstract

In two previous studies, we showed that supplementing a high-fat diet with 9% w/w *U. dioica* protects against fat accumulation, insulin resistance, and dysbiosis. This follow up study in C57BL6/J mice aimed at testing: (i) the efficacy of the vegetable at lower doses; 9%, 4% and 2%, (ii) the impact on intestinal T and B cell phenotype and secretions, (iii) impact on fat and glucose absorption during HF provision.

At all doses, the vegetable attenuated HF diet induced fat accumulation in the mesenteric, perirenal, renal fat pads and liver but not the epididymal fat pad. The 2% dose protected against insulin resistance, prevented HF diet-induced decreases in intestinal T cells and IgA^+ B cells and activated T regulatory cells (Tregs) when included both in the LF and HF diets. Increased Tregs correlated with reduced inflammation; prevented increases in IL6, IFNγ, and TNFα in intestine but not expression of TNFα in epididymal fat pad. Testing of nutrient absorption was performed in enteroids. Enteroids derived from mice fed HF supplement with *U. dioica* had reduced absorption of free fatty acids and glucose compared to enteroids from mice fed the HF diet only. In enteroids the ethanolic extract of *U. dioica* attenuated fat absorption and downregulated the expression of the receptor CD36 which facilitates uptake of fatty acids.

In conclusion, including *U. dioica* in a HF diet, attenuates fat accumulation, insulin resistance and inflammation. This may be achieved by preventing dysregulation of immune homeostasis and in the presence of HF condition, reducing fat and glucose absorption.

*The article was published in the *Journal of Nutritional Biochemistry*: Fan S, Raychaundhuri S, Ogedengbe O, Moronge V, Obanda DN. Impacts of the vegetable *Urtica dioica* on the intestinal T and B cell phenotype and macronutrient absorption in C57BL/6J mice with diet-induced obesity. *J. Nutri. Biochem.* 2024:109634.

5.1. Introduction

The genus *Urtica* comprises about 46 species that grow in a broad range of climate conditions around the world except Antarctica (Taheri et al., 2022; Kregiel et al., 2018). Among the 46 species, *Urtica dioica* (stinging nettle) and *Urtica urens* (small nettle) are the most common. Native to Europe, Africa, Asia, and North America (Kregiel et al., 2018). Shoots harvested or foraged before flowering are consumed as an herb or vegetable; spinach alternative (Kregiel et al., 2018; Ibrahim et al., 2018). Although not traditionally cultivated, nettles are abundant in supply, have been widely studied for the prevention of several diseases. The extract of *U. dioica* has been studied as an intervention for several medical conditions and dietary supplements based on the extracts are widely available. It is one of the most studied dietary supplements targeting allergy, eczema, atherosclerosis, cancer, age-related degenerative brain disorders, autoimmune diseases, such as rheumatoid arthritis, bladder disorders, hemorrhaging, inflammation, insulin resistance, and type 2 diabetes (Taheri et al., 2022; Kregiel et al., 2018; Ibrahim et al., 2018; Obanda, et al., 2016a; Obanda, et al., 2016b and Fan et al., 2020).

The phytochemical compounds in *U. dioica* include nearly 50 different lipophilic and hydrophilic compounds which include sterols, triterpenes, coumarins, phenols, flavonoids, lignans, ceramides, fatty acids, and alcohols, distributed in the roots, stem and leaves (Taheri et al., 2022; Kregiel et al., 2018; Ibrahim et al., 2018). Most studies have utilized the whole extract. Similarly, most dietary supplements available have the whole extract.

In previous studies, we have shown that the ethanolic extract of *U. dioica* is effective in preventing diet-induced insulin resistance. Specifically, the bioactive compounds protect against

lipid metabolite induced deactivation of components of the insulin signaling pathway due to a high-fat diet (Obanda, et al., 2016a; Obanda, et al., 2016b). More recently we have shown that supplementing a HF diet with the whole vegetable attenuates fat accumulation, protects against systemic insulin resistance and changes the gut microbiota composition and function (Fan et al., 2020 and 2021). Particularly *U. dioica* impacted the structure of the phylum Firmicutes, increasing the representation of the genus *Clostridium*. While this genus is well known because it is home to many pathogenic taxa like *C.difficille* or *C. botulinum*, it also houses many species that are benign and some that are beneficial. Our studies in murine obesity models have shown that animals with a high representation of *Clostridium* are resistant to diet-induced obesity (Obanda et al., 2019 and Obanda et al., 2021). Species identified in the gut microbiota of these obese resistant animals or those fed *U. dioica* include *C. celatum*, *C. disporicum* and *C. vincentii* (Fan et al., 2021; Obanda et al., 2019 and Obanda et al., 2021). The gut microbiota influences obesity phenotype through direct contact with intestinal cells or indirectly via bacterial metabolites on host cellular mechanisms. The microbiota shapes the intestinal immune system, and the immune system in turn shapes the gut microbiota (Kubinak et al., 2015; Luck et al., 2019 and Petersen et al., 2019). The microbiota and the intestinal immune system are linked by regulatory T (Treg) cells and secretory immunoglobulin A (sIgA), a B cell antibody primarily produced by plasma cells in the lamina propria. Changes in IgA-producing cells, sIgA levels and Tregs are linked to dysregulated immune homeostasis, inflammatory bowel diseases and diet-induced obesity (Kubinak et al., 2015; Luck et al., 2019 and Petersen et al., 2019). Obesity-induced reductions in IgA, worsen insulin resistance, increase intestinal permeability, microbiota encroachment, and inflammation in the intestine and metabolic tissues such as adipose (Luck et al., 2019).

The two previous dietary intervention studies in which we established that *U. dioica* vegetable is protective against diet-induced obesity, utilized a 9% vegetable w/w basis. This is too high, and not physiologically relevant especially in a human setting. In this follow-up study, we performed a dose-response study. Using tissues from the lower effective dose, we further studied the role of the vegetable on the gut immune system and used *in vitro* 3-D mini gut culture (enteroids and enteroid monolayers) to study the impact of the vegetable on glucose and free fatty acid absorption under conditions of HF provision.

5.2. Materials and Methods

5.2.1. Acquisition of Vegetable

The vegetable *Urtica dioica* L. (total herb above the root mass) used in the current and previous studies (Fan et al., 2020 and 2021) was harvested from the Green Farmacy Garden, a medicinal garden located in Fulton Maryland; latitude 39.1454180, longitude -76.9213600. The dried, washed and powdered stems and leaves were incorporated into the diets. The nutrition analysis of the vegetable using the Association of Analytical Chemists (AOAC) methods for calorific value and proximate analysis has been reported before (Fan et al., 2020).

5.2.2. Formulation of Study Diets

Our previous studies (Fan et al., 2020 and 2021) utilized 3 diets: the low fat (LF) control with 10% fat, the high fat (HF) control with 45% fat and the HF containing 9% *U. dioica* (HFUT9) (Table 2). Based on the results of study 1, a dose response is required to get a lower dose of vegetable that is physiologically relevant. Hence for this study, we formulated six diets including the LF containing 2% *U. dioica* (LFUT), the HF containing 9, 4 or 2% *U. dioica* (HFUT9,

HFUT4, HFUT2). All diets with HF were formulated to be isocaloric as shown in Table 4. Both LF diets were also formulated to be isocaloric. All diets were formulated to have the same amount of sucrose and protein considering that *U. dioica* has 16.1% protein.

Table 5. Diet Formulation for Dose-Response Study

	LF	**LFUT**	**HF**	**HFUT2**	**HFUT4**	**HFUT9**
Ingredient (g)						
Corn starch	452.2	449.8	72.8	70.87	68.84	63.92
Maltodextrin 10	75	75	100	100	100	100
Sucrose	172.8	172.8	172.8	172.8	172.8	172.8
Cellulose	50	38.4	50	40.53	30.54	6.34
Soybean oil	25	24.5	25	24.6	24.19	23.17
Lard	20	20	177.5	177.5	177.5	177.5
Casein	200	196	200	196.75	193.31	185
L-Cystein	3	3	3	3	3	3
Mineral Mix	10	10	10	10	10	10
Di calcium phosphate	13	13	13	13	13	13
Calcium carbonate	5.5	5.5	5.5	5.5	5.5	5.5
Potassium citrate	16.5	16.5	16.5	16.5	16.5	16.5
Vitamin mix	10	10	10	10	10	10
Choline Bitartrate	2	2	2	2	2	2
Urtica dioica dried powder	0	22	0	18	37	83
Total weight (g)	**1055.05**	**1058.05**	**858.15**	**861.1**	**864.23**	**871.78**
kcal						
Protein	716	715.9	716	716	716	716
Carbohydrate	2840	2839.8	1422.4	1422.4	1422.4	1422.4
Fat	405	404.9	1822.5	1822.5	1822.5	1822.5
Total kcal	**3961**	**3960.6**	**3960.9**	**3960.9**	**3960.9**	**3960.9**
Kcal (%)						
Protein	18.1	18.1	18.1	18.1	18.1	18.1
Carbohydrate	71.7	71.7	35.9	35.9	35.9	35.9
Fat	**10.2**	**10.2**	**46.0**	**46.0**	**46.0**	**46.0**
Total Kcal (%)	100	100	100	100	100	100

5.2.3. Study Animals

All data reported in this manuscript was acquired using 60 male C57BL/6J mice (Jackson Laboratories, Inc, Bar Harbor, Maine, USA). All experiments and procedures were performed in accordance to a protocol approved by the Institutional Animal Care and Use Committee (IACUC) of the University of Maryland (UMD). All mice were acquired at 7 weeks age. Mice were singly housed in shoebox cages with corncob bedding in controlled environmental conditions (22°C), 12-hour light-dark cycle with *ad libitum* access to food and water.

5.2.4. Determination of Insulin Sensitivity

Fasting (6h) blood glucose and insulin were determined at baseline (during the 1st week) from blood collected by mandibular bleeding. Blood glucose was measured using a portable glucometer (Milpitas, CA, USA). Insulin was determined by a mouse ELISA kit (Crystal Chem, Downers Grove, IL). The Insulin resistance index HOMA-IR was calculated using the formula: HOMA-IR=fasting glucose (mg/dl) x fasting insulin (ng/ml)/405 as shown before (Roza et al., 2016).

5.2.5. Sample Size Determination, Randomization and Feeding Regime

The sample size of n=9-10 for each treatment group was used based on a power analysis in our previous animal studies on obesity-induced insulin resistance, which showed 8 to be a number sufficient to generate statistically significant results. To attain a statistical power of 0.90, 8 samples are needed for a one-tailed test and 10 samples for a two-tailed test. After one week of baseline feeding on the LF diet, mice were randomized based on body weight and HOMA-IR

into six groups of 10 and the feeding study diets lasted for 12 weeks. Food intake and body weight were monitored and recorded twice weekly.

5.2.6. Euthanasia and Tissue Collection and Processing

Following 12 weeks of dietary intervention when animals were 20 weeks of age, HOMA-IR was determined as done at baseline. Two days later, animals were anesthetized by isoflurane inhalation. Terminal blood was collected by heart puncture followed by euthanasia by cervical dislocation. The serum was separated and stored at -80^{o}C to be used in later tests. The weights of the liver and spleen were determined before snap freezing.

5.2.7. Determination of fat accumulation

Abdominal fat pads (epididymal, perirenal, and retroperitoneal) and the mesenteric fat (around the intestines) were excised and their weight was determined and summed as total abdominal fat. All other tissues collected were snap frozen in liquid nitrogen and then stored at -80°C for later analysis.

5.2.8. Interscapular Brown Adipose Tissue Identification

Interscapular brown adipose tissue (iBAT) located beneath the anterior subcutaneous white adipose tissue (WAT) was separated according to the procedure shown by Bargut et al., (2017). A cut was made along the bottom of the anterior subcutaneous tissue horizontally, followed by two vertical incisions along the lateral of the depot. Using forceps to flip the depot and expose the butterfly-shaped iBAT and separate it from the surrounding WAT.

5.2.9. Immune Cell Isolation from the Intestinal Lamina Propria

Because the data showed that 2% *U. dioica* was sufficient to attenuate diet induced obesity and insulin resistance, only samples from mice fed 2% *U. dioica* were included in the following analysis. Samples from mice fed HF diet supplemented with 4% and 9% *U. dioica* were not included. The whole small intestines of LF, LFUT, HF and HFUT2 from the dose-response study were harvested from animals immediately after euthanasia for flow cytometry. To obtain samples for flow cytometry, the intestine was processed according to the procedure shown by Couter and Surana (2016). Briefly, the entire intestine was placed in 10ml cold RPMI supplemented with 10% fetal bovine serum (FBS) to maximize cell viability. After trimming off mesenteric fat and removing Peyer's patches (PP), the intestine was flushed with 15-20ml cold phosphate-buffered saline (PBS) to remove intestinal contents using an 18 G feeding needle. The cleaned intestine was cut into segments, inverted inside out, and placed in extraction media containing 30ml RPMI medium, 93ul fresh 5% (w/v) dithiothreitol (DTT), 60ul of 0.5M EDTA, and 500ul of FBS for 15 min at 37°C with vigorous stirring. After incubation, tissues were agitatedly rinsed in RPMI to remove extraction media and then minced in freshly constituted 600ul digestion medium, then transferred to 25ml RPMI, 12.5 mg dispase, 37.5 mg collagenase II, and 300ul of FBS for 30 min at 37°C with up and down pipetting. Digested tissue was filtered twice through a 100um cell strainer and rinsed with 20ml of RPMI containing 10% FBS followed by another filtration through a 40um cell strainer into Flow Cytometry Staining Buffer (Invitrogen, Carlsbad).

5.2.10. Treatment of Samples with Flow Cytometry Fluorochrome-Conjugated Antibodies

Mouse FcR Blocking Reagent was added to each sample to prevent unspecific binding, while 7-AAD (7-Aminoactinomycin D) Staining Solution was added to exclude dead cells. All antibodies and kits used to prepare samples for flow cytometry were obtained from Miltenyi Biotec (Gaithersburg, MD). To determine the total B and T cells, antibodies CD45 conjugated with APC, CD3-FITC, CD19-PE-Vio770, CD4-VioBlue, and CD8-PE were used to stain the cells. To differentiate IgA-producing B cells and plasma B cells, B220-PE and IgA-APC were used. CD4-VioBlue, CD25-PE, Foxp3-Vio67, GATA3-FITC, and RORγt-APC were used for identifying the subtypes of Tregs by intracellular staining. The IL-17 and IFN-γ secretion kits were used to identify cells producing these cytokines. All antibodies used are summarized in Table 4 below.

Table 6. Fluorochrome Conjugated Antibodies Used for Flow Cytometry

Immune cell type	Cell surface-antibody or intracellular-antibody
T cells	$CD45^+$ $CD3^+$
T helper cells	$CD4^+$ $CD25^+$
T helper subsets	$CD4^+$ $CD25^+$ $Foxp3^+$ (Tregs)
	$CD4^+$ $CD25^+$ $GATA3^+$
	$CD4^+$ $CD25^+$ $ROR\gamma t^+$
B cells	$CD45^+$ $CD3^-$ $CD19^+$
IgA-producing B cells	$CD19^+$ $B220^+$ IgA^+
Plasma B cells	$CD19^+$ $B220^-$ IgA^+

5.2.11. Cell Surface Staining

A volume containing approximately 10^6 cells (after cell counting) was aliquoted into individual tubes, centrifuged at 300xg for 10 mins at 4°C before decanting the supernatant and adding Fc-block buffer for 10 mins at 4°C followed 7-AAD, incubated in dark at room temperature (RT) for 5 mins. Cells were then washed, and cell surface-stained antibodies were added for 10 mins

at 4°C in the dark. The final wash with a 2ml flow cytometry staining buffer was performed before suspending pellets in 500ul flow cytometry staining buffer.

5.2.12. Intracellular Staining

A volume containing approximately 10^6 cells was aliquoted into single tubes and centrifuged at 300xg for 10 mins at 4°C. After washing with flow cytometry staining buffer and centrifuging into pellets, cells were resuspended in fresh fixation/permeabilization solution and incubated in the dark at 4°C. After a second wash, permeabilization buffer was added for 5 mins at 4° C after centrifuging. After repeating the washing and centrifuging, intracellular antibodies were added and incubated for 30 mins at 4°C in the dark. After a final wash in permeabilization buffer followed by 5-minute centrifugation at 4°C, cells were resuspended into 500ul flow cytometry staining buffer.

5.2.13. Cytokines Stimulation for Flow Cytometry

Cytokines IL-17 and IFN-γ were determined by secretion assay detection kits (Miltenyi Biotec Inc.). Aliquoted $1X10^6$ cells were stimulated with 2ul ionomycin and PMA (phorbol 12-myristate 13-acetate) in 1ml RPMI supplemented with 5% mouse serum and incubated at 37° C for 3 hours. After washing and centrifuging, cells were resuspended into 90ul of cold medium containing 10ul mouse IL-17 and IFN-γ catch reagent on ice for 5 mins. The warm medium was added to dilute the cells before incubation for 45 mins at 37°C, followed by labeling cells with IL-17-APC and IFN-γ-PE as described before with the cell surface staining method. Negative controls were treated the same except for the initial stimulation with ionomycin and PMA.

5.2.14. Flow Cytometry and Analysis in FlowJo

The FACSCanto II (BD Biosciences, Erembodegem, Belgium) was used to compensate for all different fluorochromes. Data obtained was analyzed by FlowJo 10.8.1 software (BD Life Sciences, Franklin Lakes, NJ). Further statistical analysis was performed by GraphPad Prism (Version 9.2.0).

5.2.15. RNA Extraction and cDNA Synthesis

RNA from 50mg WAT (epididymal fat pad) was extracted and purified using the RNAeasy lipid tissue kit according to the manufacturer's specifications. Prior to extraction, the WAT was disrupted in TRIzol with bead beating using the FastPrep®-24. Both RNA quantity and quality were determined using the Qubit 4 fluorometer. RNA samples with a concentration over 2 ng/ul and an RNA integrity number greater than 8 were used for cDNA synthesis using the high-capacity cDNA reverse transcription kit (Applied Biosystems, Vilnius, Lithuania) with 2000ng as starting RNA per sample.

5.2.16. Gene Quantification

Primer sets were used to analyze mRNA expression of selected genes involved in the browning and beiging of adipose tissue. Genes quantification included UCP1, Cidea, PRDM16, PPARα, PPARγ, PGC-1, Dio2, EBF2, FGF21, SIRT1, COX8b and two browning inhibitors ASK1 and SENP2. RT-PCR cycling conditions on the CFX 96 were 2 mins at 50°C and 2 mins at 95°C, followed by 40 cycles of three-step denaturation at 95°C for 15 seconds, annealing at 55°C for 15 seconds and extension at 72°C for 1 min. Triplicate assay samples containing 10ng cDNA, 5uM primer mix (all primers used are shown in Table 5) and PowerUp™ SYBR™ Green Master

Mix (ThermoFisher Scientific, Rockville, MD) in a final volume of 10 ul were used in the RT-PCR method. Means of triplicates were taken, and the relative amount of target mRNA were normalized to β-actin levels as an endogenous control gene. Data were analyzed according to the $2^{-\Delta\Delta CT}$ method, and the fold difference was calculated between LF and the other three groups, LFUT, HF, and HFUT2 diets. The LF group was set as a baseline for determining changes in gene expression for the other 3 groups.

Table 7. Primers Used for qPCR for Browning in Adipose Tissues

Genes	Forward Primers	Reverse Primers
β-Actin	5'-CCAGAGCAAGAGAGGTATCC-3'	5'-CTGTGGTGGTGAAGCTGTAG-3'
UCP1	5'-ACTGCCACACCTCCAGTCATT-3'	5'-CTTTGCCTCACTCAGGATTGG-3'
PGC-1α	5'-CCCTGCCATTGTTAAGACC-3'	5'-TGCTGCTGTTCCTGTTTTC-3'
PRDM16	5'-CAGCACGGTGAAGCCATTC-3'	5'-GCGTGCATCCGCTTGTG-3'
CIDEA	5'-AAACCATGACCGAAGTAGCC-3'	5'-AGGCCAGTTGTGATGACTAAGAC-3'
DIO2	5'-CTCCGAGGCATAATTGTTACCT-3'	5'-CTTCCTCCTAGATGCCTACAAAC-3'
EBF2	5'-GGAGGTGCTGTAATTAGATTGCT-3'	5'-GTCAGCATTTCAGAGTCCACA-3'
FGF21	5'-CGTCTGCCTCAGAAGGACTC-3'	5'-TCTACCATGCTCAGGGGGTC-3'
BMP7	5'-GCGTTCATGTAGGAGTTCAGA-3'	5'-GTCAGCTTCCGAGACCTTG-3'
LXR	5'-CATTCATGGCTCTGGAGAACT-3'	5'-GAGAGCATCACCTTCCTCAA-3'
SENP2	5'-CATTCCACAGTCACTCCCATT-3'	5'-TACAGGATGAAAGCAAGACCA-3'
ASK1	5'-TGTAATCCTCAGCCAGAAACC-3'	5'-AGTCCCAGCCCATAGATATCC-3'
SIRT1	5'-TGCTGGCCTAATAGAGTGGCA-3'	5'-CTCAGCGCCATGGAAAATGT-3'
COX8b	5'-GAACCATGAAGCCAACGACT-3'	5'-GCGAAGTTCACAGTGGTTCC-3'
PPARα	5'-ATGCCAGTACTGCCGTTTTCA-3'	5'-GGGCCTTGACCTTGTTCATGT-3'
PPARγ	5'-TGTGGGGATAAAGCATCAGGC-3'	5'-CCGGCAGTTAAGATCACACCTAT-3'

5.2.17. Isolation of Mouse Intestinal Crypts

Procedures used were those prescribed by Stem Cell Technologies under sterile conditions. Briefly, at euthanasia, 20cm of small intestine proximal to the stomach was removed and placed into cold PBS, trimmed of fat, flushed with cold DPBS to remove the contents, opened lengthwise, and rinsed severally with cold PBS. The sample was cut into 2 mm pieces and placed in cold PBS in a 50 ml tube and washed at least 20 times with fresh DPBS each time. After

washing 20 times, samples settled down at the bottom and were resuspended in 25 ml gentle cell dissociation reagent (GCDR) and incubated at room temperature for 15 mins on a rocking platform at 25 rpm. After incubation, tissue pieces resuspended in 10 ml cold DPBS containing 0.1% BSA were filtered through a 70um filter. The process was repeated on all sections original tissue by resuspending them in DPBS containing 0.1% BSA to generate 2–4 fractions. After centrifuging and decanting, each fraction was resuspended in fresh 10ml DPBS containing 0.1% BSA, centrifuged at 200xg for 3 mins at 4°C, and decanted to leave intestinal crypts in tubes.

5.2.18. Establishment of Intestinal Organoids

Each fraction of crypts was resuspended in 10 ml cold DMEM/F-12. About 1 ml was added to a 6-well plate for checking under the light microscope. The fraction most enriched with intestinal crypts and without much debris was selected, centrifuged at 200xg for 5 mins at 4° C, supernatant pipetted off and Matrigel added to the pellets. About 50 ul of Matrigel pellets with sample were placed on a warm 24-well plate and incubated at 37°C for 10 mins. Once the Matrigel was set, 750 ul of RT complete IntestiCult Organoids Growth Medium (StemCell Technologies, MA, Cambridge) containing penicillin-streptomycin was added. The medium was changed every two days and enteroids passaged every 7 – 10 days.

5.2.19. Passaging Mouse Intestinal Organoids

To passage organoids, the culture medium was removed from each of the wells, 1ml of GCDR was added to the dome, and the plate was incubated at RT for one minute. A pre-wetted 1000ul pipette tip was used to break up the dome by pipetting up and down 20 times before transferring the contents into a 15 ml conical tube incubating at RT for 10 mins on a rocking platform at 25

rpm and centrifuge at 300xg for 5 mins at 4°C followed by rinsing with 10 ml cold DMEM/F-12 followed by a second centrifuge. Matrigel was then added to the pellet and the processes of seeding domes on a 24-well plate were repeated.

5.2.20. Preparing Mouse Intestinal Organoids-Derived Monolayers

Monolayers were generated for use in studying extended nutrient transport (mimicking absorption). After passaging enteroids 3 times, organoids were transitioned from a mouse medium into IntestiCult Organoids Growth Medium Human media (StemCell Technologies, MA, Cambridge) for one passage before generating monolayers. After the passage, the culture was coated with Matrigel diluted in DPBS (1ul:49ul). Three domes of Matrigel are needed for each monolayer. After dissociating the Matrigel domes containing organoids as shown above for passaging, each sample was washed with 3 ml cold DMEM/F-12, centrifuged and pellets resuspended in 1 ml of warm 0.05% of Trypsin-EDTA to dissociate the organoids into single cells as much as possible. After centrifuging at 200xg for 5 mins at 4° C, the pellet was resuspended in IntestiCult Monolayer Growth Medium with ROCK inhibitor Y-27632. The growth and development of confluency in monolayers was monitored using the Transepithelial electrical resistance (TEER) meter (World Precision Instruments, Sarasota, FL).

5.2.21. Preparation of Free Fatty Acids

Media containing lipids was prepared by conjugating sodium palmitate (Sigma Aldrich, St Louis MO) with fatty acid-free bovine albumin serum (BSA) (Sigma Aldrich, St Louis MO). Briefly, a 50ml stock solution of 1000uM sodium palmitate in DMEM was prepared by dissolving 13.75mg sodium palmitate in 600ul DI water at 90°C (in a heat block). While maintained at

90°C, the dissolved fatty acid was added to 50ml warm media (40°C) in 20 ul increments while stirring rapidly with a magnetic stirrer. After all fatty acids had been added, the solution was filtered using a sterile 0.2μm filter and stored at 4°C for use in later experiments.

5.2.22. Fatty Acids Absorption and Transportation Tests

In confluent enteroid monolayers of the four treatment groups, 400 uM sodium palmitate conjugated with BSA was added to the media in the apical chamber and incubated for 16 hours at 37°C in 5% CO_2. Media from the basolateral chamber was collected after 16 hours. The total amount of triglycerides in the basolateral layer was quantified using the triglyceride colorimetric Assay Kit (Cayman, MI, USA).

5.2.23. Glucose Absorption and Transportation Tests

The procedures used were described by Hasan et al. (2021). Briefly, confluent enteroid monolayers were washed with 5 mM mannose buffer (50 mM of HEPES pH 7.4, 128 mM of NaCl, 4.7 mM of KCl, 1.25 mM of $MgSO_4$, 1.25 mM of $CaCl_2$, and 5 mM of mannose). After 30 min of incubation at 37°C, the solution from the basolateral layer were collected and marked as t = 0. Immediately, 100ul of 50 mM glucose solution was added in the apical chamber, while 600ul of 5 mM mannose buffer was added in the basolateral chamber. After 2 hours of incubation at 37° C in 5% CO_2, the basolateral solution from each well was collected and analyzed for glucose content using the Glucose Assay Kit (Sigma Aldrich, MA, USA).

5.2.24. RNA Extraction, cDNA synthesis and RT-qPCR

RNA was separately extracted from adipose tissue, small intestinal tissue and enteroids. In 2ml tubes, 100mg of epididymal fat or 10mg intestinal tissue (duodenum) was disrupted by bead beating in TRIzol using the FastPrep®-24 (MP Biomedical, Solon, Ohio) homogenizer. Enteroids were collected in TRIzol. The on-column RNA extraction procedure described in the RNeasy lipid tissue kit (Qiagen, Germantown, MD, USA) was used. RNA quantity and quality were determined by the Qubit 4 fluorometer (ThermoFisher Scientific, Rockville, MD) and only samples with RNA integrity higher than 8 were used for cDNA synthesis using the High-Capacity cDNA Reverse Transcription Kit (Qiagen, German Town, MD) with 2000ng as starting RNA. A starting amount of 10ng cDNA, 5uM primer mix (all primers used are shown in Table 6) and PowerUp™ SYBR™ Green Master Mix (ThermoFisher Scientific, Rockville, MD) in a final volume of 10 ul were used in the RT-PCR method. The cycling program was 2 mins at 50°C, 2 mins at 95°C, followed by 40 cycles of three-step denaturation at 95°C for 15 secs, annealing at 55°C for 15 secs and extension at 72°C for 1 min. Relative amounts of target mRNA expression were normalized to β-actin levels as an endogenous control. Data were analyzed using the $2^{-\Delta\Delta CT}$ method and fold changes were compared between groups. All samples were run in triplicates.

Table 8. Primers used for qPCR in Small Intestines and Enteroids

Genes	Forward Primers	Reverse Primers
β-Actin	5'-CCAGAGCAAGAGAGGTATCC-3'	5'-CTGTGGTGGTGAAGCTGTAG-3'
TGF-β	5'-GACCGCAACAACGCCATCTA-3'	5'-GGCGTATCAGTGGGGGTCAG-3'
IL-10	5'-ATGGCCTTGTAGACACCTTG-3'	5'-GTCATCGATTTCTCCCCTGTG-3'
IL-1	5'-GTGCCAGTTTCGATCCGTAGA-3'	5'-GGGCCACAGAGCACCAATCTGTG-3'
IL-1β	5'-CCAGCTTCAAATCTCACAGCAG-3'	5'-CTTCTTTGGGTATTGCTTGGGATC-3'
IL-6	5'-TCCTTAGCCACTCCTTCTGT-3'	5'-AGCCAGAGTCCTTCAGAGA-3'
IL-17A	5'-AACACTGAGGCCAAGGACTT-3'	5'-ACCCACCAGCATCTTCTCG-3'
IFN-γ	5'-CGGCACAGTCATTGAAAGCCTA-3'	5'-GTTGCTGATGGCCTGATTGTC-3'
TNF-α	5'-CACAGAAAGCATGATCCGCGACGT-3'	5'-CGGCAGAGAGGAGGTTGACTTTCT-3'
NFκB	5'-GAGTTTGCGGAAGGATGTCT-3'	5'-TGTCTGCCTCTCTCGTCTT-3'
iNOS	5'-CACCTTGGAGTTCACCCAGT-3'	5'-ACCACTCGTACTTGGGATGC-3'
IL-21	5'-GGTTTGATGGCTTGAGTTTGG-3'	5'-TGACTTGGATCCTGAACTTCTATC -3'
CD36	5'-TGGCCTTACTTGGGATTGG-3'	5'-CCAGTGTATATGTAGGCTCATCCA-3'
Mogat1	5'-GTATGTCTGATGCAGCTCTTCA-3'	5'-TTCCAGCACTACTTTGGCATA-3'
Mttp	5'-AATTAAGCCTTCCAGCCCTT-3'	5'-ACAGCCTTGACATCCTTTACTC-3'
Npc1l1	5'-GGACTGGAAGGACCATTTCC-3'	5'-GACAGGTGCCCCGTAGTCA-3'
Lipe	5'-CCATATTGTCTTCTGCGAGTGT-3'	5'-GGCGAAAAGGCAAGATCAAAG-3'
Dgat1	5'-CACCAGGATGCCATACTTGA-3'	5'-TCTTTGTTCAGCTCAGACAGTG-3'
Dgat2	5'-ATGGTACAGGTCGATGTCTTTC-3'	5'-CCTCTTCTCCTCTGACACCT-3'
Fabp1	5'-CCCTTGATGTCCTTCCCTTTC-3'	5'-TTGCCACCATGAACTTCTCC-3'
Fabp4	5'-GCTTTGCTCAGGTCTTGGA-3'	5'-CAGCGGGTCTTTCACAATAG-3'
PPARα	5'-ATGCCAGTACTGCCGTTTTCA-3'	5'-GGGCCTTGACCTTGTTCATGT-3'
PPARγ	5'-TGTGGGGATAAAGCATCAGGC-3'	5'-CCGGCAGTTAAGATCACACCTAT-3'

5.2.25. Statistical Analysis

Data were expressed or graphed as mean ± SEM. Differences between the two groups were assessed using the unpaired two-tailed student T-tests. Data sets with more than two groups were analyzed using a one-way ANOVA performed by GraphPad Prism for analysis of variance between different treatments. When significant differences were observed, post hoc tests were performed using Tukey's test of multiple comparisons. Effects were considered significant at $P \leq 0.05$.

5.3. Results

5.3.1. Food Consumption, Energy Intake and Body Weight Gain

Similar findings in the dose-response study, weekly food consumption was not significantly different between the control and 5 treatment groups (Figure 14A; p=ns; n=10). Daily energy intakes were not different in LF diet groups and HF diet groups, respectively (Figure 14B). As expected, the HF diet group significantly increased body weight compared to the LF diet group. Supplementing the HF diet with *U. dioica* at all doses significantly attenuated weight gain compared to the HF diet alone over the 12 weeks (Figure 14C and D) ($p<0.05$; n=10). No dose-response effect was observed between the 2%, 4% and 9% *U. dioica*. Including *U. dioica* in the LF diet had no effect on body weight (p=ns).

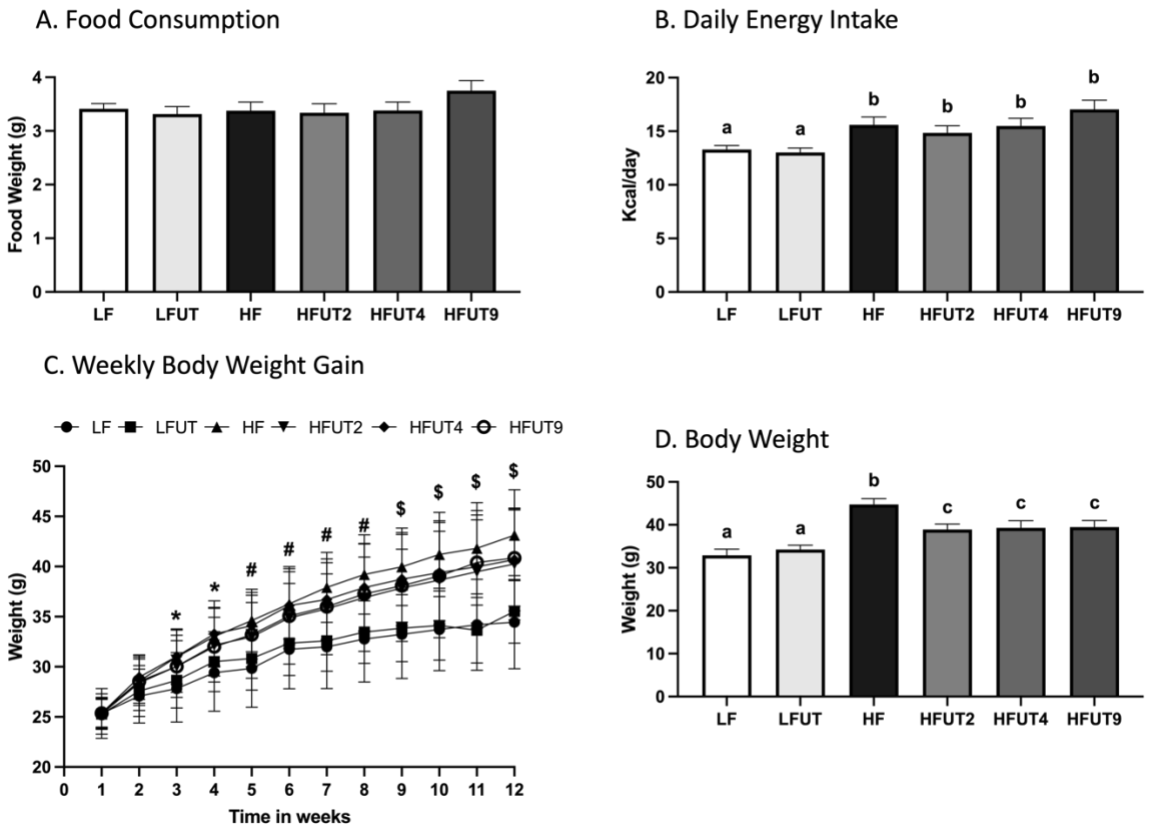

Figure 14. Supplementation with U. dioica lowered body weight.
Mice were fed with test diets for 12 weeks. Food intake was determined twice per week by determining the input and output weight plus any spillage in the cages. (A). Weekly food consumption was not different among all groups. (B). The calculated calorie consumption per day was not different among LF groups and HF groups, respectively. (C-D). The HF diet induced greater body weight gain compared to the LF diet. The Supplementation of the HF diet with *U. dioica* at all 3 doses attenuated body weight compared to the HF diet. [a]Different letters indicate significant differences between the groups ($p<0.05$; n=10).

5.3.2. Fasting Glucose, Fasting Insulin and Insulin Resistance

In the dose-response study, no difference in fasting glucose, fasting insulin and HOMA-IR were observed between the LF and LFUT groups (p=ns). As expected, the HF diet induced significantly higher fasting glucose compared to that of the LF and LFUT diet groups. Groups fed the HF diet supplemented with *U. dioica* at all 3 doses had lower fasting glucose compared to the HF diet group. The fasting glucose of HFUT2 was significantly lower than that of HFUT4

and HFUT9 (Figure 15A; $p<0.05$; n=10). As expected, the HF diet induced significantly higher fasting insulin compared to that of the LF and LFUT diet groups. However, the impact of *U. dioica* on fasting insulin in the HF groups varied depending on the doses. Only the lowest *U. dioica* dose of 2% attenuated fasting insulin. The 4% and 9% *U. dioica* did not reduce fasting insulin compared to the control HF diet (Figure 15B; p=ns). The calculated HOMA-IR index of insulin resistance mirrored the results of fasting insulin. The HF diet increased HOMA-IR compared to the LF and LFUT diet groups. The impact of *U. dioica* on HOMA-IR in the HF groups depended on the dose of *U. dioica*. Only the lowest *U. dioica* dose of 2% attenuated HOMA-IR (Figure 15C; $p<0.05$). The 4% and 9% *U. dioica* did not reduce HOMA-IR compared to the control HF diet (Figure 15C; p=ns).

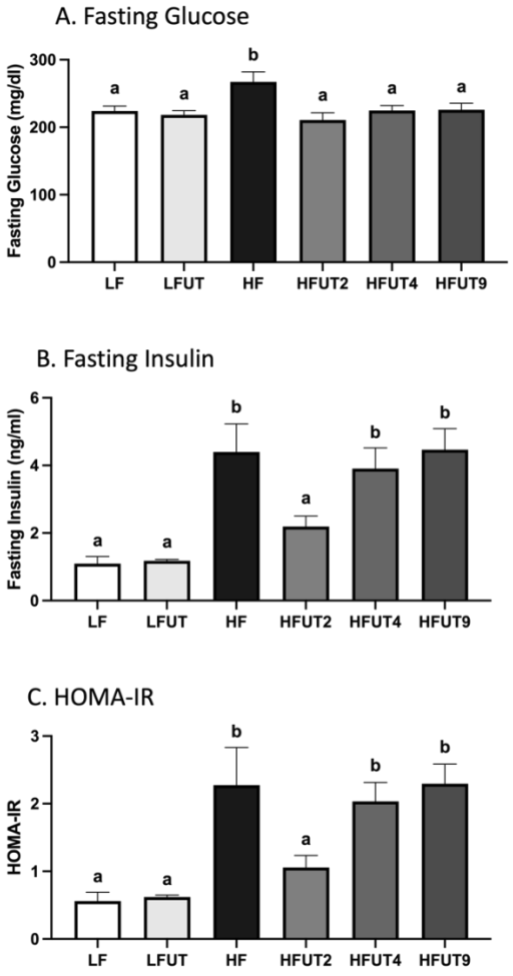

Figure 15. Effects of U. dioica vegetable on fasting glucose, fasting insulin and insulin resistance.

Fasting glucose determined by glucometer and fasting insulin determined by ELISA kit were used to calculate HOMA-IR. (A). Including *U. dioica* in both LF and HF diet at all doses lowered fasting glucose ($p<0.005$). (B). Including *U. dioica* in the LF lowered fasting insulin, but among the HF diets, only the 2% *U. dioica* dose lowered fasting insulin. (C). Including *U. dioica* in the LF diet lowered HOMA-IR, but among the HF diets, only the 2% *U. dioica* dose lowered HOMA-IR. [a]Different letters indicate significant differences between the groups ($p<0.05$; n=10).

5.3.3. Weight of the Spleen and Correlation with Insulin Resistance

In the dose-response study, the HF diet significantly increased the weight of the spleen compared to the LF diet. Dietary *U. dioica* increased the weight of the spleen compared to the LF diet (Figure 16A; $p<0.05$). Including *U. dioica* in the HF diets decreased spleen weight only at the

lowest dose of 2% (Figure 16A; p<0.05). The 4% and 9% *U. dioica* doses did not lower the weight of the spleen compared to the HF diet (Figure 16A; p=ns). A positive correlation was observed between insulin resistance and spleen weight (Figure 16B; p<0.05; n=10).

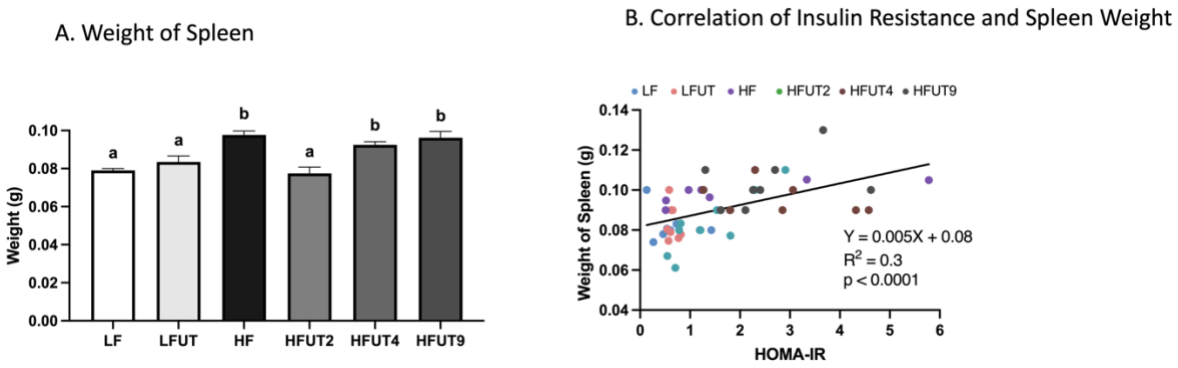

Figure 16. Effects of U. dioica vegetable on insulin resistance and spleen weight.
(A). The weight of the spleen in HF diet group increased compared to LF diets. Including 2% *U. dioica* in the HF diet attenuated spleen weight increase (p<0.0001) but the 4% and 9% *U. dioica* did not attenuate HF diet induced increased in spleen weight (p=ns). (B). Positive correlations between the weight of the spleen and HOMA-IR are significant (p<0.05). [a]Different letters indicate significant differences between the groups (p<0.05; n=10).

5.3.4. Fat Accumulation in Adipose Tissue

In the dose-response study, the HF diet induced fat accumulation in the mesenteric (depot around the intestines), perirenal, retroperitoneal and epididymal fat pads compared to the LF diet. The vegetable had no effect on fat pads' weight in the LF diet (p=ns). Compared to the HF diet, including *U. dioica* in the HF diet at all doses prevented fat accumulation in the mesenteric, perirenal and retroperitoneal fat pads (Figure 17A-C; p<0.001) but not the epididymal fat pad (p=ns). However, summing up the weight of all fat pads showed that *U. dioica* significantly attenuated HF diet-induced fat accumulation (Figure 17D; p<0.05). With 2% *U. dioica* the decrease in abdominal fat was 17%, with 4% the decrease was 26%, and with 9% the decrease was 24% (Figure 17D). The weight of the interscapular brown adipose tissue fat pad (BAT) was

not affected by the fat content of diet (not different in LF and HF diets), but it increased in mice fed the HF diets supplemented with 4% and 9% *U. dioica* but not 2% **(**Figure 17E).

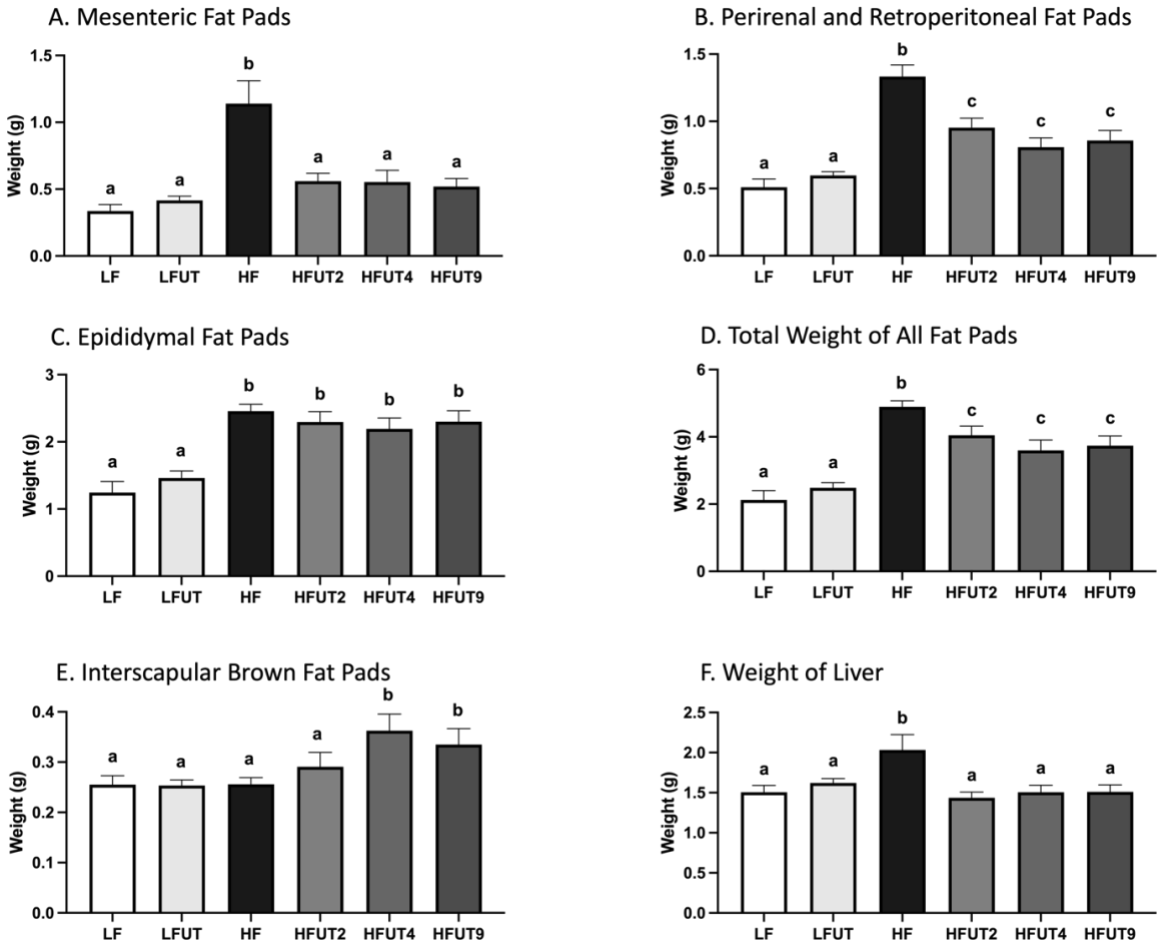

Figure 17. Supplementation with U. dioica attenuated the fat accumulation in the adipose tissues and in the liver.

The different fat depots were dissected and weighed at euthanasia. (A-C). Including *U. dioica* in the LF diet had no effect on fat mass in all depots (p=ns; n=10). Compared to the LF control, the HF diet induced an increase in fat mass in all depots ($p<0.001$; n=10). Including *U. dioica* in the HF diet prevented weight increases in the mesenteric, perirenal and retroperitoneal ($p<0.001$; n=10), but not the epididymal fat pad (p=ns). (D). Summing up all fat pads showed that including *U. dioica* in the LF diet had no effect on fat mass (p=ns; n=10). Compared to the LF control, the HF diet induced an increase in fat mass ($p<0.05$; n=10) and including *U. dioica* in the HF diet attenuated weight increases ($p<0.05$; n=10). (E). The weight of the interscapular BAT tissue was not different between LF and HF diet groups (p=ns). Compared to the HF diet, supplementation with 4% and 9% *U. dioica* increased BAT ($p<0.05$; n=10) but 2% *U. dioica* had no effect (p=ns; n=10). (F) Including *U. dioica* in the LF diet had no effect on liver weight (p=ns; n=10). Compared to the LF control, the HF diet induced an increase in liver weight ($p<0.01$; n=10). Including *U. dioica* in the HF diet prevented increases in liver weight ($p<0.001$; n=10). [a]Different letters indicate significant differences between the groups ($p<0.05$; n=10).

5.3.5. Liver Weight

In the dose-response study, the vegetable had no effect on liver weight in the LF group (Figure 17A; p=ns). The HF diet increased liver weight compared to the LF diet. At all doses, *U. dioica* prevented HF diet induced accumulation of fat in the liver; the weight of the liver was not different from the LF diet (Figure 17F; $p<0.01$).

5.3.6. T Cell Population and Subtypes

The total number of T cells was determined, followed by the population of $CD4^+$ T cells and $CD8^+$ T cells (Figure 19A-C). To determine Tregs, the singlet population was gated first, followed by lymphocyte gating. Treg cells were recognized as $CD4^+CD25^+Foxp3^+$ cells (Figure 19D). Compared to the LF diet, total T cells identified as $CD45^+CD3^+$ were decreased by a HF diet. Including *U. dioica* in the HF diet attenuated the decrease in total T cells (Figure 19A; $p<0.05$). The population of $CD4^+$ T cells was not changed by *U. dioica* in the LF diets. A HF diet increased the amounts of $CD4^+$ T cells and *U. dioica* had no effect (Figure 19B; p=ns). The cytotoxic T cells population ($CD8^+$ T cell) was not different between all 4 groups (Figure 19C; p=ns). The T regulatory cells were determined as the percentage of $CD4^+CD25^+$ cells intracellularly expressing $FOXP3^+$. There was no difference in Tregs between LF and HF diet groups. Supplementing both the LF and HF diet groups with *U. dioica* vegetable increased the population of Tregs (Figure 19D; $p<0.001$), indicating that the vegetable induced $CD4^+$ T cells antigenic stimulation. Determination of the T helper subset expressing the transcription factor RORγt common in the GI tract showed no differences between all treatment groups. However, supplementation with *U. dioica* in both LF and HF diets increased $ROR\gamma t^+$ cells, though not to a significant level (Figure 19E; p=ns). Determination of T helper subset expressing the canonical

Th2 transcription factor GATA3 that is common in the GI tract showed no differences between all treatment groups (Figure 19F; p=ns).

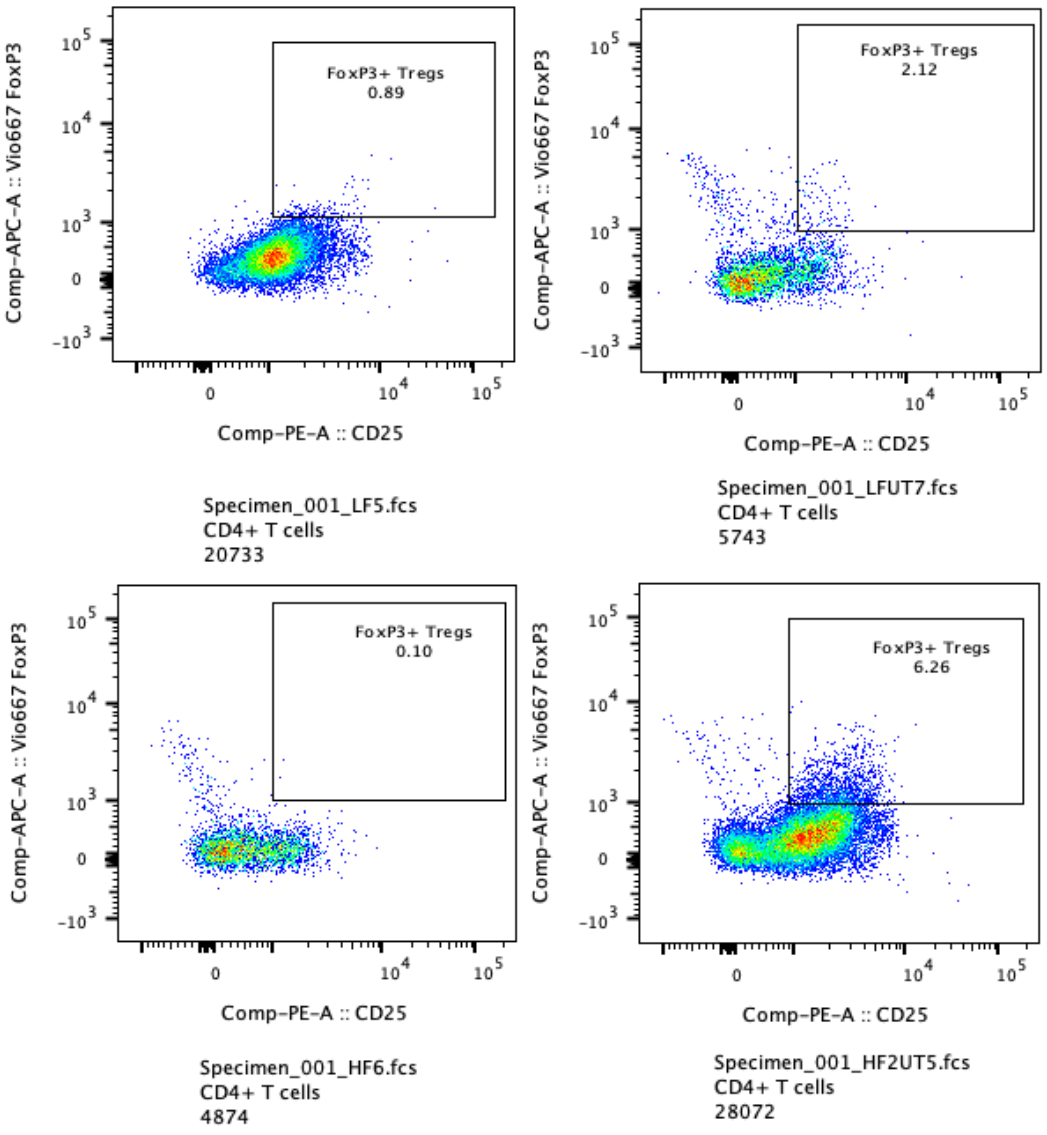

Figure 18. The representative pseudocolor plots of Tregs from LF, LFUT, HF and HFUT2 groups.

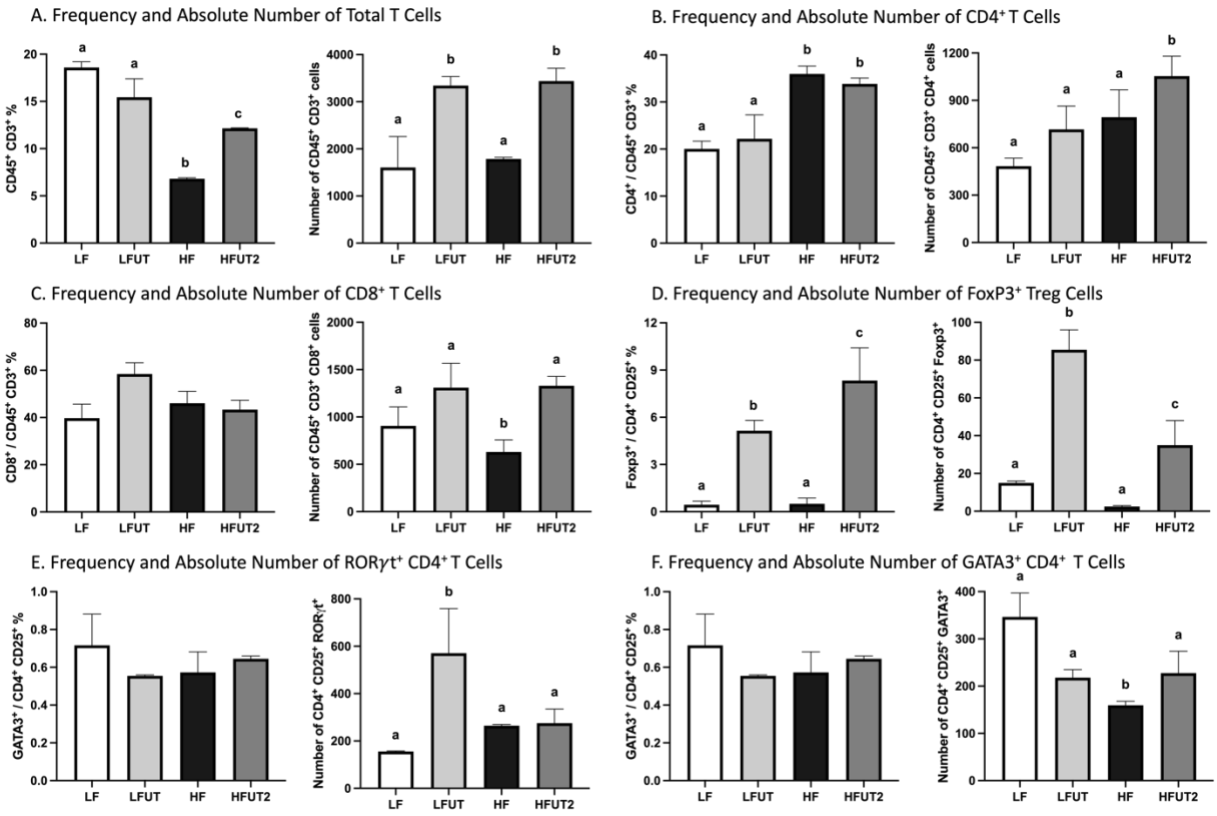

Figure 19. Effects of U. dioica on intestinal immune cell phenotype of T cells.
Cells isolated from the lamina propria of the whole intestine were incubated in blocking buffer to prevent unspecific binding, incubated in 7-AAD staining solution to exclude dead cells and then re-stained in fluorophore-conjugated monoclonal antibodies targeting different subsets of T and B immune cells. (A). The population and number of $CD45^+$ $CD3^+$ T cells was reduced by the HF diet. Supplementation with *U. dioica* prevented this decrease ($p<0.05$; n=4). (B). The HF diet increased the $CD4^+$ cell population among T cells ($p<0.05$; n=4) and *U. dioica* supplementation did not change this (p=ns; n=4). (C). The population and number of $CD8^+$ cells were not different between all dietary groups (p=ns). (D). The population and number of Tregs was increased by *U. dioica* supplementation both in LF and HF diet groups ($p<0.001$; n=4). (E and F). The population and number of $CD4^+$ T cells expressing RORγt and GATA3 transcription factors were not different among the treatment groups (p=ns). [a]Different letters indicate significant differences between the groups ($p<0.05$; n=4).

5.3.7. B Cell Population and Subtypes

The total number of B cells was determined after gating for singlets, live or dead, and lymphocytes (Figure 20A). IgA-producing ($B220IgA^+$) and plasma cells ($B220^-$ IgA^+) were separated based on B cell selection. Quantification of total B cells and IgA producing B cells did not show significant differences among diet groups (Figure 20B; p=ns). The HF diet group reduced the IgA-producing B cell population compared to the LF diet group. However,

supplementation with *U. dioica* did not restore either IgA-producing B cells or plasms B cells (Figure 20B).

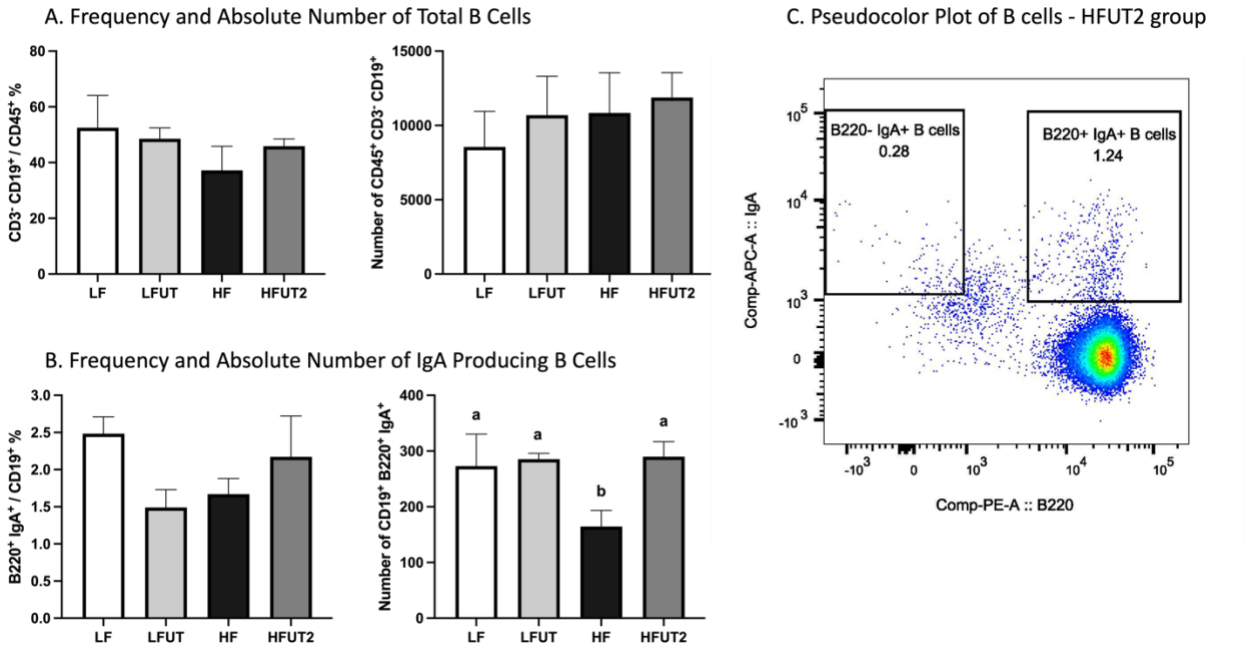

Figure 20. Effects of U. dioica on intestinal immune cell phenotype of B cells.
(A & B). Total B cells and IgA-producing B cells were not significantly different from all diet groups. (C) The representative pseudocolor plots of B cells from the HFUT2 group.

5.3.8. Cytokine Secretions in the Small Intestinal LP

Cytokines IL-17 and IFN-γ were determined by secretion assays that involved stimulating $CD4^+$ T cells with ionomycin and PMA before resuspending them in IL-17 and IFN-γ catch reagents and then labeling cells with respective antibodies before flow cytometry. Results showed that the HF diet lowered IL-17 secretion in $CD4^+$ T cells. Supplementation with *U. dioica* attenuated these and increased IL-17 secretion (Figure 21A; $p<0.05$). The HF diet increased IFN-γ secretion in $CD4^+$ T cells. Supplementation with *U. dioica* protected against this increase (Figure 21C; $p<0.001$). Cytokine secretions were quantified in the negative control and stimulated treatments

and calculated by subtracting the count number of the negative control group from the count number of the stimulation group (Figure 21E & 21F).

5.3.9. Gene Quantification

A follow-up of gene expression by qPCR of IL-17 and IFN-γ in small intestinal tissue showed that *U. dioica* vegetable enhanced expression of IL-17 when included in both LF and HF diets (Figure 21B; $p<0.01$), while attenuating expression of IFN-γ when included in both LF and HF diets (Figure 21D; $p<0.01$).

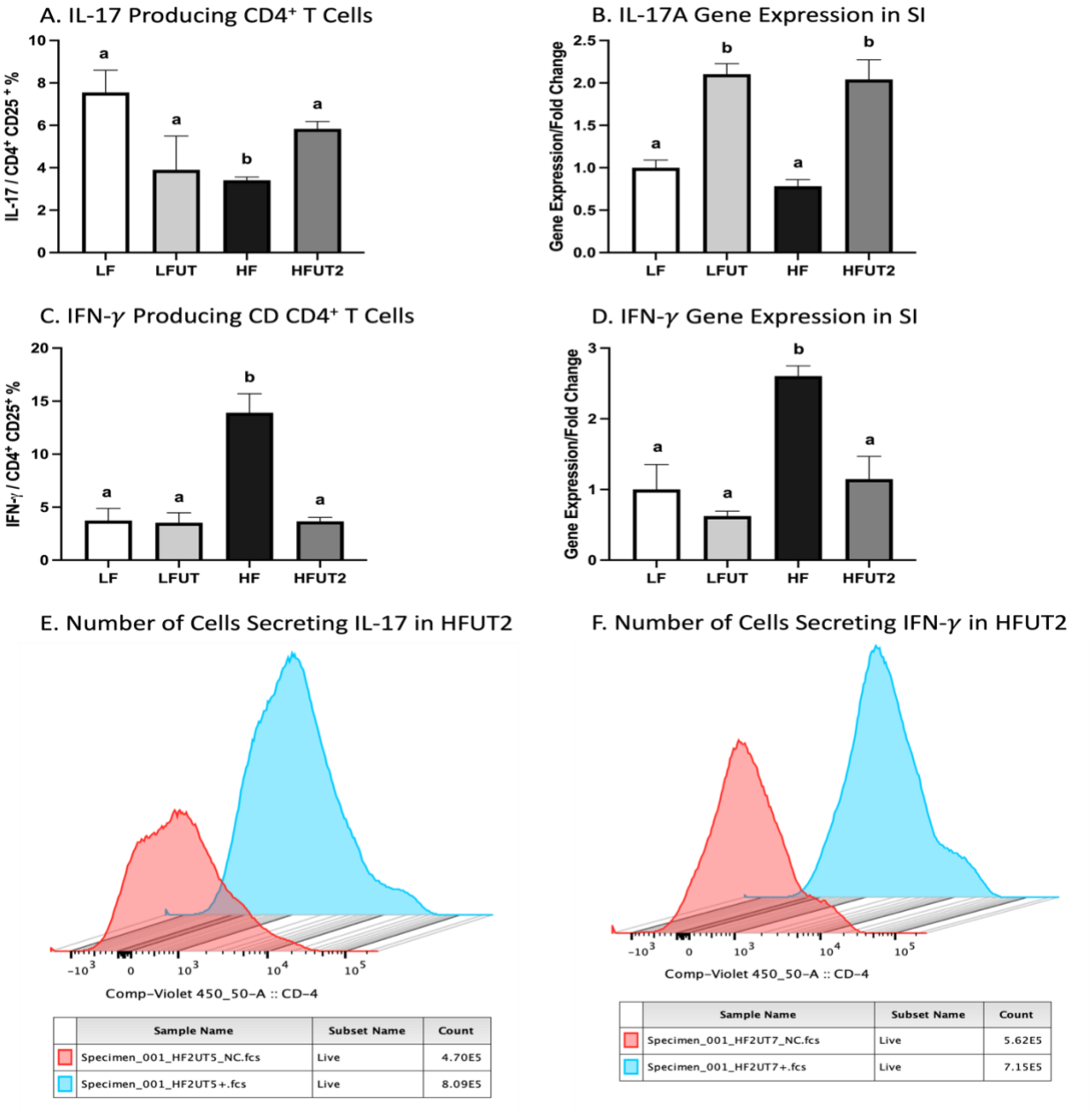

Figure 21. Effect of U. dioica on cytokine stimulation and gene expression in the SI lamina propria.

Cytokines IL-17 and IFN-γ were determined after stimulating $CD4^+$ T cells with ionomycin and PMA. (A). The population of IL-17 producing $CD4^+$ T cells was reduced by the HF diet compared to the LF diet group ($p<0.05$; n=4). Supplementation with *U. dioica* attenuated this decrease ($p<0.05$; n=4). (B). The gene expression of IL-17 in SI tissue was significantly increased by *U. dioica* supplementation in both the LF and HF diets ($p<0.05$; n=4). (C). The population of IFN-γ producing $CD4^+$ T cells was increased by the HF diet compared to the LF diet group ($p<0.05$; n=4). Supplementation with *U. dioica* prevented this increase ($p<0.05$; n=4). (D). The gene expression of IFN-γ in SI tissue of both LF and HF fed mice was significantly lower when both diets were supplemented with *U. dioica* ($p<0.05$; n=4). (E and F). Count numbers of secretory cytokines from negative control and stimulated groups of IL-17 and IFN-γ respectively. [a]Different letters indicate significant differences between the groups ($p<0.05$; n=4).

5.3.10. Gene Expression in Small Intestine Tissue

U. dioica vegetable stimulates Tregs, which facilitates secreting TGF-β. On the other hand, TGF-β also promotes Tregs generation and maturation. HF diet hampered TGF-β secretion significantly compared to the LF diet groups. However, HF supplemented with 2% *U. dioica* restored Tregs function as same as LFUT group. HF diet also inhibited IL-10 secretion locally, but HFUT2 could not restore it. Inflammatory cytokines in the small intestinal tissues were also quantified to test inflammation in the small intestines, including IL-1, IL-1β, IL-6 and TNF-α. HF diet induced pro-inflammatory cytokines, IL-1, IL-1β, IL-6, TNF-α and NF-κB. While *U. dioica* supplement significantly lowered IL-1, IL-6, TNF-α and NF-κB pro-inflammatory cytokines in small intestinal tissues to the same level of LF groups or even lower (Figure 22).

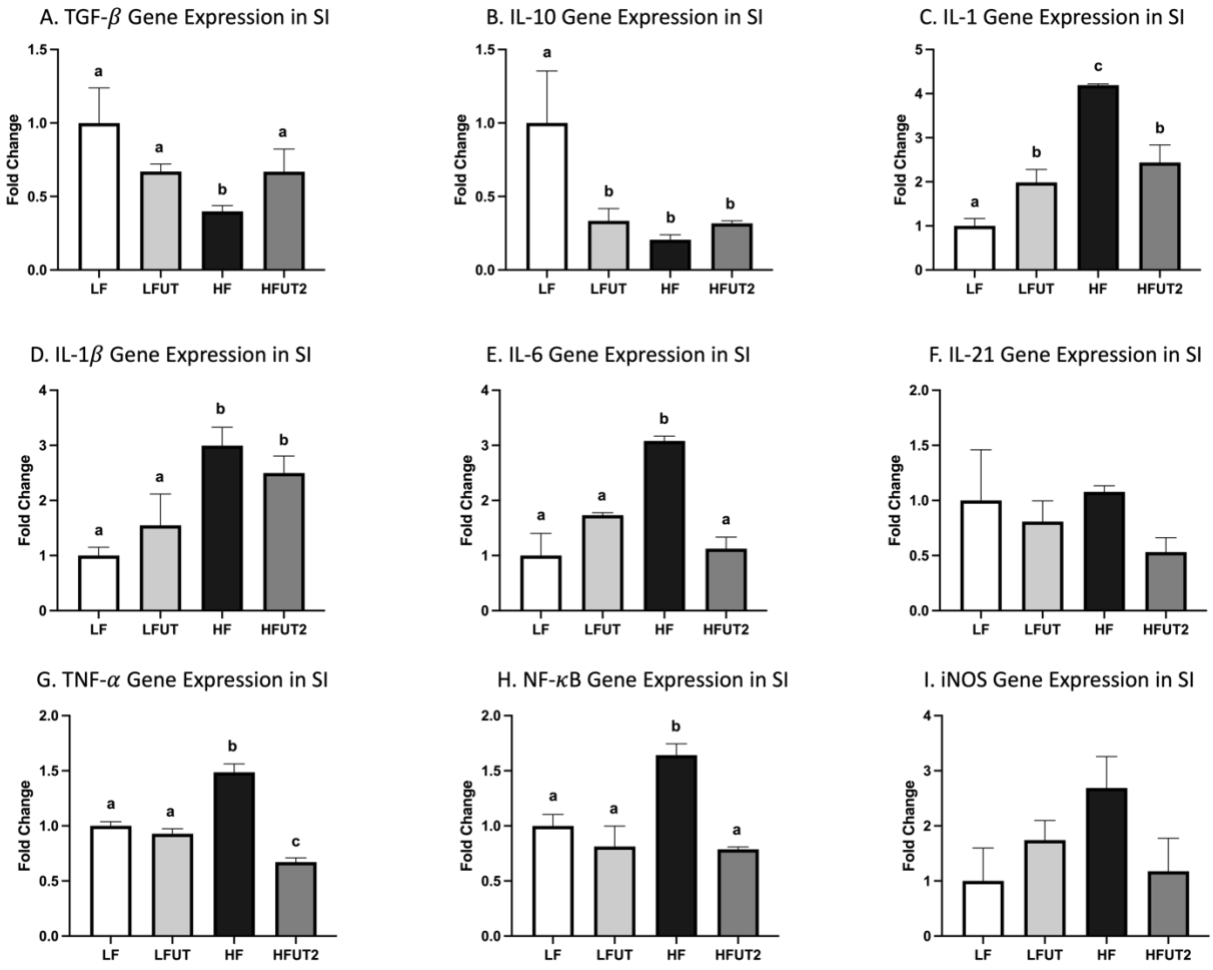

Figure 22. Gene expression of inflammatory cytokines in the small intestinal tissues.
RNA was extracted from small intestinal tissue (jejunum), cDNA was synthesized, and gene expression was determined by qPCR. The threshold cycle (Cq) values for each gene and that of β-actin as a reference gene were used to calculate gene expression by calculating $2^{-\Delta\Delta CT}$.[a]Different letters indicate significant differences between the groups ($p<0.05$; n=8).

5.3.11. Browning Gene Expression in White Adipose Tissue

UCP1 is a unique mitochondrial protein on the membrane devoted to thermogenesis. UCP1 in the HF diet group was significantly lower than LF groups (Figure 23A; $p<0.05$, n=8). However, HF supplement with 2% *U. dioica* upregulated UCP1 expression in epididymal adipose tissues. PGC-1α, PRDM16, DIO2 and PPARγ are transcription genes of browning markers in white adipose tissues. HF diet down-regulated PGC-1α and DIO2 significantly compared to LF

groups. While *U. dioica* supplementation upregulated them by twofold. Although PGC-1α and PPARγ were not significant differences between HF and LF groups, *U. dioica* supplementation significantly induced PGC-1α and PPARγ. CPT1 mediates β oxidation in mitochondria and COX8b is a mitochondrial marker to transfer the electrons for ATP generation. HF diet significantly reduced CPT-1 gene expression in the white adipose tissues, but HFUT could not restore its function (Figure 23F). COX8b gene expression were not different between HF and LF groups, but HF supplement with 2% *U. dioica* up regulated its gene expression doubled compared to both LF and HF groups (Figure 23G). SENP2 and ASK1 are two browning inhibitors, which suppress browning in white adipose tissues. Consistently in the results that HF diet highly expressed SENP2 and ASK1 genes, however, *U. dioica* supplement down regulated them significantly compared to the HF diet group (Figure 23H & I; p,0.05; n=8).

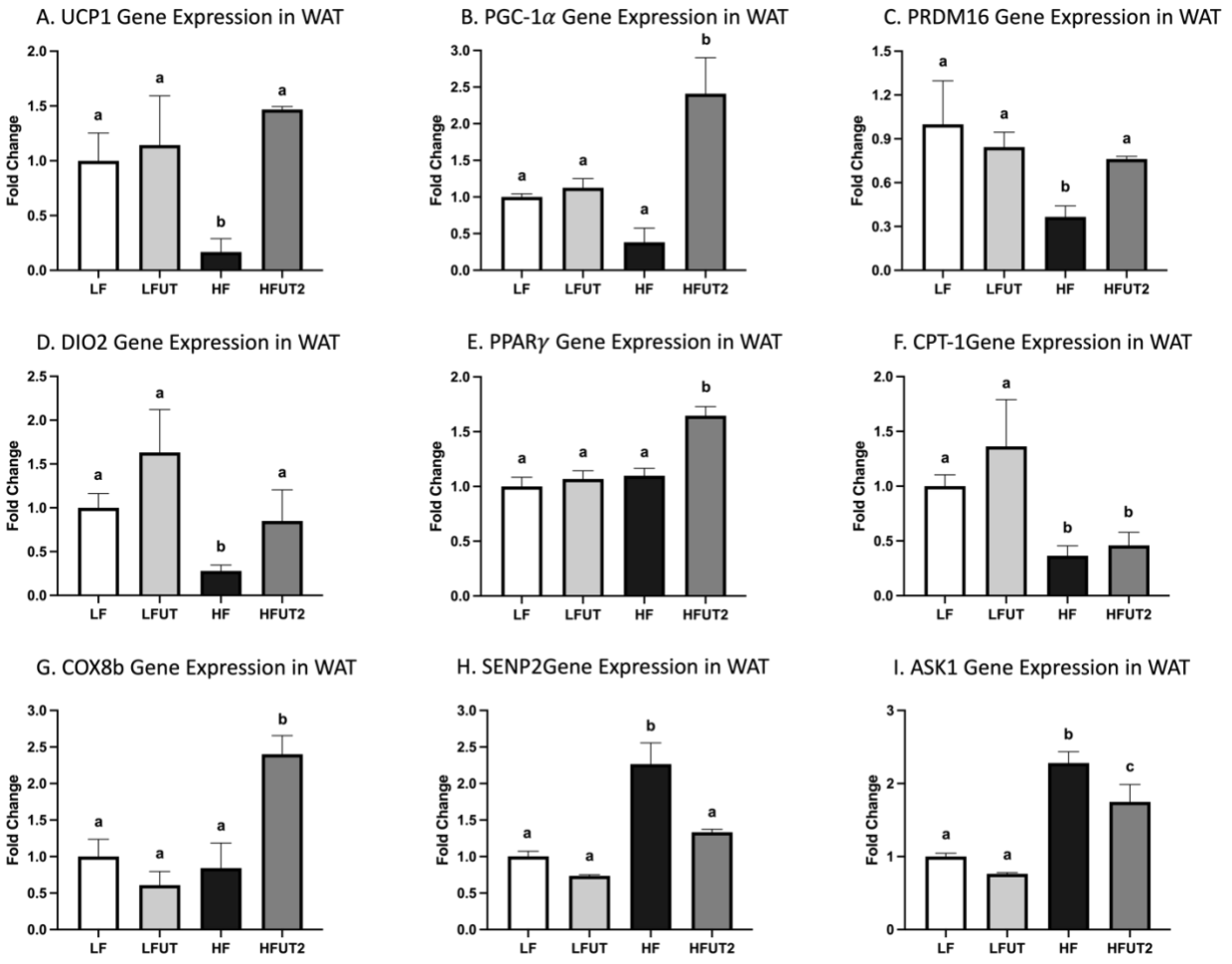

Figure 23. Gene expression of thermogenesis markers in the white adipose tissues.
RNA was extracted from small intestinal tissue (jejunum), cDNA was synthesized, and gene expression was determined by qPCR. The threshold cycle (Cq) values for each gene and that of β-actin as a reference gene were used to calculate gene expression by calculating $2^{-\Delta\Delta CT}$.[a]Different letters indicate significant differences between the groups ($p<0.05$; n=8).

5.3.12. Glucose Absorption and Transportation in Organoids-Derived Monolayers

Enteroids

Small intestinal organoids cultured from the jejunum of LF, HF and HFUT2 groups were used to quantify nutrient absorption in vitro. The transcellular transport of nutrients from the brush border side across the epithelium into circulation was mimicked by adding 50 mM glucose solution to the apical layer and determining nutrients delivered to the basolateral layer after a specific time period. Compared to the enteroids from LF group, the ones from the HF group

absorbed a significantly higher amount of glucose ($p < 0.0001$; n=3). Enteroids from the group supplemented with *U. dioica* exhibited a reduced amount of glucose absorbed compared HF group (Figure 25A; $p < 0.05$; n=3). However, testing the impact of *U. dioica* extract on glucose absorption in enteroids from the HF group treated with 50uM glucose, showed no significant effect (Figure 25B).

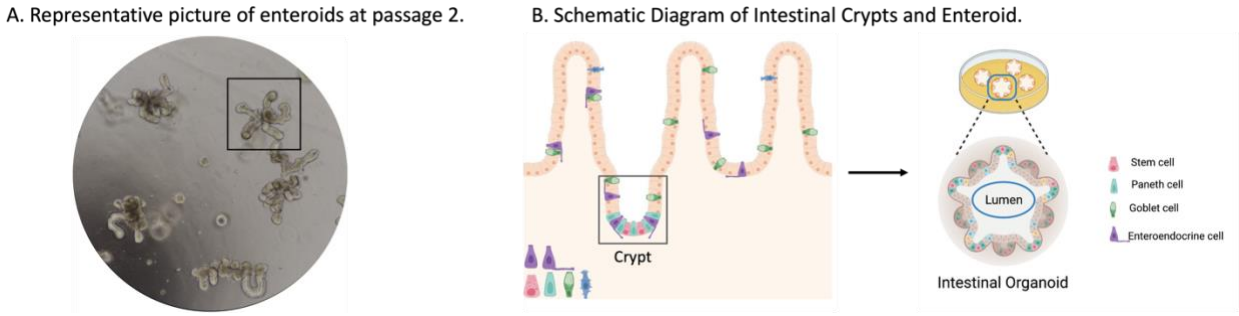

Figure 24. Representative picture of enteroids at passage 2 and schematic diagram of the intestinal crypts and enteroids.

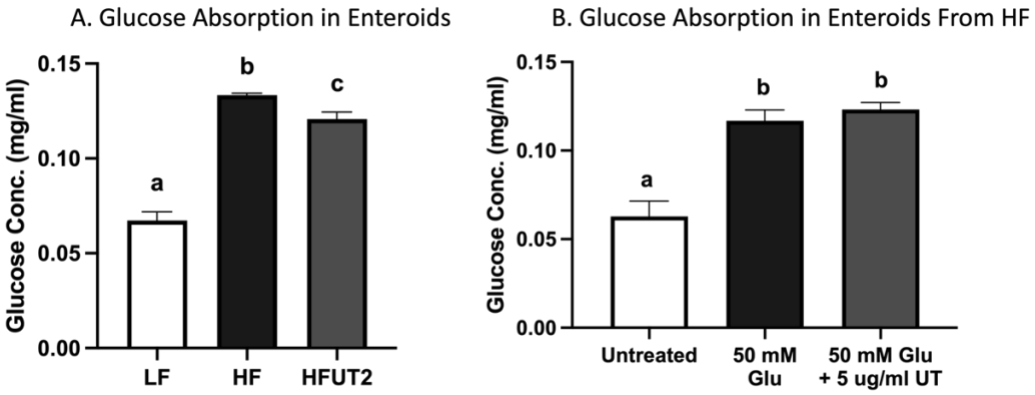

Figure 25. Effects of U. dioica on glucose absorption in the dose-response study.
(A). Glucose absorption was significantly higher in enteroids from HF fed mice compared to those from LF fed mice ($p<0.01$). Glucose absorption in enteroids from mice fed a HF diet supplemented with *U. dioica* had lower glucose absorption compared to those fed the HF diet ($p<0.05$). (B). Glucose absorption tested in enteroids treated with *U. dioica* extract and glucose did not show significant differences with the control treated with glucose only (p=ns). [a]Different letters indicate significant differences between the groups ($p<0.05$; n=3-4).

5.3.13. Fat Absorption and Transportation in Organoids-Derived Monolayers Enteroids

400 uM sodium palmitate was added to the confluent monolayers apical chamber. Fat absorption tests showed that enteroids from the HF diet group absorbed more FFAs (higher triglycerides in the basolateral layer) compared to those from LF (Figure 26A; $p<0.0001$; n=3). Enteroids from the mice fed *U. dioica* at 2% had lower amounts of fat absorbed, although statistical significance was not reached (Figure 26A; $p=0.1$; n=3). Testing the impact of *U. dioica* extract on FFAs absorption in enteroids from the HF group treated with 400uM FFAs showed that *U. dioica* extract significantly reduced the amount of FFAs absorbed, the amount of triglycerides detected in the basolateral layer (Figure 26B; $p<0.05$).

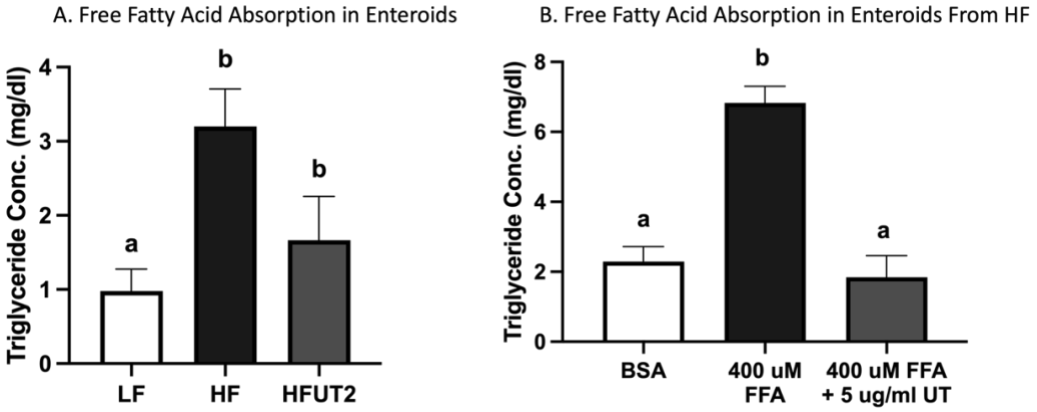

Figure 26. Effects of U. dioica on fat absorption in the dose-response study.
(A). FFAs absorption was significantly higher in enteroids from HF fed mice compared to those from LF fed mice ($p<0.01$). FFAs absorption in enteroids from mice fed a HF diet supplemented with *U. dioica* trended lower, though significance was not attained. (B). FFAs absorption was significantly lower in enteroids treated with FFA and *U. dioica* extract compared to those treated with FFA only ($p<0.05$).
[a]Different letters indicate significant differences between the groups ($p<0.05$; n=3-4).

5.3.14. Mechanistic Studies to determine the role of Genus Clostridium in attenuating Nutrition Absorption

The bacterial species *Clostridium disporicum*, *Clostridium vincentii* and *Clostridium celatum* were anaerobically cultured. Spent media were added to enteroid monolayers to determine the impact of bacterial metabolites on the absorption of fat absorption.

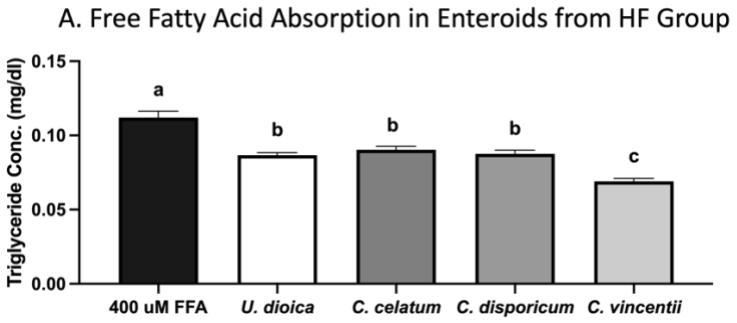

Figure 27. Effects of U. dioica on fat absorption in organoids.
All cells were treated with 400uM of FFAs. Treatments were either 5ug/ml *U. dioica* extract or 20ul of bacterial filtered spent media containing the metabolites.(A) Representative picture of enteroids used at passage 2. (B). FFAs absorption was significantly higher in enteroids treated with FFA only. Supplementing the media with *U. dioica* extract or bacterial metabolites lowered fat absorption. ($p<0.01$).

5.3.15. Gene Quantification

Changes in the expression of genes that are involved in fat transportation were determined in the enteroids used for the determination of nutrient absorption (Figure 28). RNA was extracted, cDNA was synthesized, and gene expression was determined by qPCR. The threshold cycle (Cq) values for each gene and that of β-actin as a reference gene were used to calculate gene expression by calculating $2^{-\Delta\Delta CT}$.

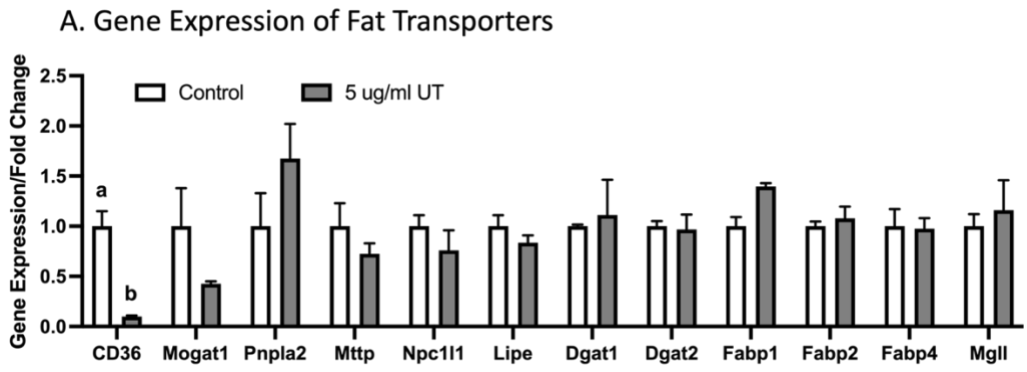

Figure 28. Effects of U. dioica extract on the gene expression of fat transporters in the dose-response study.
(A). Gene expression determined by qPCR. [a]Different letters indicate significant differences between the treatment group and control set at 1.00 for all genes shown ($p<0.05$; $n=4$).

5.4. Discussion

This study is a follow-up to two previous studies focused on *U. dioica* protective effects against diet-induced obesity and insulin resistance. Compared to previous studies which used 9% on w/w basis, we show that a lower dose of 2% attenuates HF diet-induced fat accumulation and protects against high fasting glucose and insulin and HOMA-IR. In the second part of the study, we show that the vegetable prevents HF diet induced reductions in the intestinal T cells and IgA producing B cells and increases Tregs. In addition, our results suggest that under conditions of HF supply *U. dioica* could influence both sides of the energy balance equation; namely, energy acquisition and affects host genes that regulate how energy is expended and stored.

Because our previous studies involved a high dose (9%) (Fan et al., 2020 and 2021), our initial aim was to find a lower dose that imparts the same effects. It was surprising that we did not observe a dose effect between the 2, 4 and 9% *U. dioica*. All three doses were protective against diet-induced fat accumulation and fasting glucose levels (Figures 14-17). However, the unexpected finding was that the 4% and 9% did not attenuate HF diet-induced fasting insulin and

thus HOMA-IR (Figure 15). High fasting insulin levels are an indicator of insulin sensitivity and can deteriorate glucose and lipid metabolism leading to more fat accumulation via stimulation of lipogenesis (Titchenell et al., 2016). However, in this study, the higher insulin levels did not translate into higher body weight or fat accumulation but correlated positively with spleen weight which is a correlation measure of inflammation though not a direct measure (Chassaing et al., 2014). As disease progresses, the resulting immune response leads to an increase in immune cells, thus an increase in spleen weight is indicative of the robust immune response present. While a HF diet increased spleen weight by about 20%, supplementing the HF with 4% and 9% *U. dioica* did not prevent or attenuate these while the 2% did (Figure 16A). The spleen is the largest secondary lymphoid organ in the body with lymphoid tissue containing immune cells that target blood-borne pathogens and is a site of erythrophagocytosis. Inflammation induced by HF diet changes splenic function and morphology leading to pathogenesis of diabetes and obesity-related cardiovascular disease and kidney disease (Bronte et al., 2013). Therapeutic modalities that maintain normal splenic morphology in the obese condition may be beneficial.

Another unexpected finding was that *U. dioica* prevented fat accumulation in the mesenteric fat, perirenal and retroperitoneal fat pads but not the epididymal fat pad (Figure 17). The mesenteric fat pad is most analogous or comparable to human intra-abdominal adipose tissue both in its location and biology and because it has access to the portal vein (Chusyd et al., 2016). Fat pads differ in terms of inflammatory transcriptome and secretory capacity. TNF-α is an adipokine, produced in adipose tissue and immune cells (Sethi et al., 2021). It contributes to obesity-associated metabolic disease and mediates insulin resistance. TNF-α can impair insulin receptor signaling in adipocytes by stimulating endoplasmic reticulum Ca^{2+} release, increasing cytosolic free Ca^{2+} levels and activating Ca^{2+}/calmodulin-dependent protein kinase II (Sethi et

al., 2021 and Petersen et al., 2021). TNF-α can also promote insulin resistance by regulating intracellular lipid metabolism, particularly promoting the accumulation and/or release of pro-inflammatory lipids such as ceramides which activate classic and novel PKCs (Sethi et al., 2021 and Petersen et al., 2021).

Because the intestinal immune system is linked to obesity and insulin resistance mechanisms, we determined the effect of the HF diet or *U. dioica* on intestinal immune cell phenotype and specific secretions. T cells mediate communication between the gut and other organs in the initiation and progression of metabolic-related diseases. *U dioica* prevented HF diet-induced reductions in total T cells and including *U. dioica* in either the LF or HF diet induced T cells antigenic stimulation (increased Tregs) (Figure 19A). Natural Tregs develop in the thymus and induced Tregs, derived from naive $CD4^+$ T cells in the periphery mediate peripheral tolerance. A HF diet reduces the proportions and numbers of Tregs in the lamina propria and studies have consistently shown that Tregs are decreased in the small intestine and colon of obese patients compared with lean human subjects (Luck et al., 2015). Adoptive transfer of Tregs into obese mice or preventing the decrease in Tregs improves insulin sensitivity. Tregs in the intestine regulate inflammation and induce tolerance to antigens such as dietary components or the microbiota or bacterial pathogens (Sorini et al., 2018; Hegazy et al., 2017 and Littman et al., 2010). Tregs maintain intestinal homeostasis in IL-10 and TGF-β-dependent mechanisms. *U. dioica* attenuated HF diet-induced decreases in TGF-β. Tregs are known to promote IgA secretion by B cells and *U. dioica* increased of IgA^+ secreting B cells (Figure 19D). Besides Tregs, the other abundant $CD4^+$ T cells are Th17 cells. *U. dioica* attenuated HF diet-induced reduction in IL-17 producing cells and gene expression (Figure 19 E-F). Th17 cells, induced by TGF-β through the transcription factor RORγt, are key in host defense against fungi

and maintain intestinal homeostasis through producing IL-17 and/or IL-22 (Littman et al., 2010 and Hong et al., 2017).

IFN-γ is produced by $CD4^+$ and $CD8^+$ (cytotoxic T lymphocytes) in response to cytokine and antigen stimulation (Bradley et al., 2022). The HF diet induced an increase in IFN-γ producing T cells and *U. dioica* supplementation in both the LF and HF diets lowered the amounts of $CD4^+$ T cells secreting IFN-γ and its gene expression (Figure 21 B and D). In obesity, the global effects of IFN-γ reduces Tregs and diminishes their function. In addition, IFN-γ and TNF-α induce gut permeability hence, bacterial metabolites like lipopolysaccharide get into circulation and further promote obesity and insulin resistance (Hong et al., 2017 and Bradley et al., 2022). Overall, in the intestine, *U. dioica* prevented HF diet induced increases in cytokines IL1, IL-1β, IL-6, TNF-α, IFN-γ and NFκB reinforcing the fact that it impacts the intestinal immune system, an important modulator of glucose homeostasis and obesity-associated insulin resistance. The gut immune system also impacts intestinal permeability, immune cell trafficking, and availability of intestinal hormones that impact systemic insulin resistance.

To determine the functional impact of *U. dioica* on nutrient absorption, we used enteroids cultured from the jejunum because they are an accurate representation of the epithelial layer and its different cell types. They recapitulate *in vivo* intestinal lipoprotein synthesis and secretion, have key aspects of the physiology of intact intestine and the necessary machinery for lipid absorption and chylomicron synthesis and secretion (Zachos et al., 2016 and Jattan et al., 2017). The major small intestinal cell lineages are present in the monolayer which differentiates upon forming a confluent monolayer (Kozuka et al., 2017). Enteroids from HF-fed obese animals displayed elevated glucose and fat absorption from the lumen to serosa compared to enteroids from mice fed the LF diet and enteroids from *U. dioica* fed animals (Figure 25). Adding *U.*

dioica extract in enteroids from HF-fed mice attenuated glucose absorption. This is evidence that *U. dioica* has an impact on glucose transport and fatty acid transport mechanisms and this may contribute to the mechanisms by which it attenuates diet-induced obesity. Although the expression of most of the genes involved in fat transport and metabolism were impacted by *U dioica*, statistical significance was not reached (Figure 28). Only the receptor CD36 was significantly lowered (Figure 28). CD36 facilitates high-affinity cell and tissue uptake of long-chain fatty acids and during high fat supply can contribute to lipid accumulation and metabolic dysfunction. CD36 is implicated in several aspects related to fatty acid metabolism including fat taste perception, fat intake, fat absorption, absorption-related peptide secretion and fatty acid utilization by muscle and adipose. Besides fatty acids, CD36 recognizes phospholipids, diacylglycerol and cholesterol for chylomicron production (Pepino et al., 2014 and Xu et al., 2013) and can impact fat absorption at levels involving triglyceride hydrolysis or resynthesis, fatty acid uptake, chylomicron assembly and trafficking in intestinal epithelial cells.

This study is not without its limitations. In the *in vitro* study section, we exposed enteroids to an extract of *U. dioica* rather than the whole vegetable. The extract contains water and ethanol soluble phytochemicals and soluble fiber, but some beneficial components like insoluble fiber or phytochemicals are not included. However, the most beneficial effects of the vegetable are attributed to soluble phytochemical components captured in the extract. Secondly, enteroids do not contain immune cells; hence, we could not simultaneously determine the impact of the vegetable on immune cells and gene expression in this model. However, our data builds onto previous studies and the body of knowledge on *U. dioica* as a 'super food' with a myriad of health benefits in the prevention of metabolic disease.

Chapter 6: Conclusions

A diet supplemented with *U. dioica* protects against diet induced obesity, insulin resistance and inflammation both in the intestine and in adipose tissue. It contributes to a leaner frame through impacting different pathways. In adipose tissue, it increases genes involved in adipogenesis and beiging/browning while reducing those involved in lipogenesis. In skeletal muscle, it increases the expression of genes involved in fatty acid oxidation. In the gut microbiota, *U. dioica* promotes diversity and the representation of bacterial taxa associated with a lean phenotype and enhanced insulin sensitivity (genus *Clostridium* and *Turicibacter).* Bacterial metabolic function prediction further demonstrates that *U. dioica* enriches amino acid metabolism pathways that contribute to reducing body weight and increasing insulin resistance. The change in bacterial composition and function has an impact on immune cell phenotype. The HF diet induced alterations in immune cell homeostasis but including *U. dioica* in either the LF or HF diet increased the T regulatory cells indicating that the vegetable induced T cells antigenic stimulation. Furthermore, the increased representation of *Clostridium* may contribute to immune cell homeostasis by increasing Tregs. The major function of Tregs in the intestine is to regulate inflammation and induce tolerance to antigens such as dietary components or the microbiota or other bacterial pathogens. Tregs contribute to improved insulin sensitivity and resistance to obesity. The functional study on nutrient absorption in enteroids showed that *Urtica dioica* impacts the amounts of nutrients absorbed during excess provision, as in the case of a HF diet. Enteroids from HF fed obese animals displayed elevated glucose and fat absorption from the lumen to serosa, while enteroids from *U. dioica* fed animals displayed lower glucose and fat absorption. The data builds onto previous studies and the body of knowledge on *U. dioica* as a 'superfood' with a myriad of health benefits in the prevention of metabolic disease.

Appendices

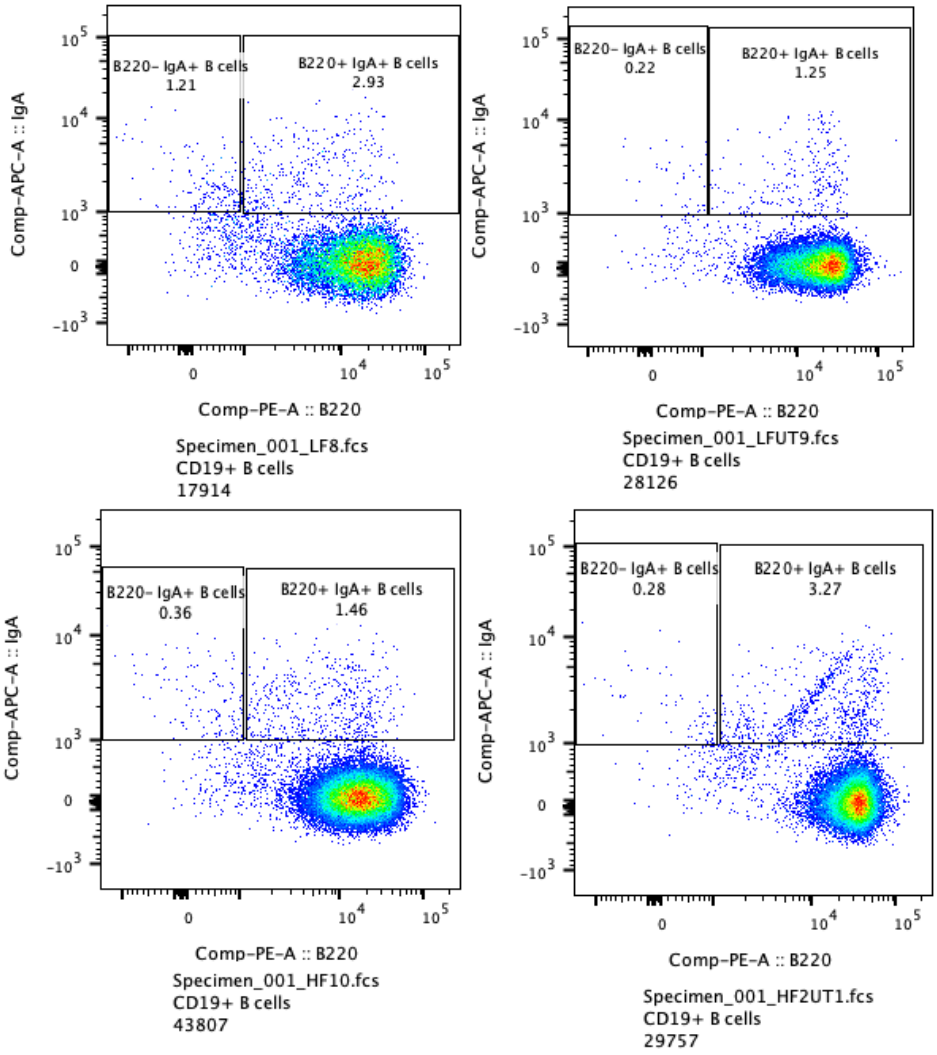

Appendix Figure A1. B cell subset population for all groups.

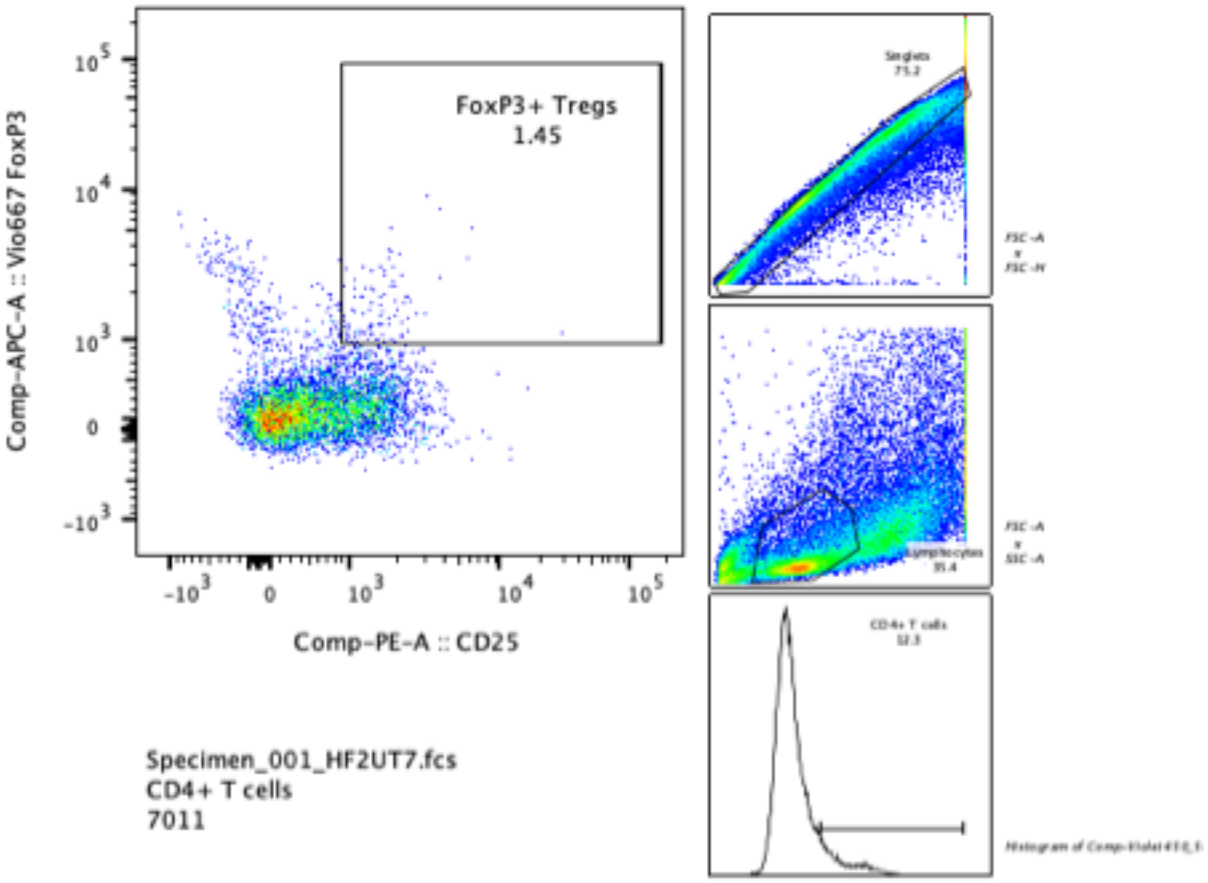

Appendix Figure A2. Gating strategies for Foxp3+ Tregs population.
Lamina propria $CD4^{+}CD25^{+}Foxp3^{+}$ Tregs represented by flow cytometry. Cells were gated on singlets and lymphocytes first.

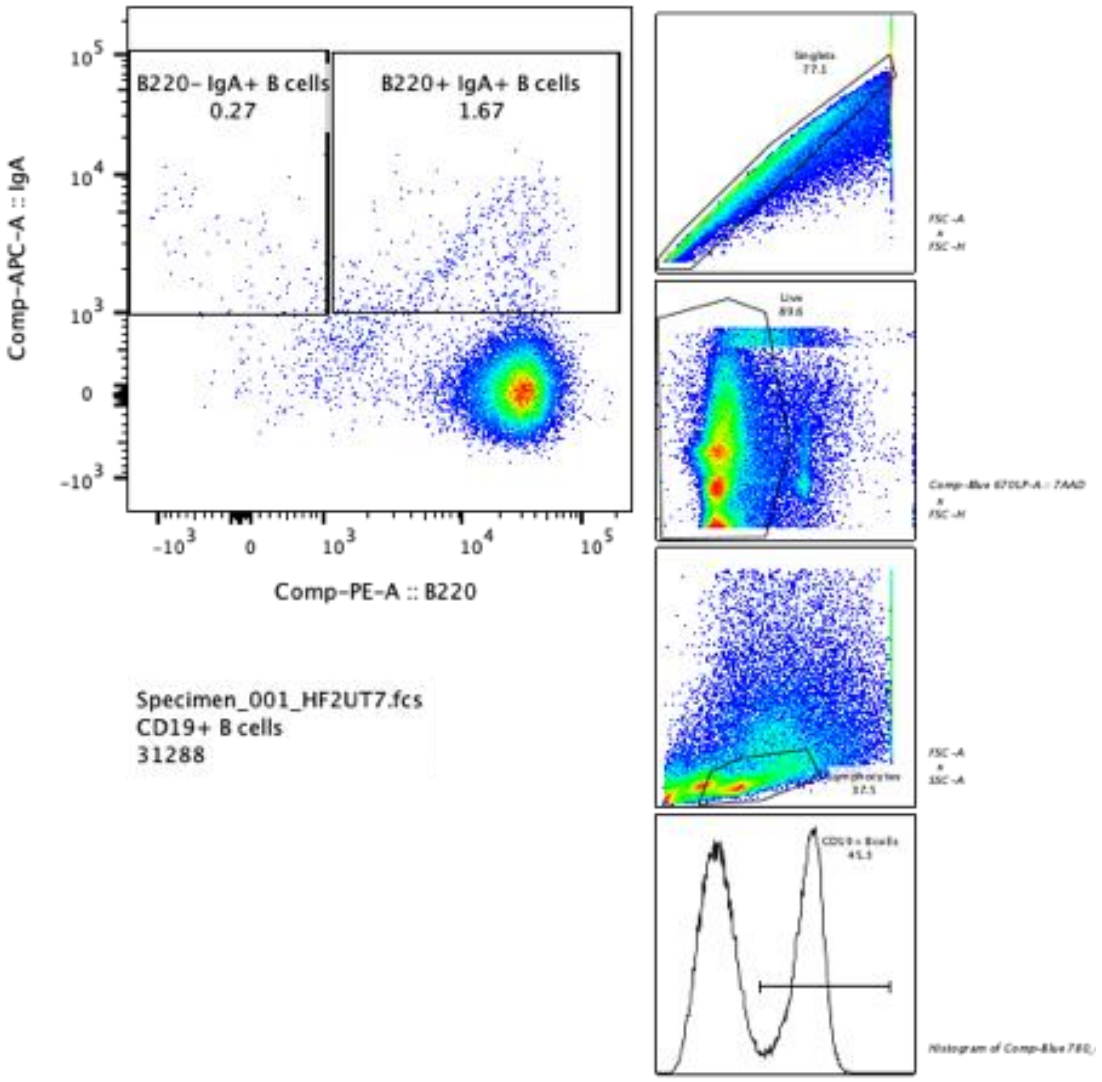

Appendix Figure A3. Gating strategies for IgA-producing B cell population in the small intestinal lamina propria.

$CD19^{+}B220^{+}IgA^{+}$ B cells were represented as IgA-producing B cells by flow cytometry. $CD19^{+}B220^{-}IgA^{+}$ B cells were represented as plasma cells by flow cytometry. Cells were gated on singlet live lymphocytes first.

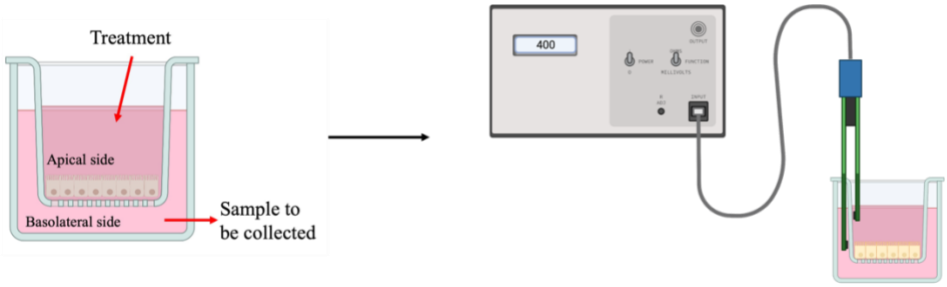

Appendix Figure A4. Schematic diagram of Enteroids Monolayer and TEER Measurement.

Bibliography

1. Winer DA, Luck H, Tsai S, Winer S. The Intestinal Immune System in Obesity and Insulin Resistance. *Cell Metabolism*. 2016;23(3):413-426.
2. Patel PS, Buras ED, Balasubramanyam A. The Role of the Immune System in Obesity and Insulin Resistance. *Journal of Obesity*. 2013; 2013:1-9.
3. Mokdad AH, Ford ES, Bowman BA, et al. Prevalence of Obesity, Diabetes, and Obesity-Related Health Risk Factors, 2001. *JAMA*. 2003;289(1):76-79.
4. Portero McLellan KC, Wyne K, Villagomez ET, Hsueh WA. Therapeutic interventions to reduce the risk of progression from prediabetes to type 2 diabetes mellitus. *Ther Clin Risk Manag*. 2014; 10:173-188.
5. Gérard P. Gut microbiota and obesity. *Cell Mol Life Sci*. 2016;73(1):147-162.
6. García-Montero C, Fraile-Martínez O, Gómez-Lahoz AM, et al. Nutritional Components in Western Diet Versus Mediterranean Diet at the Gut Microbiota–Immune System Interplay. Implications for Health and Disease. *Nutrients*. 2021;13(2):699.
7. Greer R, Dong X, Morgun A, Shulzhenko N. Investigating a holobiont: Microbiota perturbations and transkingdom networks. *Gut Microbes*. 2016;7(2):126-135.
8. Carding S, Verbeke K, Vipond DT, Corfe BM, Owen LJ. Dysbiosis of the gut microbiota in disease. *Microbial Ecology in Health and Disease*. 2015;26(s2):26191.
9. Turnbaugh PJ, Bäckhed F, Fulton L, Gordon JI. Diet-Induced Obesity Is Linked to Marked but Reversible Alterations in the Mouse Distal Gut Microbiome. *Cell Host & Microbe*. 2008;3(4):213-223.
10. David LA, Maurice CF, Carmody RN, et al. Diet rapidly and reproducibly alters the human gut microbiome. *Nature*. 2014;505(7484):559-563.
11. Ley RE, Bäckhed F, Turnbaugh P, Lozupone CA, Knight RD, Gordon JI. Obesity alters gut microbial ecology. *Proceedings of the National Academy of Sciences*. 2005;102(31):11070-11075.
12. Mandard S, Zandbergen F, Straten E van, et al. The Fasting-induced Adipose Factor/Angiopoietin-like Protein 4 Is Physically Associated with Lipoproteins and Governs Plasma Lipid Levels and Adiposity *. *Journal of Biological Chemistry*. 2006;281(2):934-944.
13. Sagar NM, Cree IA, Covington JA, Arasaradnam RP. The Interplay of the Gut Microbiome, Bile Acids, and Volatile Organic Compounds. *Gastroenterology Research and Practice*. 2015;2015: e398585.
14. Boutagy NE, McMillan RP, Frisard MI, Hulver MW. Metabolic endotoxemia with obesity: Is it real and is it relevant? *Biochimie*. 2016; 124:11-20.
15. Cani PD, Amar J, Iglesias MA, et al. Metabolic Endotoxemia Initiates Obesity and Insulin Resistance. *Diabetes*. 2007;56(7):1761-1772.

16. Wiertsema SP, van Bergenhenegouwen J, Garssen J, Knippels LMJ. The Interplay between the Gut Microbiome and the Immune System in the Context of Infectious Diseases throughout Life and the Role of Nutrition in Optimizing Treatment Strategies. *Nutrients*. 2021;13(3):886.
17. Kubinak JL, Petersen C, Stephens WZ, et al. MyD88 Signaling in T Cells Directs IgA-Mediated Control of the Microbiota to Promote Health. *Cell Host & Microbe*. 2015;17(2):153-163.
18. Luck H, Khan S, Kim JH, et al. Gut-associated IgA+ immune cells regulate obesity-related insulin resistance. *Nat Commun*. 2019;10(1):3650.
19. Kim KS, Hong SW, Han D, et al. Dietary antigens limit mucosal immunity by inducing regulatory T cells in the small intestine. *Science*. 2016;351(6275):858-863.
20. Devkota HP, Paudel KR, Khanal S, et al. Stinging Nettle (Urtica dioica L.): Nutritional Composition, Bioactive Compounds, and Food Functional Properties. *Molecules*. 2022;27(16):5219.
21. Orčić D, Francišković M, Bekvalac K, et al. Quantitative determination of plant phenolics in Urtica dioica extracts by high-performance liquid chromatography coupled with tandem mass spectrometric detection. *Food Chemistry*. 2014; 143:48-53.
22. Upton R. Stinging nettles leaf (*Urtica dioica* L.): Extraordinary vegetable medicine. Journal of Herbal Medicine 2013; 3:9–38.
23. Obanda DN, Ribnicky D, Yu Y, Stephens J, Cefalu WT. An extract of Urtica dioica L. mitigates obesity induced insulin resistance in mice skeletal muscle via protein phosphatase 2A (PP2A). *Sci Rep*. 2016;6(1):22222.
24. Obanda DN, Zhao P, Richard AJ, Ribnicky D, Cefalu WT, Stephens JM. Stinging Nettle (Urtica dioica L.) Attenuates FFA Induced Ceramide Accumulation in 3T3-L1 Adipocytes in an Adiponectin Dependent Manner. *PLOS ONE*. 2016;11(3): e0150252.
25. Sun L, Ma L, Ma Y, Zhang F, Zhao C, Nie Y. Insights into the role of gut microbiota in obesity: pathogenesis, mechanisms, and therapeutic perspectives. *Protein Cell*. 2018;9(5):397-403.
26. Ridaura VK, Faith JJ, Rey FE, et al. Gut Microbiota from Twins Discordant for Obesity Modulate Metabolism in Mice. *Science*. 2013;341(6150):1241214.
27. Muccioli GG, Naslain D, Bäckhed F, et al. The endocannabinoid system links gut microbiota to adipogenesis. *Molecular Systems Biology*. 2010;6(1):392.
28. Le Chatelier E, Nielsen T, Qin J, et al. Richness of human gut microbiome correlates with metabolic markers. *Nature*. 2013;500(7464):541-546.
29. Obanda DN, Husseneder C, Raggio AM, et al. Abundance of the species Clostridium butyricum in the gut microbiota contributes to differences in obesity phenotype in outbred Sprague-Dawley CD rats. *Nutrition*. 2020; 78:110893.
30. Obanda DN, Keenan MJ, Page R, et al. Gut Microbiota Composition and Predicted Microbial Metabolic Pathways of Obesity Prone and Obesity Resistant Outbred Sprague-

Dawley CD Rats May Account for Differences in Their Phenotype. *Frontiers in Nutrition*. 2021;8. Accessed November 27, 2022.
31. Rampelli S, Schnorr SL, Consolandi C, et al. Metagenome Sequencing of the Hadza Hunter-Gatherer Gut Microbiota. *Current Biology*. 2015;25(13):1682-1693
32. Lee CJ, Sears CL, Maruthur N. Gut microbiome and its role in obesity and insulin resistance. *Annals of the New York Academy of Sciences*. 2020;1461(1):37-52.
33. Petersen C, Bell R, Klag KA, et al. T cell–mediated regulation of the microbiota protects against obesity. *Science*. 2019;365(6451): eaat9351.
34. Gizard F, Fernandez A, De Vadder F. Interactions between gut microbiota and skeletal muscle. *Nutr Metab Insights*. 2020; 13:1178638820980490.
35. Bäckhed F, Manchester JK, Semenkovich CF, Gordon JI. Mechanisms underlying the resistance to diet-induced obesity in germ-free mice. *Proceedings of the National Academy of Sciences*. 2007;104(3):979-984.
36. Lee JY, Ye J, Gao Z, et al. Reciprocal Modulation of Toll-like Receptor-4 Signaling Pathways Involving MyD88 and Phosphatidylinositol 3-Kinase/AKT by Saturated and Polyunsaturated Fatty Acids *. *Journal of Biological Chemistry*. 2003;278(39):37041-37051.
37. Rastelli M, Cani PD, Knauf C. The Gut Microbiome Influences Host Endocrine Functions. *Endocrine Reviews*. 2019;40(5):1271-1284.
38. Kelley DE, Goodpaster B, Wing RR, Simoneau JA. Skeletal muscle fatty acid metabolism in association with insulin resistance, obesity, and weight loss. *American Journal of Physiology-Endocrinology and Metabolism*. 1999;277(6): E1130-E1141.
39. Lahiri S, Kim H, Garcia-Perez I, et al. The gut microbiota influences skeletal muscle mass and function in mice. *Science Translational Medicine*. 2019;11(502): eaan5662.
40. Bleau C, Karelis AD, St-Pierre DH, Lamontagne L. Crosstalk between intestinal microbiota, adipose tissue and skeletal muscle as an early event in systemic low-grade inflammation and the development of obesity and diabetes. *Diabetes/Metabolism Research and Reviews*. 2015;31(6):545-561.
41. Tripathi A, Debelius J, Brenner DA, et al. The gut–liver axis and the intersection with the microbiome. *Nat Rev Gastroenterol Hepatol*. 2018;15(7):397-411.
42. Parséus A, Sommer N, Sommer F, et al. Microbiota-induced obesity requires farnesoid X receptor. *Gut*. 2017;66(3):429-437.
43. Henao-Mejia J, Elinav E, Jin C, et al. Inflammasome-mediated dysbiosis regulates progression of NAFLD and obesity. *Nature*. 2012;482(7384):179-185.
44. Arrese M, Cabrera D, Kalergis AM, Feldstein AE. Innate Immunity and Inflammation in NAFLD/NASH. *Dig Dis Sci*. 2016;61(5):1294-1303.
45. Baffy G. Kupffer cells in non-alcoholic fatty liver disease: The emerging view. *Journal of Hepatology*. 2009;51(1):212-223.
46. Han H, Yi B, Zhong R, et al. From gut microbiota to host appetite: gut microbiota-derived metabolites as key regulators. *Microbiome*. 2021;9(1):162.

47. Noble EE, Hahn JD, Konanur VR, et al. Control of Feeding Behavior by Cerebral Ventricular Volume Transmission of Melanin-Concentrating Hormone. *Cell Metabolism*. 2018;28(1):55-68. e7.
48. Li Z, Yi CX, Katiraei S, et al. Butyrate reduces appetite and activates brown adipose tissue via the gut-brain neural circuit. *Gut*. 2018;67(7):1269-1279.
49. Hardy OT, Czech MP, Corvera S. What causes the insulin resistance underlying obesity? *Curr Opin Endocrinol Diabetes Obes*. 2012;19(2):81-87.
50. Lee YS, Li P, Huh JY, et al. Inflammation Is Necessary for Long-Term but Not Short-Term High-Fat Diet–Induced Insulin Resistance. *Diabetes*. 2011;60(10):2474-2483.
51. Luck H, Tsai S, Chung J, Clemente-Casares X, Ghazarian M, Revelo X.S, et al. Regulation of obesity-related insulin resistance with gut anti-inflammatory agents. Cell Metab. 2015; 21(4):527–542.
52. Gutzeit C, Magri G, Cerutti A. Intestinal IgA production and its role in host-microbe interaction. *Immunological Reviews*. 2014;260(1):76-85.
53. Machado S.A., Pasquarelli-do-Nascimento G., da Silva D. et al. Browning of the white adipose tissue regulation: new insights into nutritional and metabolic relevance in health and diseases. Nutr Metab (Lond) 19, 61 (2022).
54. Zhang C, Zhang M, Wang S, et al. Interactions between gut microbiota, host genetics and diet relevant to development of metabolic syndromes in mice. *ISME J*. 2010;4(2):232-241.
55. Sonnenburg ED, Smits SA, Tikhonov M, Higginbottom SK, Wingreen NS, Sonnenburg JL. Diet-induced extinctions in the gut microbiota compound over generations. *Nature*. 2016;529(7585):212-215.
56. Florowska A, Krygier K, Florowski T, Dłużewska E. Prebiotics as functional food ingredients preventing diet-related diseases. *Food & Function*. 2016;7(5):2147-2155.
57. Langlands SJ, Hopkins MJ, Coleman N, Cummings JH. Prebiotic carbohydrates modify the mucosa associated microflora of the human large bowel. *Gut*. 2004;53(11):1610-1616.
58. Kregiel D, Pawlikowska E, Antolak H. Urtica spp.: Ordinary Plants with Extraordinary Properties. *Molecules; Basel*. 2018;23(7):1664.
59. Rutto L.K.; Xu Y.; Ramirez E.; Brandt M. Mineral properties and dietary value of raw and processed stinging nettle (Urtica dioica L.). Int. J. Food Sci. 2013.
60. Adhikari B.M.; Bajracharya A.; Shrestha A.K. Comparison of nutritional properties of stinging nettle (Urtica dioica) flour with wheat and barley flours. Food Sci. Nutr. 2016, 4, 119–124259.
61. Klingelhoefer S, Obertreis B, Quast S, Behnke B. Antirheumatic effect of IDS 23, a stinging nettle leaf extract, on in vitro expression of T helper cytokines. J Rheumatol 1999;26:2517–22.
62. Mukundi MJ, Mwaniki NE, Piero NM, Murugi NJ, Kelvin JK, A Yusuf A, John MK, Alex NK, Daniel AS, Peter GK, et al. Potential Anti-diabetic Effects and Safety of

Aqueous Extracts of Urtica dioica Collected from Narok County, Kenya. Pharm Anal Acta [Internet] 2017;08.
63. Sharafetdinov Kh Kh, Kiseleva Tl, Kochetkova Aa, Mazo Vk. Promising Plant Sources of Anti-Diabetic Micronutrients. J Diabetes Metab [Internet] 2017;8.
64. Roza NAV, Possignolo LF, Palanch AC, Gontijo JAR. Effect of long-term high-fat diet intake on peripheral insulin sensibility, blood pressure, and renal function in female rats. *Food & Nutrition Research*. 2016;60(1):28536.
65. Patsouris D.; Li P.-P.; Thapar D.; Chapman J.; Olefsky J.M.; Neels J.G. Ablation of CD11c-positive cells normalizes insulin sensitivity in obese insulin resistant animals. Cell Metab. 2008, 8, 301–309.
66. Wu H.; Perrard X.D.; Wang Q.; Perrard J.L.; Polsani V.R.; Jones P.H.; Smith C.W.; Ballantyne C.M. CD11c expression in adipose tissue and blood and its role in diet-induced obesity. Arterioscler. Thromb. Vasc. Biol. 2010, 30, 186–192.
67. Yoshida K.; Shimizugawa T.; Ono M.; Furukawa H. Angiopoietin-like protein 4 is a potent hyperlipidemia-inducing factor in mice and inhibitor of lipoprotein lipase. J. Lipid Res. 2002, 43, 1770–1772.
68. Guerre-Millo M.; Gervois P.; Raspe E.; Madsen L.; Poulain P.; Derudas B.; Herbert J.-M.; Winegar DM, Willson TM, Fruchart J.-C. et al. PPARa activators improve insulin sensitivity and reduce adiposity. J. Biol. Chem. 2000.
69. Goto TLee, J.Y.; Teraminami, A.; Kim, Y.I.; Hira, S.; Uemura, T.; Inoue, H.; Takahashi, N.; Kawada, T. Activation of peroxisome proliferator-activated receptor-alpha stimulates both differentiation and fatty acid oxidation in adipocytes. J. Lipid Res. 2011, 52, 873–884
70. Wondisford A.R.; Xiong L.; Chang E.; Meng S.; Meyers D.J.; Li M.; Cole P.A.; He, L. Control of Foxo 1 Gene Expression by Co-activator P300. Control of Foxo 1 Gene Expression by Co-activator P300. J. Biol. Chem. 2014, 289, 4326–4333.
71. Bruce C.R.; Hoy A.J.; Turner N.; Watt W.J.; Allen T.L.; Carpenter K.; Cooney G.J.; Febbraio A.; Kraegen E. Overexpression of carnitine palmitoyltransferase-1 in skeletal muscle is sufficient to enhance fatty acid oxidation and improve high-fat diet–induced insulin resistance. Diabetes 2009, 58, 550–558.
72. Matthias B. Obesity: global epidemiology and pathogenesis. Nat Rev Endocrinol 2019;15:288–98.
73. Bäckhed F, Ding H, Wang T, Hooper LV, Koh GY, Nagy A, et al. The gut microbiota as an environmental factor that regulates fat storage. Proceedings of the National Academy of Sciences 2004;101:15718–23.
74. Liu H, Ivarsson E, Dicksved J, Lundh T, Lindberg JE. Inclusion of Chicory (Cichorium intybus L.) in Pigs' Diets Affects the Intestinal Microenvironment and the Gut Microbiota. Applied and Environmental Microbiology 2012;78:4102–9.

75. Ramnani P, Gaudier E, Bingham M, Van Bruggen P, Tuohy T, Gibson G. Pre- biotic effect of fruit and vegetable shots containing Jerusalem artichoke in- ulin: a human intervention study. British J Nutr 2010; 104:233–40.
76. Otles S, Yalcin B. Phenolic compounds analysis of root, stalk, and leaves of net- tle. Sci World J 2012;564367.
77. Fan S, Raychaudhuri S, Kraus O, Shahinozzaman M, Lofti L, Obanda D.N. Urtica dioica Whole Vegetable as a Functional Food Targeting Fat Accumulation and Insulin Resistance-a Preliminary Study in a Mouse Pre-Diabetic Model. Nutrients. 2020; 12(4):1059.
78. Oldham AL, Duncan KE. Similar Gene Estimates from Circular and Linear Standards in Quantitative PCR Analyses Using the Prokaryotic 16S rRNA Gene as a Model. *PLOS ONE*. 2012;7(12): e51931.
79. Kable ME, Srisengfa Y, Xue Z, Coates LC, Marco ML. Viable and Total Bacterial Populations Undergo Equipment- and Time-Dependent Shifts during Milk Processing. Applied and Environmental Microbiology. 2019;85(13): e00270-19.
80. Kubinak JL, Peterson C, Stephens WZ, Soto R, Bake E, O'Connel RM, et al. MyD88 signaling in T cells directs IgA-mediated control of the microbiota to promote health. Cell Host Microbe 2015; 17:153–63.
81. Fadlallah J, El Kafsi H, Sterlin D, Juste C, Parizot C, Dorgham K, et al. Micro- bial ecology perturbation in human IgA deficiency. Sci Transl Med 2018;10 pii: eaan1217.
82. Shang H, Sun J, Chen YQ. Clostridium butyricum GMCC0313.1 modulates lipid profile, insulin resistance and colon homeostasis in obese mice. PLoS One 2016;11:e0154373.
83. Atarashi K, Tanoue T, Oshima K, Suda W, Nagano Y, Nishikawa H, et al. Treg induction by a rationally selected mixture of Clostridia strains from the human microbiota. Nature 2013; 500:232–6.
84. Atarashi K, Tanoue T, Shima T, Imaoka A, Kuwahara T, Momose Y, et al. Induction of colonic regulatory T cells by indigenous Clostridium species. Science 2011; 331:337–41.
85. Chiba T, Seno H. Indigenous Clostridium species regulate systemic immune responses by induction of colonic regulatory T cells. Gastroenterology 2011; 141:1114–16.
86. Chávez-Carbajal A, Nirmalkar K, Pérez-Lizaur A, Hernández-Quiroz F, Ramírez- del-Alto S, García-Mena J, et al. Gut microbiota and predicted metabolic pathways in a sample of Mexican women affected by obesity and obesity plus metabolic syndrome. Int J Mol Sci 2019; 20:438.
87. Wexler HM. Bacteroides: the good, the bad, and the nitty-gritty 2007. Clin Microbiol Rev 2007; 20:593–621.
88. Xu J, Gordon JI. Honor thy symbionts. 2003. PNAS 2003;100:10452–9.
89. Jobgen W, Meininger CJ, Jobgen SC, Li P, Lee MJ, Smith SB, et al. Dietary L-arginine supplementation reduces white fat gain and enhances skeletal muscle and brown fat masses in diet-induced obese rats. J Nutr 2009; 139: 230-237.

90. Wiklund P, Zhang X, Pekkala S, Autio R, Kong L, Yang Y, et al. Insulin resistance is associated with altered amino acid metabolism and adipose tissue dysfunction in normoglycemic women. Sci Rep 2016; 6:1–1.
91. Taheri Y, Quispe C, Herrera-Bravo J, Sharifi-Rad J, Ezzat SM, Merghany RM, et al. *Urtica dioica*-Derived Phytochemicals for Pharmacological and Therapeutic Applications. Evidence-Based Complementary and Alternative Medicine 2022;2022:e4024331.
92. Ibrahim M, Rehman K, Razzaq A, Hussain I, Farooq T, Hussain A, et al. Investigations of Phytochemical Constituents and Their Pharmacological Properties Isolated from the Genus *Urtica*: Critical Review and Analysis. CRE 2018;28.
93. Fan S, Raychaudhuri S, Page R, Shahinozzaman M, Obanda D.N. Metagenomic insights into the effects of Urtica dioica vegetable on the gut microbiota of C57BL/6J obese mice, particularly the composition of Clostridia. J. Nutri. Biochem. 2021; 91:108594.
94. Bargut TCL, Souza-Mello V, Aguila MB, Mandarim-de-Lacerda CA. Browning of white adipose tissue: lessons from experimental models. *Hormone Molecular Biology and Clinical Investigation*. 2017;31(1).
95. Couter CJ, Surana NK. Isolation and Flow Cytometric Characterization of Murine Small Intestinal Lymphocytes. *JoVE (Journal of Visualized Experiments)*. 2016;(111): e54114.
96. Hasan NM, Johnson KF, Yin J, et al. Intestinal stem cell-derived enteroids from morbidly obese patients preserve obesity-related phenotypes: Elevated glucose absorption and gluconeogenesis. *Molecular Metabolism*. 2021; 44:101129.
97. Titchenell P.M, Quinn W.J, Lu M, Chu Q, Lu W, Li C, et al. Direct hepatocyte insulin signaling is required for lipogenesis but is dispensable for the suppression of glucose production. Cell Metab. 2016; 23(6):1154–66.
98. Chassaing B, Aitken J.D, Malleshappa M, Vijay-Kumar, M. Dextran sulfate sodium (DSS)-induced colitis in mice. Curr. Protoc. Immunol. 2014; 104:15.25.1–15.25.14.
99. Bronte V, Pittet M.J. The spleen in local and systemic of immunity. Immunity. 2013; 39(5):806-818.
100. Chusyd DE, Wang D, Huffman DM, Nagy TR. Relationships between Rodent White Adipose Fat Pads and Human White Adipose Fat Depots. Front Nutr 2016;3:10.
101. Sethi JK, Hotamisligil GS. Metabolic Messengers: tumour necrosis factor. Nat Metab 2021;3:1302–12.
102. Sorini C, Cardoso R.F, Gagliani N, Villablanca E.J. Commensal Bacteria-Specific Cd4+ T Cell Responses in Health and Disease. Front Immunol. 2018; 9:2667.
103. Hegazy A.N, West N.R, Stubbington M.J.T, Wendt E, Suijker K.I.M, Datsi A, et al. Circulating and Tissue-Resident Cd4+ T Cells With Reactivity to Intestinal Microbiota Are Abundant in Healthy Individuals and Function Is Altered During Inflammation. Gastroenterology. 2017; 153(5):1320–1337.e16.
104. Littman D.R, Rudensky A.Y. Th17 and regulatory T cells in mediating and restraining inflammation. Cell. 2010; 140(6):845–858.

105. Hong C-P, Park A, Yang B-G, Yun C.H, Kwak M.J, Lee G-W, *et al*. Gut-specific delivery of T-helper 17 cells reduces obesity and insulin resistance in mice. Gastroenterology. 2017; 152(8):1998–2010.
106. Bradley D, Smith A.J, Blaszczak A, Shantaram D, Bergin S.M, Jalilvand A, et al. Interferon gamma mediates the reduction of adipose tissue regulatory T cells in human obesity. Nat Commun. 2022; 13(1):5606.
107. Zachos N.C, Kovbasnjuk O, Foulke-Abel J, In J, Blutt SE, Jonge H.R, et al. Human enteroids/colonoids and intestinal organoids functionally recapitulate normal intestinal physiology and pathophysiology. J. Bio Chem. 2016; 291(8):3759-3766.
108. Jattan J, Rodia C, Li D, Diakhate A, Dong H, Bataille A, et al. Using primary murine intestinal enteroids to study dietary TAG absorption, lipoprotein synthesis, and the role of apoC-III in the intestine. J Lipid Res. 2017; 58(5):853–865.
109. Kozuka K, He Y, Koo-McCo S, Kumaraswamy P, Nie B, Shaw K, et al. Development and characterization of a human and mouse intestinal epithelial cell monolayer platform. Stem cells Reports. 2017; 9(6):1976-1990.
110. Pepino M.Y, Kuda O, Samovski D, Abumrad NA. Structure-function of CD36 and importance of fatty acid signal transduction in fat metabolism. Annu Rev Nutr. 2014; 34(1):281-303.
111. Xu S, Jay A, Brunaldi K, Huang N, Hamilton J.A. CD36 enhances fatty acid uptake by increasing the rate of intracellular esterification but not transport across the plasma membrane. Biochemistry. 2013; 52(41):7254–7261.